STRESS DISTRIBUTION AROUND HOLES IN LAMINATED COMPOSITE PLATES

by

Chi-Hung Huang

Dissertation submitted to the Graduate Faculty of the

Virginia Polytechnic Institute and State University

in partial fulfillment of the requirements for the degree of

DOCTOR OF PHILOSOPHY

in

Engineering Mechanics

APPROVED:

Daniel Frederick, Chairman

R. A. Heller

E. G. Henneke

C. B. Ling

G. W. Swift

May, 1975

Blacksburg, Virginia

ACKNOWLEDGMENTS

This research was supported by the U.S. Department of Defense, Project THEMIS, Contract Number DAA F07-69-0444, with Watervliet Arsenal, Watervliet, New York. This financial support is gratefully acknowledged.

The author sincerely appreciates the guidance and encouragement provided by Dr. Daniel Frederick, Director of Project THEMIS and Chairman of his committee, throughout the investigation.

The author expresses his thanks to Dr. Richard M. Barker for help and advice in finite element portion and to Dr. C. B. Ling, Dr. G. W. Swift , Dr. R. A. Heller and Dr. E. G. Henneke for serving on his graduate committee and for their assistance during the investigation.

Special appreciation is extended to for his advice on the computer program.

The patience and support of the author's wife, , is gratefully acknowledged.

TABLE OF CONTENTS

LIST OF FIGURES

FIGURES (Continued)

FIGURES (Continued)

FIGURES (Continued)

LIST OF TABLES

LIST OF SYMBOLS

τ_{ij}	Shear stress components on the plane normal to the i axis in the j direction
σ_i	Normal stress on the plane normal to the i axis in the i direction
u, v, w	Displacements of a point in x, y, z directions
h	Thickness of laminated composite plate
e_i	Normal strain in the i axis direction
γ_{ij}	Shear strain in i-j plane
a_{ij}	Elastic constants
B_{ij}	Components of stiffness matrix
x, y, z	Rectangular Cartesian coordinates
$Z, \bar{Z}$	Complex coordinates in Z-plane
$\Omega(Z), \omega(Z)$	Complex potential functions
M_x, M_y, M_{xy}	Stress couples with respect to the Cartesian coordinates
Q_x, Q_y	Shear forces with respect to the Cartesian coordinates
E	Young's modulus
ν	Poisson's ratio
G	Shear modulus
T^{ij}	Contravariant stress tensors in $(Z, \bar{Z})$ coordinates
$\zeta, \bar{\zeta}$	Complex coordinates in ζ-plane
Γ^{ij}	Contravariant stress tensors in $(\zeta, \bar{\zeta})$ coordinates
R, θ, z	Cylindrical coordinates

$K_n(x)$, $I_n(x)$ $n = 0,1,2,...$	nth-order modified Bessel functions of the second kind
$FeK_n(x)$, $GeK_n(x)$, $n = 0,1,2,...$	nth-order modified Matheiu functions of the second kind
$C_{en}(x)$, $S_{en}(x)$, $n = 0,1,2,...$	nth-order Mathieu functions of the second kind
a	Major axis of elliptical hole, radius of circular hole
b	Minor axis of elliptical hole
D	Diameter of hole
$\bar{e}_1$, $\bar{e}_2$	Base vectors with respect to Cartesian coordinates (x, y)
$\bar{a}_1$, $\bar{a}_2$	Base vectors with respect to complex coordinates (Z, $\bar{Z}$)
ξ, η, z	Elliptical coordinates, curvilinear coordinates
$M_{\xi\xi}$, $M_{\eta\eta}$, $M_{\xi\eta}$	Stress couples with respect to the curvilinear coordinates (ξ, η, z)
Q_ξ, Q_η	Shear forces with respect to the curvilinear coordinates (ξ, η, z)
x_o, y_o, z_o	Dimensionless Cartesian coordinates
r, θ, z	Dimensionless cylindrical coordinates

I. INTRODUCTION

Composite materials have existed for centuries. They have been used in a wide variety of man-made structures, from houses and bridges to furniture, laminated tennis rackets, and skis. However, the idea of designing a composite for a specific purpose is comparatively recent.

In the past, the engineer was forced to choose from available materials to design a particular structure. Soon, however, he may be in a position to prescribe material properties in the expectation that an appropriate composite will be fabricated. For example, consider the case of a proposed laminated composite for future building applications. It has been suggested that such a composite might have an outside layer comprising a structural and insulating sandwich covered with a weather-resistant film. In addition, it could have an inside skin consisting of a metallic sheet to provide either radiant heat or cooling along with a fluorescent material for internal lighting. The task of fabricating such a composite is formidable.

The main structural problems that have been solved by these materials are those involving strength, weight, and stiffness. Thus, they have been used in the construction of ships, submarines, aircraft radomes, wing and empennage structures, and helicopter blades. The use of composites increases the capacity of a commercial

plane for passengers and cargo. Composite helicopter blades provide lower inertial loads while maintaining stiffness and providing good damping and fatigue properties.

Materials that can provide strength and are at the same time corrosion-resistant, rot-proof, thermally insulating, and nonmagnetic are obviously desirable in ship construction. Materials like GRP (glass fiber reinforced plastic composites) have been used in the sonardome, master fairing, and superstructures of submarines and in the mast, cutaway rudder, and ventilation system of surface ships. In aircraft, these materials have been used in the honeycomb sandwich, nose radome, fuselage, wings, and even the jet engine compressor blades.

Composites have not been utilized to great extent in space vehicles. However, they have potential structural application as propellant tanks, payload shrouds, and rocket nozzles of launch vehicles; pressure vessels, antennas, meteoroid shields, and trusses of spacecraft; thermal shields, aeroshells, and deployable decelerators for entry vehicles; and energy absorbers, framework, and cabin walls of landing craft. Hence, bright prospects are anticipated for the broad application of these materials in space vehicles and allied fields. The present obstacles are results of the relative newness of the technology, limited design methods, and occasional low reliability. All these are characteristic of an immature technology; future research and development will overcome them.

The objectives of this dissertation are to investigate the distribution of stresses around holes in composite plates under pure bending and to calculate the stress concentration factor, which plays an important role in structural design. The analysis is also intended to provide information that is especially important in such engineering problems as the fatigue and fracture of these materials. At this point, a review of some current theories that may be apposite to the analysis will be reviewed.

The lamination theory, first introduced by Smith and further developed by many authors, was capable of describing the gross responses of laminated composite plates. This theory, based on the classical plate assumptions, took the structural geometry and the anticipated deformation characteristics into account in order to arrive at simplified governing equations, which were appropriate for the analysis of a larger class of plate configurations.

Modified lamination theory, also called high-order theory, has been introduced by releasing some assumptions of classical plate theory. In this way, the effects of transverse shear deformation and rotary inertia can be included. This approach is applicable for thick laminates and sandwich construction for which classical lamination theory fails to give accurate gross responses because of the relatively soft interlaminar shear modulus in high performance composites.

The continuum theory of homogeneous materials has also been developed for the laminate analysis. However, it obviously cannot

be used for determining local stress or strain fields at discontinuities because it represents a heterogeneous composite possessing discontinuous materials as an equivalent homogeneity.

Of all the aforementioned theories, modified lamination theory is appropriate for analyzing the stress concentration around a hole in a laminated composite plate since this approach takes into account the contribution of shear deformations and provides the interlaminar shear stresses that are especially important in the neighborhood of the free edge of a hole in a composite plate. To familiarize the reader with the theory and the assumptions on which it is based, derivations of the governing differential equations and their boundary conditions are discussed in Chapter III. This discussion reveals the nature of the problem: solving the governing differential equations with appropriate boundary conditions. Unfortunately, until now no general form of solution for these general differential equations has been presented. However, the scope of this dissertation is limited to the case of laminated heterogeneous composites; hence, the governing differential equations may be solved with the techniques presented here.

In the theoretical treatment of classical two-dimensional problems, the application of the method of complex stress functions was very successful. This fruitful method was developed primarily by the Russian mathematician Muskhelishvili and his followers. With the application of conformal mapping, it was possible to solve many important problems involving stress concentrations. In reviewing

its past history, this technique has been used to solve for the stress distribution in infinite composite plates with a hole under pure bending; the method is discussed in Chapter IV. The application of the technique for a circular and an elliptical hole is described in Chapter V, and for general curvilinear holes in Chapter VI. However, significant mathematical difficulties will be encountered, especially for the establishment of suitable conformal mappings; and therefore, one is not able to solve all problems of arbitrary cases of stress concentration even in this way.

It must be stated that numerical analytical techniques are also very important in the investigation of stress concentration problems. Some cases of two- and three-dimensional stress concentration problems have been investigated by the finite element method. The accuracy of this method, however, is limited. But for many engineering and design problems, the finite element method is of great importance. In view of these facts, the finite element analysis is presented in Chapter VII. The solutions have been compared with the results obtained from the analytical method. It can be seen that the two methods generally agree.

II. LITERATURE REVIEW

The classical lamination theory for the bending of composite plates laminated of thin orthotropic plates, or plies, was first introduced by Smith [1]* in 1953. He investigated plates that possessed two perpendicular axes of elastic symmetry. All plies were assumed to be identical in thickness and elastic properties. Kirchhoff's approximations and the assumptions of small deflections and displacement gradients were used to formulate the governing differential equations. In 1959, Pister and Dong [2] studied the problem of nonlinear bending of plates comprising two or more bonded, thin isotropic layers. Their results showed that for large deflections, the transverse and in-plane deflections were coupled; however, this coupling disappeared when the deflections were small. Therefore, for the latter case, solutions may be obtained directly from corresponding single-layer plate problems by transposing composite plate parameters.

Reissner and Stravsky [3] were the first to recognize the coupling phenomenon between in-plane stretching and transverse bending for non-symmetric laminated plates. Stravsky [4] also showed that, even for the small deflection theory of Pister and Dong [2], no simple transposition of single-layer plate solutions was possible because stretching and bending are still coupled

---

*Numbers in brackets [ ] refer to references listed in REFERENCES.

through the boundary conditions, even though the differential equations were uncoupled. The coupling phenomenon does not occur in the theory of homogeneous plates and thus had been overlooked by earlier authors.

A general small deflection theory for the elastostatic extension and flexure of thin, laminated anisotropic shells and plates was formulated by Dong, Pister, and Taylor [5]. The multi-layered composite was composed of an arbitrary number of bonded layers, each of a different thickness, orientation, and/or anisotropic elastic properties. In their theory, the Kirchhoff-Love assumptions were retained, the effects of transverse shear deformations were neglected, and the interlamina shear stresses were derived from the equilibrium equations.

The previously described theory, called the classical laminated plate theory, CLT, is clearly outlined and discussed in detail in references [6] through [9]. Numerous example problems are presented in references [8] and [9].

Currently, with wider application of advanced composite materials, there is increasing use of thick laminates and sandwich construction. In these applications, because of the relatively soft interlaminar shear modulus used in high performance composites, the classical laminated plate theory is not accurate for determining such gross responses as plate deflection and the internal stress distribution. Also, the CLT fails to predict the interlaminar shear stresses at the intersection of the interfaces and free edges,

where the stress gradients are very steep. Therefore, a theory for laminated plates analogous to that presented by Reissner [10] and Mindlin [11] for isotropic plates assumes greater importance. The introduction of shear deformation into laminated plate theory was evidently first accomplished by Stravsky [12] for isotropic layers having identical Poisson's ratios. Ambartsumyan [13] developed a slightly different approach, in which the transverse shear stresses were defined to satisfy the required continuity conditions at the layer interfaces. This bending theory allowed for the specification of three boundary conditions per edge. Whitney [14] recently extended Ambartsumyan's approach to solve certain specific boundary value problems involving more general material and geometric properties than those considered by Ambartsumyan [13].

The most general linear laminate theory is attributed to Yang, Norris, and Stravsky [15], who extended Mindlin's theory [11] for homogeneous plates to laminates consisting of an arbitrary number of bonded anisotropic layers. Although this approach is much less cumbersome than that of Ambartsumyan [13], its consequences have not been explored because of a lack of solutions to specific boundary value problems. They only solved the frequency equations for the propagation of harmonic waves in a two-layer isotropic plate of infinite extent.

Recently, Sun, Achenbach, and Herrmann [16] proposed a continuum theory called the effective stiffness theory, in which they treated the problem of a laminated system comprising a large number of

alternating layers of two different isotropic materials. This theory has exhibited reasonable agreement with exact elasticity solutions for dispersion curves. However, the theory is not intended for determining internal stresses in more complex composite systems, which is the goal of the study presented herein.

Owing to the rapid development of modern high-speed electronic computers, matrix techniques and finite element methods have received much attention by engineers. Pryor [17] recently presented a finite element method for laminated anisotropic plates consisting of rectangular 28 DOF (degrees of freedom) element, which was employed in the analysis of rectangular anisotropic laminated plates. Later, Lin [18] presented an improved version of this element, which was an isoparametric, 72 DOF element developed for the three-dimensional analysis of laminated composites. The results of Pryor and Lin were in good agreement with exact elasticity solutions. Application of the 72 DOF element for determining stress concentration factors near holes in laminated composites under uniform in-plane tension was described by Barker, Dana, and Pryor [19]. The good results of these investigators provided the motivation for using similar finite element methods in the present work.

Because of the complicated geometry and boundary conditions, analytical solutions for the stress distributions around holes in laminated composite plates have not been presented in general form in the literature. Solutions obtained by classical plate theory, as given in references [20] through [22], provided inaccurate

internal stress distributions near the edge of the hole. To date, only one three-dimensional finite element analysis [19] has been presented for the state of stress around a circular hole in a laminated composite under uniform tension. Several experimental investigations were made, as reported in references [23], [24] and [25]; however, these techniques are basically two-dimensional in nature.

This study presents a detailed investigation of the stress distributions around holes in laminated plates composed of an arbitrary number of bonded anisotropic layers, each having one plane of material symmetry parallel to the central plane of the plate. The theory developed in references [13] and [14] is employed for formulating the governing equations. General solutions for the system of governing equations are generally not available owing to the considerable difficulties in the mathematical analysis. However, techniques for obtaining exact solutions, as developed in references [22], [10], and [20] for circular and elliptical holes and in references [26], [27], and [28] for general curvilinear holes, are used to obtain solutions for the case of isotropic, laminated composite plates.

III. FORMULATION OF GOVERNING EQUATIONS

3.1. Introduction

The basic equations presented in this dissertation to describe the behavior of composite materials were originally derived by Ambartsumyan [13]. These equations, together with the assumptions on which they are based, form a theory of thick elastic plates, which is commonly referred to as Reissner's shearing deformation theory. To allow for as much understanding as possible, the derivation of the theory is carried out in this chapter. It proceeds by first describing the underlying assumptions of the theory. This is followed by derivations of the expressions which relate stresses and displacements in a composite, the equations of motion of a plate element, and the boundary conditions that are to be used with the theory.

Before proceeding to the aforementioned topics, the laminated composite plates to be studied are described. The composite plate is to be a thin, multi-layered plate consisting of an odd number $(2m + 1)$ of uniform anisotropic layers arranged symmetrically with respect to the plate middle plane xoy (see Figures 1 and 2). In general, a rectangular cartesian coordinate system is used with its origin located in the middle plane and with its positive z axis downward normal to the plane. The layers are bonded to each other and numbered in a sequence as shown in Figure 2. It is also assumed that each layer possesses a plane of elastic symmetry parallel to

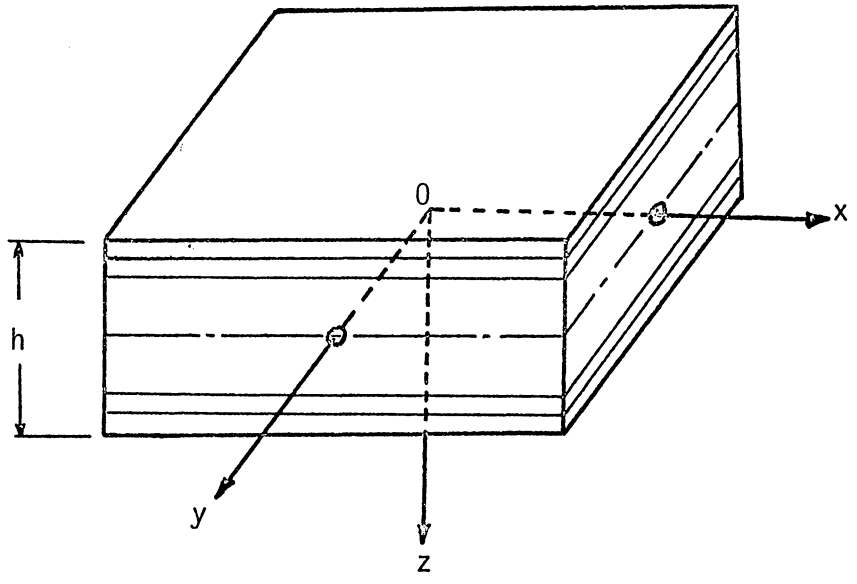

Figure 1. Configuration of Laminated Composite Plate and Coordinate System

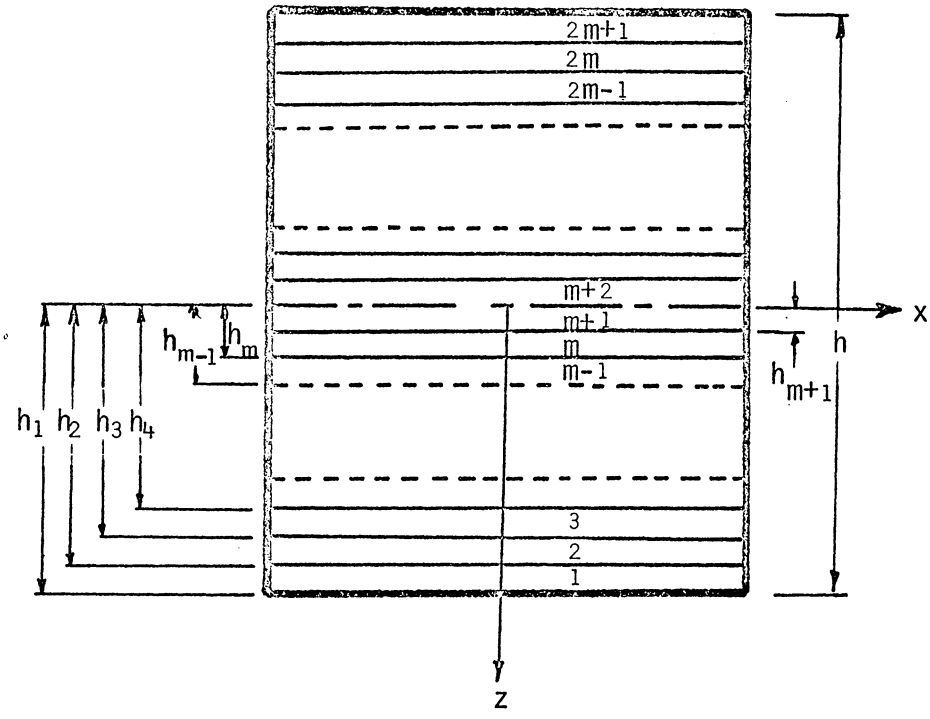

Figure 2. Stacking Sequence of Laminated Composite Plate

xoy plane and obeys the generalized Hooke's law. In addition, all layers remain elastically bonded together and do not slip against each other during deformation, nor are there traction forces on the top and bottom boundaries of the composite plate. These boundary conditions are expressed as

$$\tau_{xy}(x, y, \pm h/2) = 0, \quad \tau_{yz}(x, y, \pm h/2) = 0, \tag{3.1}$$

$$\sigma_z(x, y, \pm h/2) = 0 . \tag{3.2}$$

3.2. Basic Assumptions

The theory is based on the following postulates:

(i) The displacement w normal to plate middle plane does not depend on the z coordinate.

(ii) The deflections, slopes, and rotations of the plate are small.

(iii) The shear stresses τ_{xy} and τ_{yz} or the corresponding strains γ_{xy} and γ_{yz} change according to a postulated law with respect to the z coordinate.

As mentioned in section 3.1, certain continuity conditions must be satisfied at each interface of layers. According to reference [30] this task is fulfilled when the following expressions hold:

$$u^i(x, y, h_{i+1}) = u^{i+1}(x, y, h_{i+1}) ,$$

$$v^i(x, y, h_{i+1}) = v^{i+1}(x, y, h_{i+1}) ,$$

$$w^i(x, y, h_{i+1}) = w^{i+1}(x, y, h_{i+1}) \tag{3.3}$$

and

$$\tau_{xz}^{i}(x, y, h_{i+1}) = \tau_{xz}^{i+1}(x, y, h_{i+1}) ,$$

$$\tau_{yz}^{i}(x, y, h_{i+1}) = \tau_{yz}^{i+1}(x, y, h_{i+1}) ,$$

$$\sigma_{z}^{i}(x, y, h_{i+1}) = \sigma_{z}^{i+1}(x, y, h_{i+1}) \qquad (3.4)$$

where

$i = 1, 2, 3, \ldots, m+1$,

u,v,w = displacement components in the x, y, and z direction, respectively ,

$\tau_{\alpha\beta}$ = shear stress components ,

$\alpha, \beta = x, y, z$,

σ_{α} = normal stress ,

$\alpha = x, y, z$,

h = thickness of the composite plate ,

and index i stands for the ith layer.

In assumption (iii), the selection of the function that governs the relation of τ_{xz} and τ_{yz} to the coordinate should preferably be based on the analysis of the shear stress distribution τ_{xz} and τ_{yz}, using the sufficiently accurate theories for the bending of thick plates [10, 29]. This analysis shows that shear stresses τ_{xz} and τ_{yz} for the case of thick as well as thin plates have a parabolic distribution. Therefore, for each layer the stresses τ_{xz}^{i} and τ_{yz}^{i} can be expressed as

$$\tau_{xz}^{i} = \left[\frac{1}{2}B_{55}^{i}\left(\frac{h^2}{4} - z^2\right) + A_{i}^{5}\right]\phi(x, y)$$

$$\tau_{yz}^{i} = \left[\frac{1}{2}B_{44}^{i}\left(\frac{h^2}{4} - z^2\right) + A_i^4\right]\psi(x, y) \qquad (3.5)$$

where $\phi(x, y)$ and $\psi(x, y)$ are two arbitrary undetermined functions, and B_{55}^{i} and B_{44}^{i} are the components of stiffness matrix for ith layer. They are discussed later. The constants A_i^5 and A_i^4 are parameters for ith layer. They are used for making the shear stresses satisfy the continuity condition equations (3.4) as well as the boundary condition Eqs. (3.1). By considering the symmetry condition with respect to the middle plane of the plate, expressions for A_i^5 and A_i^4 are obtained as follows:

$$A_i^5 = \sum_{\alpha=1}^{i-1} \frac{1}{2}\left(\frac{h^2}{4} - h_{\alpha+1}^2\right)(B_{55}^{\alpha} - B_{55}^{\alpha+1}) ,$$

$$A_i^4 = \sum_{\alpha=1}^{i-1} \frac{1}{2}\left(\frac{h^2}{4} - h_{\alpha+1}^2\right)(B_{44}^{\alpha} - B_{44}^{\alpha+1}) ,$$

$$A_i^{\alpha} = A_{2m+2-i}^{\alpha}, \; A_1^{\alpha} = A_{2m+1}^{\alpha} = 0, \; \alpha = 4,5,$$

and $i = 1, 2, 3, \ldots, m+1$. (3.6)

Assumption (iii) permits reference of all derivations and calculations to the original configuration of the plate and, together with Hooke's law, assures that the resulting theory will be linear, elastic one.

The assumption that the displacement w does not depend on the z coordinate implies no transverse normal strain. It is expected that this assumption will be generally valid for thin plates except

in the vicinity of highly transverse concentrated loads. As a consequence of the first and second postulates, the strain-displacement equations for the arbitrary ith layer can be expressed as

$$e_x^i = \frac{\partial u^i}{\partial x}, \quad e_y^i = \frac{\partial v^i}{\partial y}, \quad \gamma_{xy}^i = \frac{\partial u^i}{\partial y} + \frac{\partial v^i}{\partial x}$$

$$\gamma_{xz}^i = \frac{\partial w}{\partial x} + \frac{\partial u^i}{\partial z}, \quad \gamma_{yz}^i = \frac{\partial w}{\partial y} + \frac{\partial v^i}{\partial z}. \tag{3.7}$$

3.3. Displacement Functions

As stated in previous sections, each uniform anisotropic layer possesses a plane of elastic symmetry parallel to the xoy plane; thereby, the constitutive equations of the anisotropic material having such an elastic symmetric plane for the ith layer can be shown as

$$\begin{Bmatrix} e_x \\ e_y \\ \gamma_{xy} \\ e_z \end{Bmatrix}_i = \begin{bmatrix} a_{11} & a_{12} & a_{13} & a_{16} \\ a_{12} & a_{22} & a_{23} & a_{26} \\ a_{16} & a_{26} & a_{36} & a_{66} \\ a_{13} & a_{23} & a_{33} & a_{36} \end{bmatrix}_i \begin{Bmatrix} \sigma_x \\ \sigma_y \\ \sigma_z \\ \tau_{xy} \end{Bmatrix}_i \tag{3.8}$$

$$\begin{Bmatrix} \gamma_{xz} \\ \gamma_{yz} \end{Bmatrix}_i = \begin{bmatrix} a_{55} & a_{45} \\ a_{45} & a_{44} \end{bmatrix} \begin{Bmatrix} \tau_{xz} \\ \tau_{yz} \end{Bmatrix}_i \tag{3.9}$$

where the a_{ij} values are the elastic constants with symmetric properties, $a_{ij} = a_{ji}$. In general, thirteen independent elastic constants are needed in this system. However, if a given layer is a fiber-reinforced composite material, it can be treated as an orthotropic sheet. The axes of material symmetry are parallel and normal to the fiber direction; thus, only nine rather than thirteen coefficients are independent in this case.

In terms of the elastic stiffnesses, Eqs. (3.8) and (3.9) become

$$\begin{bmatrix} \sigma_x \\ \sigma_y \\ \tau_{xy} \end{bmatrix}_i = \begin{bmatrix} B_{11} & B_{12} & B_{16} \\ B_{12} & B_{22} & B_{26} \\ B_{16} & B_{26} & B_{66} \end{bmatrix}_i \left\{ \begin{bmatrix} e_x \\ e_y \\ \gamma_{xy} \end{bmatrix} - \begin{bmatrix} a_{13} \\ a_{23} \\ a_{36} \end{bmatrix} \sigma_z \right\}_i \tag{3.10}$$

$$\begin{Bmatrix} \tau_{xz} \\ \tau_{yz} \end{Bmatrix}_i = \begin{bmatrix} B_{55} & B_{45} \\ B_{45} & B_{44} \end{bmatrix}_i \begin{Bmatrix} \gamma_{xz} \\ \gamma_{yz} \end{Bmatrix}_i \tag{3.11}$$

where the B_{ij} values are the components of the elastic stiffness matrix. They relate elastic constants a_{ij} in the following relations:

$$\begin{Bmatrix} B_{11} \\ B_{22} \\ B_{12} \end{Bmatrix} = \frac{1}{\Delta} \begin{Bmatrix} \tilde{a}_{2266} \\ \tilde{a}_{1166} \\ -\tilde{a}_{1266} \end{Bmatrix}, \begin{Bmatrix} B_{16} \\ B_{26} \\ B_{66} \end{Bmatrix} = \frac{1}{\Delta} \begin{Bmatrix} \tilde{a}_{2126} \\ \tilde{a}_{1216} \\ \tilde{a}_{1122} \end{Bmatrix}, \begin{Bmatrix} B_{44} \\ B_{55} \\ B_{45} \end{Bmatrix} = \frac{1}{D} \begin{Bmatrix} a_{55} \\ a_{44} \\ -a_{45} \end{Bmatrix} \tag{3.12}$$

and

$$\tilde{a}_{ijkl} = a_{ij}a_{kl} - a_{ik}a_{jl} \tag{3.13}$$

$$\Delta \equiv (a_{12}a_{26} - a_{22}a_{16})a_{16} + (a_{12}a_{16} - a_{11}a_{26})a_{26} + (a_{11}a_{22} - a_{12}^2)a_{66}$$

$$D \equiv a_{44}a_{55} - a_{45}^2 \, . \tag{3.14}$$

Now the displacement functions u^i and v^i can be derived in terms of w and two unknown functions, ϕ and ψ, by integrating the last two equations of Eq. (3.7) with respect to z. It should also be noted that the strains γ_{xz}^i and γ_{yz}^i are given by Eq. (3.9) while the shear stresses τ_{xz}^i and τ_{yz}^i are given as assumed in Eq. 3.5. After some manipulation, the expressions for the displacement functions are obtained as

$$u^i = -z\frac{\partial w}{\partial x} + (J_{555}^i + R_{555}^i + za_{55}^i A_i^5)\phi(x,y) + (J_{445}^i + R_{445}^i + za_{45}^i A_1^4)\psi(x,y) \tag{3.15}$$

$$v^i = -z\frac{\partial w}{\partial y} + (J_{444}^i + R_{444}^i + za_{44}^i A_i^4)\psi(x,y) + (J_{545}^i + R_{545}^i + za_{45}^i A_i^5)\phi(x,y) \tag{3.16}$$

where $J_{\gamma\alpha\beta}$ and $R_{\gamma\alpha\beta}$ are functions designed to guarantee that the displacement functions u^i and v^i are continuous across the interface between the layers. By substituting Eqs. (3.15) and (3.16) into (3.3) the values for $J_{\gamma\alpha\beta}$ and $R_{\gamma\alpha\beta}$ are obtained as follows:

$$J_{\gamma\alpha\beta} = \frac{z}{2}\, a_{\alpha\beta}^i B_{\gamma\gamma}\left(\frac{h^2}{4} - \frac{z^2}{3}\right)$$

and

$$R^{i}_{\gamma\alpha\beta} = \sum_{i=1}^{m-i+1} [J^{i+1}_{\gamma\alpha\beta}(h_{i+1}) - J^{i}_{\gamma\alpha\beta}(h_{i+1}) + h_{i+1}(a^{i+1}_{\alpha\beta}A_{i+1} - a^{i}_{\alpha\beta}A_{i})]$$

$$R^{m+1}_{\gamma\alpha\beta} = 0, \quad \gamma = 4, 5, \quad \alpha,\beta = 4, 5 . \qquad (3.17)$$

Knowing the displacement functions, the strains can be calculated from Eq. (3.7) and stresses from Eq. (3.10). As can be seen, the strains and stresses are linearly distributed across the thickness of the plate. Because the thickness is small, it is convenient to integrate the stress distributions through the thickness of the plate and to replace the usual consideration of stresses with a consideration of statically equivalent stress resultants and stress couples. In this way, the variations with respect to z are completely eliminated thereby giving a two-dimensional theory.

3.4. Stress Resultants and Stress Couples

As normally defined in plate theory, the stress resultants and stress couples are given by

$$(M_x, M_y, M_{xy}) = \int_{-h/2}^{h/2} (\sigma_x, \sigma_y, \sigma_{xy})_i z dz , \qquad (3.18)$$

$$(N_x, N_y, N_{xy}) = \int_{-h/2}^{h/2} (\sigma_x, \sigma_y, \sigma_{xy}) dz$$

$$(Q_x, Q_y) = \int_{-h/2}^{h/2} (\tau_{xz}, \tau_{yz})_i dz \qquad (3.19)$$

It should be noted that the stress resultants and stress couples are defined per unit of length on the middle plane. Notice, in these equations, that the in-plane stress resultants N_x, N_y, and N_{xy} disappear because of the nature of the symmetric property of the plate with respect to the middle plane. This result can also be justified immediately since the stresses σ_x^i, σ_y^i, and τ_{xy}^i are an odd function in the z variable.

The stress resultants are to be found by integrating the stresses given by Eqs. (3.10) across the plate. However, this integration cannot be completed yet since the value of σ_z^i has not yet been determined.

The normal stress σ_z^i for each layer can be determined by examining the third equation of stress equilibrium, which is given by

$$\frac{\partial \sigma_{\beta z}}{\partial \beta} = 0, \quad \beta = x, y, z \ . \tag{3.20a}$$

Eq. (3.20a) holds true at every point in the composite plate, and for each individual layer. Therefore, for the ith layer it can be rewritten as

$$\frac{\partial \tau_{xy}^i}{\partial x} + \frac{\partial \tau_{yz}^i}{\partial y} + \frac{\partial \sigma_z^i}{\partial z} = 0 \ . \tag{3.20b}$$

To solve Eq. (3.20b) for σ_z^i, it is first necessary to substitute for the shear stresses τ_{xz}^i and τ_{yz}^i from Eq. (3.5) and then to integrate with respect to the z coordinate. The final result is in the following.

$$\sigma_z^i = -\left[\frac{z}{2}\left(\frac{h^2}{4} - \frac{z^2}{3}\right)B_{55}^i + zA_i^5 - S_{55}^i\right]\frac{\partial\phi}{\partial x} - \left[\frac{z}{2}\left(\frac{h^2}{4} - \frac{z^2}{3}\right)B_{44}^i + zA_i^4 - S_{44}^i\right]\frac{\partial\psi}{\partial y} \tag{3.21}$$

where $S_{\alpha\alpha}$ ($\alpha = 4, 5$) are integration constants designed to ensure that the normal stress is continuous across the interface between the layers. In view of the last equation in the continuity Eqs. (3.4), the value of $S_{\alpha\alpha}$ is given by

$$S_{\alpha\alpha}^i = \frac{h^3}{24}B_{\alpha\alpha}^1 + \sum_{J=2}^{i-1}\left[\frac{h_j}{2}\left(\frac{h^2}{4} - h_j^2\right)(B_{\alpha\alpha}^i - B_{\alpha\alpha}^{J-1}) + (A_j^\alpha - A_{j-1}^\alpha)h_j\right], \tag{3.22}$$

$i = 1, 2, 3, \ldots, m+1, \qquad \alpha = 4, 5.$

Having the displacements u^i and v^i and normal stress σ_z^i in terms of three unknown functions w, ϕ, and ψ, the expressions for the stresses can be determined through Eq. (3.10) and strains through (3.7) in terms of these unknown functions. In the interest of brevity, the intermediate steps are not presented; instead, the final expression for the stresses σ_x^i, σ_y^i, and τ_{xy}^i are given by

$$\sigma_y^i = -z\left(B_{12}^i\frac{\partial^2 w}{\partial x^2} + 2B_{26}^i\frac{\partial^2 w}{\partial x\partial y} + B_{22}^i\frac{\partial^2 w}{\partial y^2}\right) + (B_{22}^i J_{444}^{*i} + B_{26}^i J_{445}^{*i} + \tilde{B}_2^i C_4^i)\frac{\partial\psi}{\partial y}$$

$$+ (B_{22}^i J_{545}^{*i} + B_{26}^i J_{555}^{*i})\frac{\partial\phi}{\partial y} + (B_{12}^i J_{555}^{*i} + B_{26}^i J_{545}^{*i} + \tilde{B}_2^i C_5^i)\frac{\partial\phi}{\partial x}$$

$$+ (B_{12}^i J_{445}^{*i} + B_{26}^i J_{444}^{*i})\frac{\partial\psi}{\partial x} \tag{3.23}$$

$$\sigma_x^i = -z\left(B_{11}^i \frac{\partial^2 w}{\partial x^2} + 2B_{16}^i \frac{\partial^2 w}{\partial x \partial y} + B_{12}^i \frac{\partial^2 w}{\partial y^2}\right) + \left(B_{11}^i \overset{*}{J}{}_{555}^i + B_{16}^i \overset{*}{J}{}_{545}^i + \tilde{B}_1^i C_5^i\right)\frac{\partial \phi}{\partial x}$$

$$+ \left(B_{11}^i \overset{*}{J}{}_{445}^i + B_{16}^i \overset{*}{J}{}_{444}^i\right)\frac{\partial \psi}{\partial x} + \left(B_{12}^i \overset{*}{J}{}_{545}^i + B_{16}^i \overset{*}{J}{}_{555}^i\right)\frac{\partial \phi}{\partial y}$$

$$+ \left(B_{12}^i \overset{*}{J}{}_{444}^i + B_{16}^i \overset{*}{J}{}_{445}^i + \tilde{B}_1^i C_4^i\right)\frac{\partial \psi}{\partial y}, \qquad (3.24)$$

$$\tau_{xy}^i = -z\left(B_{16}^i \frac{\partial^2 w}{\partial x^2} + 2B_{66}^i \frac{\partial^2 w}{\partial x \partial y} + B_{26}^i \frac{\partial^2 w}{\partial y^2}\right) + \left(B_{66}^i \overset{*}{J}{}_{555}^i + B_{26}^i \overset{*}{J}{}_{545}^i\right)\frac{\partial \phi}{\partial y}$$

$$+ \left(B_{66}^i \overset{*}{J}{}_{445}^i + B_{26}^i \overset{*}{J}{}_{444}^i + \tilde{B}_6^i C_4^i\right)\frac{\partial \psi}{\partial y} + \left(B_{66}^i \overset{*}{J}{}_{444}^i + B_{16}^i \overset{*}{J}{}_{445}^i\right)\frac{\partial \psi}{\partial x}$$

$$+ \left(B_{66}^i \overset{*}{J}{}_{545}^i + B_{16}^i \overset{*}{J}{}_{555}^i + \tilde{B}_6^i C_5^i\right)\frac{\partial \phi}{\partial x}, \qquad (3.25)$$

where

$$\overset{*}{J}{}_{n\alpha\beta}^i = J_{n\alpha\beta}^i(z) + z a_{\alpha\beta}^i A_i^n + R_{n\alpha\beta}^i,$$

$$C_n^i = \frac{1}{2} B_{nn}^i \left(\frac{h^2}{4} - z^2\right) + A_i^n - S_{nn}^i,$$

$$\alpha, \beta = 4, 5,$$

$$n = 4, 5 .$$

Now the stress resultants and stress couples may be obtained in terms of the unknown functions w, ϕ, and ψ. By substituting Eqs. (3.23) through (3.25) into (3.18) the relationships between the stress couples and the three unknown functions are obtained in the following way.

$$\begin{pmatrix} M_x \\ M_y \\ M_{xy} \end{pmatrix} = - \begin{pmatrix} D_{11} & D_{12} & D_{16} \\ D_{12} & D_{22} & D_{26} \\ D_{16} & D_{26} & D_{66} \end{pmatrix} \begin{pmatrix} \frac{\partial^2 w}{\partial x^2} \\ \frac{\partial^2 w}{\partial y^2} \\ 2\frac{\partial^2 w}{\partial x \partial y} \end{pmatrix} + \begin{pmatrix} P^5_{1116} & P^4_{1216} & \bar{P}^5_{1216} & \bar{P}^4_{1116} \\ P^5_{1226} & P^4_{2226} & \bar{P}^5_{2226} & \bar{P}^4_{1226} \\ P^5_{1666} & P^4_{2666} & \bar{P}^5_{2666} & \bar{P}^4_{1666} \end{pmatrix} \begin{pmatrix} \frac{\partial \phi}{\partial x} \\ \frac{\partial \psi}{\partial y} \\ \frac{\partial \phi}{\partial y} \\ \frac{\partial \psi}{\partial x} \end{pmatrix} \tag{3.26}$$

The expressions for the resultant shear forces Q_x and Q_y can also be calculated by substituting Eq. (3.5) into Eq. (3.19). This results in the following:

$$\begin{pmatrix} Q_x \\ Q_y \end{pmatrix} = \begin{pmatrix} K_5 & 0 \\ 0 & K_4 \end{pmatrix} \begin{pmatrix} \phi \\ \psi \end{pmatrix}, \tag{3.27}$$

where the constants D_{ij}, $\bar{P}_{ijkl}$, P_{ijkl} and K_i, respectively, have been defined as

$$D_{ij} = \frac{2}{3}\left[B^{m+1}_{ij} h^3_{m+1} + \sum_{s=1}^{m} (h^3_s - h^3_{s+1}) B^s_{ij}\right] \tag{3.28}$$

$$P^n_{ijkl} = 2\left[B^{m+1}_{ij} \tilde{J}^{m+1}_{nnn} + B^{m+1}_{kl} \tilde{J}^{m+1}_{n45} + \tilde{B}^{m+1}_{k} C^{m+1}_{n} + \sum_{\alpha=1}^{m} (B^{\alpha}_{ij} \tilde{J}^{\alpha}_{nnn} + B^{\alpha}_{kl} \tilde{J}^{\alpha}_{n45} + \tilde{B}^{\alpha}_{k} C^{\alpha}_{n})\right] \tag{3.29}$$

$$\tilde{P}^n_{ijkl} = 2\left[B^{m+1}_{ij} \tilde{J}^{m+1}_{n45} + B^{m+1}_{kl} \tilde{J}^{m+1}_{nnn} + \sum_{\alpha=1}^{m} (B^{\alpha}_{ij} \tilde{J}^{\alpha}_{n45} + B^{\alpha}_{kl} \tilde{J}^{\alpha}_{nnn})\right] \tag{3.30}$$

$$K_n = 2\left\{B^{m+1}_{nn} h_{m+1}\left(\frac{h^2}{4} - \frac{h^2_{m+1}}{3}\right) + A^n_{m+1} h_{m+1} \sum_{\alpha=1}^{m} \left[B^{\alpha}_{nn} \tilde{J}^{\alpha}_n + A^n_{\alpha}(h_{\alpha} - h_{\alpha+1})\right]\right\} \quad (3.31)$$

$n = 4, 5;\ i, j, k, l = 1, 2, 6$, and where

$$J^i_{n\alpha\beta} = \left[B^i_{nn} a^i_{\alpha\beta} z^3\left(\frac{h^2}{12} - \frac{z^2}{30}\right) + \frac{z^3}{30} a^i_{\alpha\beta} A^n_i + \frac{z^2}{2} R^i_{n\alpha\beta}\right]\Bigg|_{h_i}^{h_{i-1}} \quad (3.32)$$

$$\tilde{J}^{m+1}_{n\alpha\beta} = B^{m+1}_{nn} a^i_{\alpha\beta} h^3_{m+1}\left(\frac{h^2}{12} - \frac{h^2_{m+1}}{30}\right) + \frac{h^3_{m+1}}{3} a^{m+1}_{\alpha\beta} A^n_{m+1} + \frac{h^2_{m+1}}{2} R^{m+1}_{n\alpha\beta} \quad (3.33)$$

$$C^{\alpha}_n = \left[\frac{B^{\alpha}_{nn}}{6} z^3\left(\frac{h^2}{4} - \frac{z^2}{5}\right) + \frac{z^3}{3} A^n_{\alpha} - \frac{z^2}{2} S^{\alpha}_{55}\right]\Bigg|_{h_{\alpha}}^{h_{\alpha-1}} \quad (3.34)$$

$$C^{m+1}_n = \frac{B^{m+1}_{nn}}{6} h^3_{m+1}\left(\frac{h^2}{4} - \frac{h^2_{m+1}}{5}\right) + \frac{h^3_{m+1}}{3} A^n_{m+1} - \frac{h^2_{m+1}}{2} S^{m+1}_{55} \quad (3.35)$$

$$\tilde{B}^{\alpha}_k = B^{\alpha}_{k1} a^{\alpha}_{13} + B^{\alpha}_{k2} a^{\alpha}_{23} + B^{\alpha}_{k6} a^{\alpha}_{63}, \quad k = 1, 2, 6 \quad (3.36)$$

$$\tilde{J}^{\alpha}_n = \left[z\left(\frac{h^2}{4} - \frac{z^2}{3}\right) + z A^n_{\alpha}\right]\Bigg|_{h_{\alpha}}^{h_{\alpha-1}}, \quad n = 4, 5 \quad (3.37)$$

3.5. Equations of Equilibrium

It is now appropriate to establish the relationships that express the equilibrium of a fundamental element of a composite plate. For linear static elasticity without body forces, the stress equations of motion at any point are given in

$$\frac{\partial \sigma_x}{\partial x} + \frac{\partial \tau_{xy}}{\partial y} + \frac{\partial \tau_{xy}}{\partial z} = 0 \quad (3.38a)$$

$$\frac{\partial \tau_{xy}}{\partial x} + \frac{\partial \sigma_y}{\partial y} + \frac{\partial \tau_{zy}}{\partial z} = 0 \quad (3.38b)$$

$$\frac{\partial \tau_{xz}}{\partial x} + \frac{\partial \tau_{yz}}{\partial y} + \frac{\partial \sigma_z}{\partial z} = 0 \qquad (3.38c)$$

These equations hold everywhere in the domain of interest. However, since by means of integrations through the thickness, the consideration of stresses has replaced consideration of stress resultants and couples, it is appropriate to alter the definition of the fundamental element of a composite plate accordingly. As shown in Figure 4 such an element extending throughout the thickness is acted upon by the internal stress resultants and couples defined in the preceding section. Therefore, the equilibrium equations of this element should be in terms of stress resultants and couples. Of the many procedures available for the derivation of the force equations of motion of a composite plate, the approach of direct integration of Eqs. (3.38) is chosen. By multiplying Eqs. (3.38a) and (3.38b) by the z coordinate and integrating them, respectively, accross the plate thickness, the two force equations of motion as given in Eqs. (3.39a) and (3.39b) are obtained. To derive the last equation, the evaluation of σ_z from the previous section is recalled. By integrating either Eq. (3.38c) or (3.20b) across the plate thickness and noting the condition that was stated in Eq. (3.1), the third equation of motion is obtained. Following these procedures, the results are

$$\frac{\partial M_x}{\partial x} + \frac{\partial M_{xy}}{\partial y} - Q_x = 0 \ , \qquad (3.39a)$$

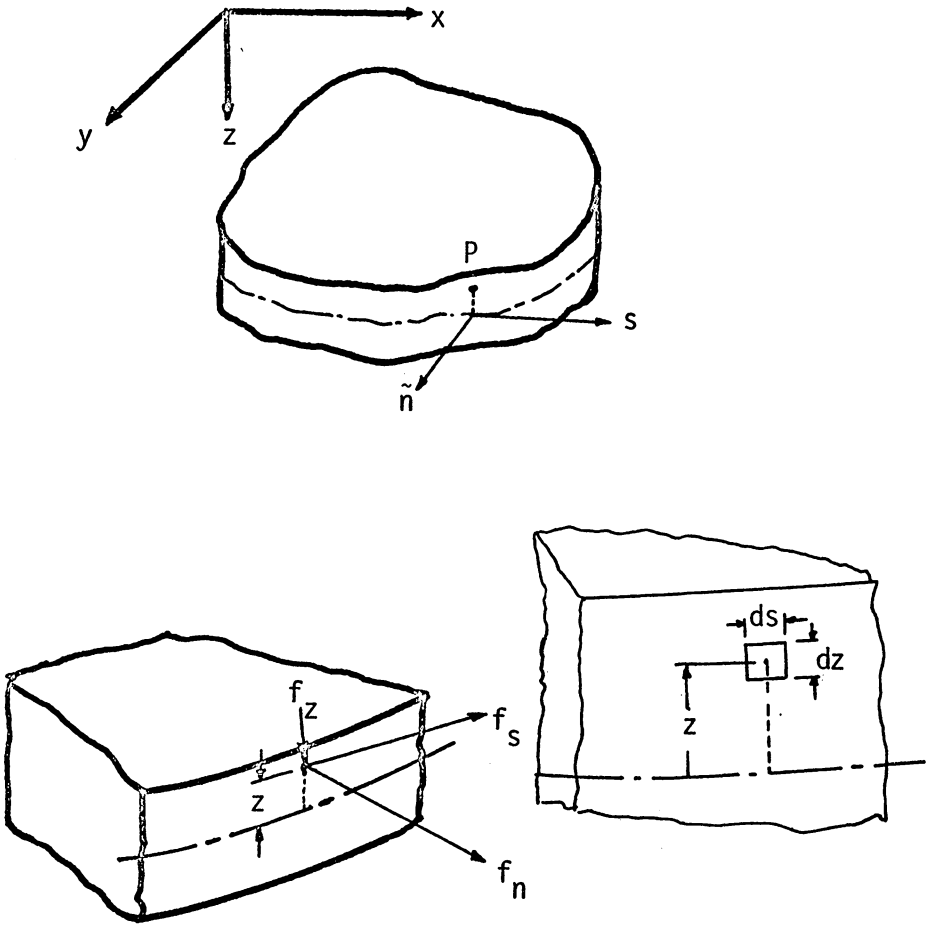

Figure 3. Boundary Element and Boundary Conditions

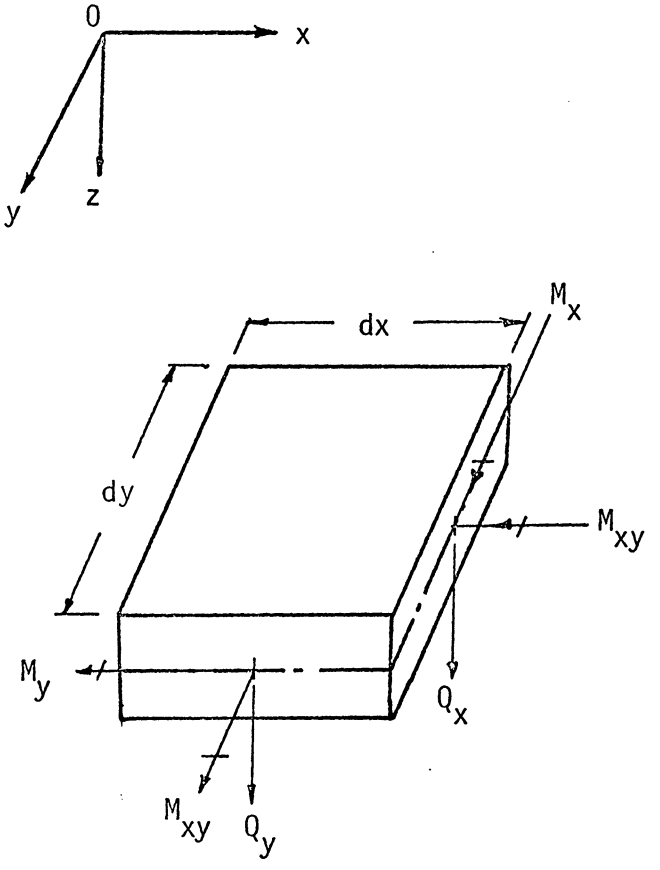

Figure 4. Nomenclature for Stress Resultants and Stress Couples

$$\frac{\partial M_{xy}}{\partial x} + \frac{\partial M_y}{\partial y} - Q_y = 0 \ , \qquad (3.39b)$$

$$\frac{\partial Q_x}{\partial x} + \frac{\partial Q_y}{\partial y} = 0 \ . \qquad (3.40)$$

This completes the derivation of the differential equations of motion in terms of stress resultants and couples. In fact, however, Eqs. (3.39) and (3.40) are not used directly, since it is desirable to obtain the solution in terms of the unknown functions w, ϕ, and ψ. Thus, the whole problem can be reduced to the solution of the governing equations for these three unknown functions. For this purpose, the stress resultants and couples given by Eqs. (3.26) and (3.27) are substituted into Eqs. (3.39) and (3.40). After some algebraic combinations and reductions the following governing differential equations are obtained.

$$D_{11}\frac{\partial^3 w}{\partial x^3} + 3D_{16}\frac{\partial^3 w}{\partial x^2 \partial y} + (D_{12} + 2D_{66})\frac{\partial^3 w}{\partial x \partial y^2} + D_{26}\frac{\partial^3 w}{\partial y^3} - P^5_{1116}\frac{\partial^2 \phi}{\partial x^2}$$
$$- (P^5_{1666} + \bar{P}^5_{1216})\frac{\partial^2 \phi}{\partial x \partial y} - \bar{P}^5_{2666}\frac{\partial^2 \phi}{\partial y^2} - \bar{P}^4_{1116}\frac{\partial^2 \psi}{\partial x^2}$$
$$- (\bar{P}^4_{1666} + P^4_{1216})\frac{\partial^2 \psi}{\partial x \partial y} - P^4_{2666}\frac{\partial^2 \psi}{\partial y^2} + K_5 \phi = 0$$

$$D_{16}\frac{\partial^3 w}{\partial x^3} + (D_{12} + 2D_{66})\frac{\partial^3 w}{\partial x^2 \partial y} + 3D_{26}\frac{\partial^3 w}{\partial x \partial y^2} + D_{22}\frac{\partial^3 w}{\partial y^3} - P^5_{1666}\frac{\partial^2 \phi}{\partial x^2}$$
$$- (\bar{P}^5_{2666} + P^5_{1226})\frac{\partial^2 \phi}{\partial x \partial y} - \bar{P}^5_{2226}\frac{\partial^2 \phi}{\partial y^2} - \bar{P}^4_{1666}\frac{\partial^2 \psi}{\partial x^2}$$

$$- (P^4_{2666} + \bar{P}^4_{1226}) \frac{\partial^2 \psi}{\partial x \partial y} - P^4_{2226} \frac{\partial^2 \psi}{\partial y^2} + K_4 \psi = 0$$

$$K_5 \frac{\partial \phi}{\partial x} + K_4 \frac{\partial \psi}{\partial y} = 0 \ . \qquad (3.41)$$

Now the problem has been reduced to the solution of the system of equations above for three functions w, ϕ, and ψ, which must also satisfy the appropriate boundary conditions.

3.6. Boundary Conditions

In addition to the governing differential equations, it is necessary to specify the boundary conditions in order to prescribe the problem fully. For convenience in later derivations, an arbitrary curvilinear boundary shape is considered as shown in Figure 3. The arc length s is measured along a neutral line from initial point s = 0 to a general point s, and its unit normal at that point is $\tilde{n}$. In general, either the displacements of the stresses on the boundaries can be specified. For the case of force-specified boundary conditions an infinitesimal element P, which is just above the point s, is considered. Acting on it is the state of stress: σ_x, σ_y, τ_{xy}, τ_{xz}, and τ_{yz}. If the specified infinitesimal forces per unit length f_n, f_s, f_z act on the element, then the force equilibrium conditions for this element can be written as

$$f_n ds = [\sigma_{xx} \cos(n, x) + \tau_{xy} \cos(n, y)] ds dz \qquad (3.42a)$$

$$f_s ds = [\tau_{xy} \cos(n, x) + \sigma_y \cos(n, y)]dsdz \qquad (3.42b)$$

$$f_z ds = [\tau_{xz} \cos(n, x) + \tau_{yz} \cos(n, y)]dsdz \qquad (3.42c)$$

As mentioned in the previous section, the consideration of stresses has been replaced with the consideration of stress resultants and couples. Therefore, it is appropriate to alter the form of Eqs. (3.42). If the integrals below are examined

$$\int_{-h/2}^{h/2} f_n z dz, \quad \int_{-h/2}^{h/2} f_s z dz, \quad \text{and} \quad \int_{-h/2}^{h/2} f_z dz,$$

it is quite obvious that the first integral becomes the applied normal moment $\bar{M}_n$, the second becomes the applied shear moment $\bar{M}_{ns}$, and the last becomes the shear force $\bar{Q}_n$. In light of these consequences, the boundary conditions in terms of stress resultants and couples can be derived by the integration of Eq. (3.42c) as well as Eqs. (3.42a and 3.42b) across the plate thickness after multiplying by the z coordinate. The definitions of stress resultants and couples given in Eq. (3.18 and Eq. (3.19) should also be recalled. These final considerations lead to the following

$$\bar{M}_n = M_x \cos(n, x) + M_{xy} \cos(n, y) , \qquad (3.43a)$$

$$\bar{M}_{ns} = M_{xy} \cos(n, x) + M_y \cos(n, y) , \qquad (3.43b)$$

$$\bar{Q}_n = Q_x \cos(n, x) + Q_y \cos(n, y) . \qquad (3.43c)$$

It should be noted that three boundary conditions as contrasted with two in classical laminated plate theory are required in the present theory.

IV. COMPLEX VARIABLE METHOD

4.1. Introduction

Eqs. (3.41) are recognized as the governing differential equations for multiple-layer, laminated plates. The coefficients D_{ij} and P^n_{ijkl} are constants but vary with different materials and geometries. Eqs. (3.41) are more general than those given in reference [13]. They include the normal stress and consider anisotropic rather than orthotropic materials.

No general solution of Eq. (3.41) is available at present, but some special problems have been solved, e.g., a simply supported plate undergoing cylindrical bending and the buckling of such a plate. The frequency equations for certain wave propagation problems have also been solved and are given in references [13], [14] and [8]. The problem of stress distribution near a hole has not been solved because it is a more complicated boundary value problem and requires a more general solution. Mathematical analysis to obtain a general solution is very difficult. Ambartsumyan attempted to solve these equations following the Lekhnitsky [21] approach of solving the generalized plane stress problem by introducing an auxiliary function (also called a generalized function). Thereby, the system of equations can be reduced and described by a single equation of higher order. In classical plate theory, this single differential equation is in the form of

$\sum a_{jk} \frac{\partial^{j+k} F}{\partial x^j \partial x^k}$, with $j + k = 4$. Its solution is shown to be a polyharmonic function. In the shear deformation theory, this reduced single differential equation becomes a sixth-order irreducible equation in the form of $\sum a_{jk} \frac{\partial^{j+k} F}{x^j x^k}$, with $j + k = 6$. This causes the problem to be very difficult to solve. Little data are given in the literature for the characteristics of this differential equation. So far, insufficient mathematical techniques are available to solve this equation. Further studies in this aspect are necessary. To date, only approximate numerical solutions of these equations have been obtained.

For the case of heterogeneous, isotropic laminated composite plates, the coefficients D_{ij} and P^n_{ijkl} can be reduced to a simple form in terms of the Young's modulus, Poission's ratio, and thickness of the plate. Thus, the system of Eqs. (3.41) can be reduced and simplified to a biharmonic equation and a Helmholtz equation. These, in turn, can be solved by analytical methods. At this point, instead of solving the general Eqs. (3.41), attention will be limited to the solution of the special equations for heterogenous isotropic medium since such a medium will provide a clear picture of the way stresses are transfered between the layers.

4.2. Heterogeneous Isotropic Composites

In the case of isotropic laminates, the stress-strain equations of the ith layer given in Eq. (3.10) are simply expressed

in the following form:

$$\begin{Bmatrix} \sigma_x \\ \sigma_y \\ \tau_{xy} \end{Bmatrix}_i = \begin{bmatrix} \frac{E}{1-\nu^2} & \frac{\nu E}{1-\nu^2} & 0 \\ \frac{\nu E}{1-\nu^2} & \frac{E}{1-\nu^2} & 0 \\ 0 & 0 & \frac{E}{2(1+\nu)} \end{bmatrix}_i \begin{Bmatrix} e_x \\ e_y \\ \gamma_{xy} \end{Bmatrix}_i \qquad (4.1)$$

$$\begin{Bmatrix} \tau_{xz} \\ \tau_{yz} \end{Bmatrix} = \begin{bmatrix} \frac{E}{2(1+\nu)} & 0 \\ 0 & \frac{E}{2(1+\nu)} \end{bmatrix}_i \begin{Bmatrix} \gamma_{xz} \\ \gamma_{yz} \end{Bmatrix}_i .$$

By recalling Eqs. (3.21), (3.22), and (3.36) as well as the definitions of K_4 and K_5 in the case of a heterogeneous isotropic composite plate, it can be seen that σ_z^i vanishes automatically. Thus σ_z^i does not appear in Eq. (4.1). Comparing Eq. (4.1) with (3.10) the following correlations are obtained:

$$B_{16} = B_{26} = B_{45} = 0, \quad B_{11} = B_{22} = \frac{E}{1-\nu^2}, \quad B_{12} = \frac{\nu E}{1-\nu^2},$$

$$B_5 = B_{44} = B_{66} = \frac{E}{2(1+\nu)} = \frac{1}{G}, \qquad (4.2)$$

where G is shear modulus and in association with the vanishing of σ_z ; $C_4 = C_5 = 0$.

For an isotropic medium, the values of A_i^n, $J_{\gamma\alpha\beta}^i$, and $R_{\gamma\alpha\beta}^i$ defined in Eqs. (3.6) and (3.7) become

$$J^i_{\gamma\alpha\beta} = 0, \quad R^i_{\gamma\alpha\beta} = 0, \ \gamma \neq \alpha \neq \beta,$$

$$J_\alpha = J^i_{\alpha\alpha\alpha} = \frac{z}{2}\left(\frac{h^2}{4} - \frac{z^2}{3}\right),$$

$$A_i = A^n_i = \sum_{\alpha=1}^{i-1} \frac{1}{2}\left(\frac{h^2}{4} - h^2_{\alpha+1}\right)\left[\frac{E^\alpha}{2(1+\nu^\alpha)} - \frac{E^{\alpha+1}}{2(1+\nu^{\alpha+1})}\right],$$

$$R^i = R^i_{nnn} = \sum_{i=1}^{m-i+1} [h_{j+1}(a^{i+1}A_{i+1} - a^i A_i)], \quad n = 4, 5 \qquad (4.3)$$

where $a^i = a^i_{44} = a^i_{55} = 1/G^i$. In the consideration of Eq. (4.3), the displacement functions u^i and v^i in Eqs. (3.15) and (3.16) are changed to the following forms:

$$u^i = -z\frac{\partial w}{\partial x} + \left[\frac{z}{2}\left(\frac{h^2}{4} - \frac{z^2}{3}\right) + z\frac{A_i}{G^i} + R^i\right]\phi,$$

$$v^i = -z\frac{\partial w}{\partial y} + \left[\frac{z}{2}\left(\frac{h^2}{4} - \frac{z^2}{3}\right) + z\frac{A_i}{G^i} + R^i\right]\psi. \qquad (4.4)$$

Now, the expressions for the stress resultants and couples for this case yield the following:

$$\begin{pmatrix} M_x \\ M_y \\ M_{xy} \end{pmatrix} = -\begin{pmatrix} D_{11} & D_{12} & 0 \\ D_{12} & D_{11} & 0 \\ 0 & 0 & D_{66} \end{pmatrix}\begin{pmatrix} \frac{\partial^2 w}{\partial x^2} \\ \frac{\partial^2 w}{\partial y^2} \\ 2\frac{\partial^2 w}{\partial x \partial y} \end{pmatrix} + \begin{pmatrix} P_{11} & P_{12} & 0 & 0 \\ P_{12} & P_{11} & 0 & 0 \\ 0 & 0 & P_{66} & P_{66} \end{pmatrix}\begin{pmatrix} \frac{\partial \phi}{\partial x} \\ \frac{\partial \psi}{\partial y} \\ \frac{\partial \phi}{\partial y} \\ \frac{\partial \psi}{\partial x} \end{pmatrix} \qquad (4.5)$$

$$\begin{pmatrix} Q_x \\ Q_y \end{pmatrix} = \begin{pmatrix} K & 0 \\ 0 & K \end{pmatrix} \begin{pmatrix} \phi \\ \psi \end{pmatrix} \tag{4.6}$$

where the constant D_{ij} is still in the form given in Eq. (3.26). However, the other expressions change as indicated below.

$$P_{ij} = P^n_{ijkl} = \tilde{P}^n_{ijkl} = 2(B^{m+1}_{ij}\,\tilde{J}^{m+1} + \sum_{\alpha=1}^{m} B^{\alpha}_{ij}\,\tilde{J}^{\alpha}) \ , \tag{4.7}$$

$$K = K_4 = K_5 = 2\left\{\frac{E^{m+1}h_{m+1}}{2(1+\nu^{m+1})}\left(\frac{h^2}{4} - \frac{h^2_{m+1}}{3}\right) + A_{m+1}h_{m+1}\right.$$

$$\left. + \sum_{\alpha=1}^{m}\left[\frac{E^{\alpha}}{2(1+\nu^{\alpha})}\,\tilde{\tilde{J}}^{\alpha} + A_{\alpha}(h_{\alpha} - h_{\alpha+1})\right]\right\} \tag{4.8}$$

$$\tilde{J}^{m+1} = \tilde{J}^{m+1}_4 = \tilde{J}^{m+1}_5 \equiv \tilde{\tilde{J}}^{m+1}_{nnn} = h^3_{m+1}\left(\frac{h^2}{12} - \frac{h^2_{m+1}}{30}\right) + \frac{h^3_{m+1}}{3}\frac{A_{m+1}}{G^{m+1}} + \frac{h^2_{m+1}}{2}R^{m+1} \tag{4.9}$$

$$\tilde{J}^{\alpha} = \left[z^3\left(\frac{h^2}{12} - \frac{z^2}{30}\right) + \frac{z^3}{3}\frac{A}{G^{\alpha}} + \frac{z^2}{2}R^{\alpha}\right]\Bigg|_{h_{\alpha}}^{h_{\alpha-1}} \tag{4.10}$$

In view of Eqs. (4.7) through (4.10) and (4.2), relationships between the material constants D_{ij} and P_{ij} can be determined as follows:

$$D_{11} - D_{12} = 2D_{66} \tag{4.11a}$$

and

$$P_{11} - P_{12} = 2P_{66} \ . \tag{4.11b}$$

With the aid of the results given above, the system of Eqs. (3.41) become

$$\frac{\partial}{\partial x}\left(D_{11}\frac{\partial^2 w}{\partial x^2} + D_{11}\frac{\partial^2 w}{\partial y^2}\right) - P_{11}\frac{\partial^2 \phi}{\partial x^2} - P_{66}\frac{\partial^2 \phi}{\partial y^2} - (P_{66}+P_{12})\frac{\partial^2 \psi}{\partial x \partial y} + k\phi = 0, \tag{4.12a}$$

$$\frac{\partial}{\partial y}\left(D_{11}\frac{\partial^2 w}{\partial x^2} + D_{11}\frac{\partial^2 w}{\partial y^2}\right) - (P_{66}+P_{12})\frac{\partial^2 \phi}{\partial x \partial y} - P_{66}\frac{\partial^2 \psi}{\partial x^2} - P_{11}\frac{\partial^2 \psi}{\partial y^2} + k\psi = 0, \tag{4.12b}$$

$$\frac{\partial \phi}{\partial x} + \frac{\partial \psi}{\partial y} = 0. \tag{4.12c}$$

Eqs. (4.12) are simpler than those of (3.41). These sets can be solved in several ways one of which, the complex variable method, is used for Eqs. (4.12). In order to do this, they must be reduced to such a form that the complex variable method can be employed.

4.3. Complex Variable Method

From Eq. (4.12c) note that a function χ can be defined such that it is satisfied identically.

$$\phi = -\frac{\partial \chi}{\partial y}, \quad \psi = \frac{\partial \chi}{\partial x}. \tag{4.13}$$

This new function is known as the stress function. Now, by substituting Eq. (4.13) and the relationships between the D_{ij} and P_{ij} given in Eq. (4.11), Eqs. (4.12a) and (4.12b) are altered to the forms

$$\frac{\partial}{\partial x}(D_{11}\nabla^2 w) + \frac{\partial}{\partial y}(-K\chi + P_{66}\nabla^2 \chi) = 0, \tag{4.14a}$$

$$\frac{\partial}{\partial y}(D_{11}\nabla^2 w) - \frac{\partial}{\partial x}(-K\chi + P_{66}\nabla^2 \chi) = 0, \tag{4.14b}$$

where ∇^2 is the two-dimensional Laplacian operator defined as

$$\nabla \equiv \frac{\partial^2}{\partial x^2} + \frac{\partial^2}{\partial y^2} .$$

In Eqs. (4.14), the quantities $D_{11}\nabla^2 w$ and $-K\chi + P_{66}\nabla^2\chi$ satisfy the Cauchy-Reimann conditions. Therefore, these two quantities are harmonic functions and conjugate to each other. Of several available ways to solve Eqs. (4.14), the complex variable analysis based on conformal mapping techniques will be used. Let the function χ be separated into two parts in such a way that

$$\frac{\partial \chi}{\partial x} = \frac{\partial \chi_o}{\partial x} + \frac{\partial \Phi}{\partial y} , \quad \frac{\partial \chi}{\partial y} = \frac{\partial \chi_o}{\partial y} - \frac{\partial \Phi}{\partial x} \qquad (4.15)$$

where Φ is a harmonic function that satisfies the Laplacian equation $\nabla^2\Phi = 0$, and the function χ_o is chosen to satisfy the Helmholtz equation below,

$$\nabla^2\chi_o - \frac{K}{P_{66}}\chi_o = 0 . \qquad (4.16)$$

It follows from Eqs. (4.15) and (4.16) that Eqs. (4.14) are separated into two parts; one is Eq. (4.16) and the other is given in the following form:

$$\frac{\partial}{\partial x}(D_{11}\nabla^2 w) = K\frac{\partial \Phi}{\partial x} ,$$

$$\frac{\partial}{\partial y}(D_{11}\nabla^2 w) = K\frac{\partial \Phi}{\partial y} . \qquad (4.17)$$

Obviously, Eq. (4.17) can be further simplified and reduced to a harmonic equation by eliminating the function Φ. The result is

$$\nabla^2(D_{11}\nabla^2 w) = 0 \ . \qquad (4.18)$$

Now the problem is reduced to the solution of the beharmonic Eq. (4.18) and the Helmholtz Eq. (4.16), as well as the harmonic function Φ through Eqs. (4.17). Therefore, the problem is solvable as long as solutions may be found for the biharmonic and Helmholtz equations. The biharmonic equation has been solved and its solution is given in the references [22], [31], and [20]. Expressed in terms of general functions the solution for w has the form

$$w = \bar{Z}\Omega(Z) + Z\,\bar{\Omega}(\bar{Z}) + \omega(Z) + \bar{\omega}(\bar{Z}) \qquad (4.19)$$

where Z is a complex variable defined as $x + iy$ and the $\bar{Z}$ is the conjugate of Z. (Note: the complex variable Z should not be confused with the coordinate Z in the x, y, z.) The functions $\Omega(Z)$ and $\omega(Z)$ are harmonic functions of a complex variable Z, and $\Omega(Z)$ and $\bar{\omega}(\bar{Z})$ are the conjugate functions of $\Omega(Z)$ and $\omega(Z)$, respectively. From Eqs. (4.17) and (4.19), the function Φ can be obtained in terms of $\Omega(Z)$. The result is

$$\Phi = -\frac{4D_{11}}{K}\left\{\bar{\Omega}'(\bar{Z}) + \Omega'(Z)\right\} \qquad (4.20)$$

where $\bar{\Omega}'(\bar{Z})$ is defined as $\frac{d\bar{\Omega}(\bar{Z})}{d\bar{Z}}$ and $\Omega'(Z)$ is defined as $\frac{d\Omega(Z)}{dZ}$. Recalling the identities

$$\frac{\partial}{\partial x} = \left(\frac{\partial}{\partial Z} + \frac{\partial}{\partial \bar{Z}}\right) \quad \text{and} \quad \frac{\partial}{\partial y} = i\left(\frac{\partial}{\partial Z} - \frac{\partial}{\partial \bar{Z}}\right), \qquad (4.21)$$

Eqs. (4.15) can be modified in terms of complex coordinates (Z and $\bar{Z}$) as follows.

$$\frac{\partial \chi}{\partial Z} = \frac{\partial \chi_o}{\partial Z} + i \frac{\partial \Phi}{\partial Z} ,$$

$$\frac{\partial \chi}{\partial \bar{Z}} = \frac{\partial \chi_o}{\partial \bar{Z}} - i \frac{\partial \Phi}{\partial \bar{Z}} . \qquad (4.22)$$

Integrating Eqs. (4.22) along with the value of Φ given in Eq. (4.20), the final results are obtained as follows,

$$\chi = \chi_o + i \frac{4D_{11}}{K} [\bar{\Omega}'(\bar{Z}) - \Omega'(Z)] . \qquad (4.23)$$

For convenience later in employing tensor notation, the complex coordinates (Z, $\bar{Z}$) are denoted as (Z^1, Z^2).

$$Z = x + iy = Z^1, \quad \bar{Z} = x - iy = Z^2 . \qquad (4.24)$$

The Cartesian coordinates x, y, and z will be denoted by x^1, x^2 and x^3, respectively. In this way, the stress resultants and stress couples in complex coordinates (Z^1, Z^2, X^3) may be evaluated from the stress resultants and stress couples in Cartesian coordinates (X^1, X^2, X^3) by the tensor transformation formula

$$T^{rS} = \frac{\partial Z^r}{\partial X^m} \frac{\partial Z^S}{\partial X^n} M^{mn} , \quad m, n, r, S = 1, 2, 3 \quad (4.25)$$

where T^{rS} are contravariant stress resultant components. Recall that in Cartesian coordinates covariant and contravariant tensor components are identical. Therefore, $M^{mn} = M_{mn}$, and M_{mn} are also the physical

stress resultants. Eq. (4.25) can also be written in expanded form as follows.

$$T^{11} = M_{11} - M_{22} + 2iM_{12} = M_{xx} - M_{yy} + 2iM_{xy}$$

$$T^{22} = M_{xx} - M_{yy} - 2iM_{xy}$$

$$T^{12} = M_{xx} + M_{yy}$$

$$T^{13} = Q_x + iQ_y$$

$$T^{23} = Q_x - iQ_y \qquad (4.26)$$

Now with the help of Eqs. (4.5), (4.6),(4.13), (4.19) and (4.23), Eqs. (4.26) can be written in terms of the complex potential functions $\Omega(Z)$ and $\omega(Z)$ and function χ_o in the following way.

$$T^{11} = 8\left\{iP_{66}\frac{\partial^2\chi_o}{\partial\bar{Z}^2} - D_{66}[Z\bar{\Omega}''(\bar{Z}) + \bar{\omega}(\bar{Z})]\right\} - \frac{32}{K}D_{11}P_{66}\bar{\Omega}'''(\bar{Z}),$$

$$T^{22} = 8\left\{-iP_{66}\frac{\partial^2\bar{\chi}_o}{\partial Z^2} - D_{66}[\bar{Z}\Omega''(Z) + \omega''(Z)]\right\} - \frac{32}{K}D_{11}P_{66}\Omega'''(Z),$$

$$T^{12} = -4(D_{11} + D_{22})[\Omega'(Z) + \bar{\Omega}'(\bar{Z})],$$

$$T^{13} = 2Ki\frac{\partial\chi_o}{\partial\bar{Z}} - 8D_{11}\bar{\Omega}''(\bar{Z}),$$

$$T^{23} = -2Ki\frac{\partial\bar{\chi}_o}{\partial\bar{Z}} - 8D_{11}\Omega''(Z). \qquad (4.27)$$

As for the displacements, $u^i + iv^i$ can also be expressed in terms of $w(Z)$ and χ through Eqs. (4.4) and (4.13), leading to the following results:

$$u^i + iv^i = -2Z \frac{\partial w}{\partial Z} + 2\left[\frac{z}{2}\left(\frac{h^2}{4} - \frac{z^2}{3}\right) + z \frac{A_i}{G^i} + R^i\right] i \frac{\partial \chi}{\partial Z} \quad (4.29a)$$

With the help of Eqs. (4.19) and (4.21), Eq. (4.29a) can be expressed in terms of $\Omega(Z)$, $w(Z)$, and χ_o as follows:

$$u^i + iv^i = -2Z[\Omega(Z) + Z\bar{\Omega}'(\bar{Z}) + \bar{\omega}'(\bar{Z})] + 2i\left[\frac{z}{2}\left(\frac{h^2}{4} - \frac{z^2}{3}\right)\right.$$

$$\left. + z \frac{A_i}{G^i} + R^i\right]\left[\frac{\partial \chi_o}{\partial \bar{Z}} + i \frac{4D_{11}}{K} \bar{\Omega}''(\bar{Z})\right] \quad (4.29b)$$

Up to this point, stress resultants and couples as well as the displacements have been expressed in the basic complex variable formulation. The conformal transformation is employed to extend the basic complex variable formulation to the transformed problem.

4.4. Conformal Transformation

The curvilinear coordinate system $(\xi, \eta,)$ with the ξ-curve and η-curve form an orthogonal system. Let its complex variables be defined as follows:

$$\zeta = \xi + i\eta, \quad \bar{\zeta} = \xi - i\eta. \quad (4.30)$$

Consider the transformation $Z = F(\zeta)$ which maps the points (ξ, η, z) of region R_ζ in the ζ-plane into points (x^1, x^2, x^3) of a region R_Z in the Z-plane of a rectangular cartesian coordinate

system. Now assume that

$$\frac{dZ}{d\zeta} = Je^{i\varepsilon} \tag{4.31}$$

where J and ε are real values. For convenience in later work, the coordinate system (ξ, η, z) is replaced by $(\theta_1, \theta_2, x^3)$, and its complex coordinate system $(\zeta, \bar{\zeta}, x^3)$ is replaced by (ζ^1, ζ^2, x^3). Then the square of a general line element in space is expressed as

$$dS^2 = dZd\bar{Z} + dx^3dx^3 = J^2(d\xi d\xi + d\eta d\eta) + dx^3dx^3 \ . \tag{4.32}$$

Therefore, the metric tensors g_{ij} and g^{ij} corresponding to θ_α-curves are obtained as

$$g_{11} = g_{22} = J^2, \quad g_{12} = g^{12} = 0, \quad \text{and } g^{11} = g^{22} = 1/J^2 \tag{4.33}$$

Now Eq. (4.25) can be expressed as

$$\Gamma^{rs} = \frac{\partial \zeta^r}{\partial \theta^m} \frac{\partial \zeta^s}{\partial \theta^n} M^{mn} \tag{4.34}$$

where the Γ^{rs} is denoted as the contravariant stress tensor in complex coordinates $(\zeta, \bar{\zeta}, z)$.

In the system (θ^1, θ^2) the contravariant tensor M^{nm} is not equal to M_{nm}, the physical stress tensor, but they are related by the following formula:

$$M_{mn} = \sqrt{g_{mn}/g^{mm}}\, M^{mn} \quad m, n = 1, 2, 3 \ . \tag{4.35}$$

From Eq. (4.33), Eq. (4.35) can be rewritten in expanded form as follows:

$$M_{\xi\xi} = J^2 M^{\xi\xi}, \quad M_{\eta\eta} = J^2 M^{\eta\eta}, \quad M_{\eta\xi} = J^2 M^{\eta\xi}, \quad Q_{\xi} = JQ^{\xi}, \quad Q_{\eta} = JQ^{\eta}. \tag{4.36}$$

The transformation from Γ^{rS} in coordinates (ζ^1, ζ^2, x^3) to the T^{rS} in coordinates (Z^1, Z^2, x^3) can be formulated by the tensor transformation law; it is given in the following form:

$$T^{rS} = \frac{\partial Z^r}{\partial \zeta^m} \frac{\partial Z^S}{\partial \zeta^n} \Gamma^{mn} . \tag{4.37}$$

By means of Eq. (4.31), Eq. (4.37) becomes

$$T^{11} = J^2 e^{2i\varepsilon} \Gamma^{11}, \quad T^{22} = J^2 e^{-2i\varepsilon} \Gamma^{22}, \quad T^{12} = J^2 \Gamma^{12},$$

$$T^{13} = Je^{i\varepsilon} \Gamma^{13}, \quad T^{23} = Je^{-i\varepsilon} \Gamma^{23} . \tag{4.38}$$

Now from Eqs. (4.34) and (4.36) the Γ^{rS} in terms of the physical stress resultant component referred to ξ, η-curves are given as follows:

$$\Gamma^{11} = (M^{\xi\xi} - M^{\eta\eta} + 2iM^{\xi\eta}) = J^{-2}(M_{\xi\xi} - M_{\eta\eta} + 2iM_{\eta\xi}) ,$$

$$\Gamma^{22} = J^{-2}(M_{\xi\xi} - M_{\eta\eta} - 2iM_{\xi\eta}) ,$$

$$\Gamma^{12} = J^{-2}(M_{\xi\xi} + M_{\eta\eta}) ,$$

$$\Gamma^{13} = J^{-1}(Q_{\xi} + iQ_{\eta}) ,$$

$$\Gamma^{23} = J^{-1}(Q_{\xi} - iQ_{\eta}) . \qquad (4.39)$$

Comparing Eqs. (4.38) and (4.39) yields the following useful expressions, which transform the stress components in Cartesian coordinates (x, y, z) to the curvilinear coordinates (ξ, η, z). These transformation equations are

$$M_{\xi\xi} - M_{\eta\eta} + 2iM_{\xi\eta} = e^{-2i\epsilon}\{M_{xx} - M_{yy} + 2iM_{xy}\} ,$$

$$M_{\xi\xi} - M_{\eta\eta} - 2iM_{\xi\eta} = e^{2i\epsilon}\{M_{xx} - M_{yy} - 2iM_{xy}\} ,$$

$$M_{\xi\xi} + M_{\eta\eta} = M_{xx} + M_{yy} ,$$

$$Q_{\xi} + iQ_{\eta} = e^{-i\epsilon}\{Q_x + iQ_y\} ,$$

$$Q_{\xi} - iQ_{\eta} = e^{i\epsilon}\{Q_x - iQ_y\} . \qquad (4.40)$$

Now the stress components $M_{\xi\xi}$, $M_{\eta\eta}$, $M_{\xi\eta}$, Q_{ξ}, and Q_{η} in curvilinear coordinates (ξ, η, z) can be expressed in terms of complex potential functions $\Omega(Z)$, $\omega(Z)$ and function χ_0 by substituting Eqs. (4.27)

into (4.40) and noting the definition of ζ and $\bar{\zeta}$ given in Eq. (4.30); the results are

$$M_{\xi\xi} - M_{\eta\eta} + 2iM_{\xi\eta} = e^{-2i\varepsilon}\left\{8\left[\left[iP_{66}\frac{\partial^2\chi_o}{\partial\bar{\zeta}^2} - D_{66}[\zeta\bar{\Omega}''(Z) + \bar{\omega}''(\bar{Z})]\right]\right]\right.$$

$$\left. - \frac{32}{K}D_{11}P_{66}\bar{\Omega}'''(\bar{Z})\right\}$$

$$M_{\xi\xi} + M_{\eta\eta} = -4(D_{11} + D_{12})\left[\frac{\Omega'(\zeta)}{F'} + \frac{\bar{\Omega}'(\bar{\zeta})}{\bar{F}'}\right]$$

$$Q_\xi + iQ_\eta = 2K_i\frac{\partial\chi_o}{\partial\bar{\zeta}} - 8D_{11}\bar{\Omega}''(\bar{Z}) \qquad (4.41)$$

where F' is defined as $dF/d\zeta$ and $\bar{F}'$ is a conjugate function of F'. $M_{\xi\xi} - M_{\eta\eta} - 2iM_{\xi\eta}$ and $Q_\xi - iQ_\eta$ are the conjugate functions of $M_{\xi\xi} - M_{\eta\eta} + 2iM_{\xi\eta}$ and $Q_\xi + iQ_\eta$, respectively. $\Omega''(Z)$, $\omega''(Z)$, and $\Omega'''(Z)$ are defined as

$$\Omega''(Z) = \Omega''(\zeta)\left(\frac{d\zeta}{d\bar{Z}}\right)^2 + \Omega'(\zeta)\left(\frac{d^2\zeta}{dZ^2}\right)\left(\frac{d\zeta}{dZ}\right),$$

$$\omega''(Z) = \omega''(\zeta)\left(\frac{d\zeta}{dZ}\right)^2 + \omega'(\zeta)\left(\frac{d^2\zeta}{dZ^2}\right)\left(\frac{d\zeta}{dZ}\right),$$

$$\Omega'''(Z) = \Omega'''(\zeta)\left(\frac{d\zeta}{d\bar{Z}}\right)^3 + 3\Omega''(\zeta)\left(\frac{d^2\zeta}{dZ^2}\right)\left(\frac{d\zeta}{dZ}\right)^2$$

$$+ \Omega'(\zeta)\left(\frac{d\zeta}{d\bar{Z}}\right)\left[\left(\frac{d^2\zeta}{dZ^3}\right) + \left(\frac{d^2\zeta}{dZ^2}\right)^2\right] \qquad (4.42)$$

4.5. Boundary Conditions

In the preceding chapter the boundary conditions on an arbitrary curve S are given by Eq. (3.40) or (3.39). However, in this analysis it is preferable to express them in terms of complex coordinates $(Z, \bar{Z})$. Suppose that an infinitesimal element is cut off from the edge contour S, and the shear forces Q_x, Q_y and stress couples M_x, M_y, and M_{xy} are acting on this element in positive directions as shown in Figure 4. Then the moment about the x- and y-axes can be written as

$$dL = -M_y dx - M_{xy} dy + yQ_y dx + yQ_x dy$$

$$dL' = M_x dy + M_{xy} dx - xQ_x dy - xQ_y dx \qquad (4.43)$$

where L and L' are the components of the couple $\bar{M}$ about the x- and y-axes, respectively. dL and dL' represent the differential quantities. x and y are the coordinates of an arbitrary point on the contour, which is considered a function of the arc length s taken from a certain initial point to that point. The integral of Eq. (4.43) with respect to the arc length s from a certain initial point (say s = 0) to the variable point s has the following form:

$$L = \int_s \{-M_y dx - M_{xy} dy + yQ_y dx + yQ_x dy\} ,$$

$$L' = \int_s \{M_x dy + M_{xy} dx - xQ_x dy - xQ_y dx\} . \quad (4.44)$$

Let $\vec{e}_1$ and $\vec{e}_2$ be the base vectors in coordinates (x, y) and $\vec{a}_1$ and $\vec{a}_2$ be the base vectors in complex coordinates $(Z, \bar{Z})$; therefore, the transformation between the $\vec{e}_i$ and $\vec{a}_i$ is

$$\vec{a}_1 = \frac{\partial Z}{\partial x}\vec{e}_1 + \frac{\partial Z}{\partial y}\vec{e}_2, \quad \vec{a}_2 = \frac{\partial \bar{Z}}{\partial x}\vec{e}_1 + \frac{\partial \bar{Z}}{\partial y}\vec{e}_2 . \quad (4.45)$$

From Eqs. (4.24) and (4.45), $\vec{e}_1$ and $\vec{e}_2$ can be evaluated in terms of $\vec{a}_1$ and $\vec{a}_2$ as

$$\vec{e}_1 = \frac{1}{2}(\vec{a}_1 + \vec{a}_2), \quad \vec{e}_2 = -\frac{i}{2}(\vec{a}_1 + \vec{a}_2) . \quad (4.46)$$

As usual, the couple $\vec{M}$ can be expressed either in Cartesian coordinates (x, y) or in complex coordinates $(Z, \bar{Z})$ through Eq. (4.46). That is,

$$\vec{M} = L\vec{e}_1 - L'\vec{e}_2 = \frac{1}{2}(L + iL')\vec{a}_1 + \frac{1}{2}(L - iL')\vec{a}_2 . \quad (4.47)$$

By using Eq. (4.44) and the expressions for T^{rS} in Eq. (4.26), after some algebraic combinations and reductions Eq. (4.47) is transformed to the following expression

$$\vec{M} = \vec{m}\vec{a}_1 + \bar{m}\vec{a}_2,$$

and where

$$m = -\frac{1}{2}\int_S [(T^{12} - ZT^{23})d\bar{Z} - (T^{11} - ZT^{13})dZ] \quad (4.48)$$

where $\bar{m}$ is the conjugate function of m. If the boundary is along the contour where Z is a constant line and the moment along this edge is denoted by m_c, then

$$m_c = -\frac{1}{2}\int_S [(T^{12} - ZT^{23})d\bar{Z} - (T^{11} - ZT^{13})dZ]. \quad (4.49)$$

Thus, Eqs. (3.43a) and (3.43b) are then replaced by one Eq. (4.49) in the present analysis. Similarly, the last Eq. (3.43c) can also be expressed in terms of χ or χ_o and function $\Omega(Z)$, by substituting Q_x and Q_y given in Eqs. (4.6) and (4.13), and by writing cos(n, x) and cos(n, y) in terms of the arc length s of the contour in the following form:

$$\cos(n, x) = \frac{dy}{dS},$$

$$\cos(n, y) = \frac{dx}{dS}.$$

This leads to

$$\bar{Q}_n dS = -K d\chi \quad (4.50a)$$

The integral of Eq. (4.50a) along the arc length s, as with the moment, is given by

$$F_Z = -K\chi = -K\chi_o - 4D_{11}i[\bar{\Omega}'(\bar{Z}) - \Omega'(Z)] \qquad (4.50)$$

where F_Z is the specified shear force on the boundary. Similarly, m_c can be expressed in terms of functions $\Omega(Z)$ and $\chi(Z)$ by substituting the Eq. (4.27) into Eq. (4.49). After some manipulations the final form is obtained as follows:

$$m_c = -2(3D_{11} + D_{12})\Omega(Z) + 4D_{66}\bar{\omega}'(\bar{Z}) + 4D_{11}Z\Omega'(Z) - 2(D_{11} + D_{12})Z\Omega'(Z)$$

$$+ \frac{16}{K} D_{11}P_{66}\bar{\Omega}''(\bar{Z}) + iKZ\chi_o - 4P_{66}i \frac{\partial \chi_o}{\partial \bar{z}} \qquad (4.51)$$

Eqs. (4.50) and (4.51) are the two boundary conditions in this analysis in contrast to the one boundary condition for classical plate theory [5],[21] when the complex variable method is used.

Now consider a composite plate containing an unstressed hole loaded by uniform force or moment on the boundary, then the shear force F_z and moment m_c vanish at the hole boundary. For this case, then Eq. (4.50b) becomes

$$\chi_o + i \frac{4D_{11}}{K}[\bar{\Omega}'(\bar{Z}) - \Omega'(Z)] = 0 . \qquad (4.52)$$

Multiplying Eq. (4.52) by iKZ and replacing the term $iKZ\chi_o$ in Eq. (4.51) with $4D_{11}Z[\bar{\Omega}'(\bar{Z}) - \Omega'(Z)]$, an expression of Eq. (4.51) is obtained as follows:

$$-2(3D_{11} + D_{12})\Omega(Z) + 4D_{66}[\bar{\omega}'(\bar{Z}) + Z\bar{\Omega}'(\bar{Z})] + \frac{16}{K} D_{11}P_{66}\bar{\Omega}''(\bar{Z})$$

$$- 4P_{66}i \frac{\partial \chi_o}{\partial Z} = 0. \qquad (4.53)$$

Now the problem has been reduced to simply seeking harmonic functions $\Omega(Z)$ and $\omega(Z)$, and a function χ_o which satisfies the Helmholtz Eq. (4.16). These functions must satisfy the boundary conditions (4.52) and (4.53) at the hole edge as well as (4.50) and (4.51) at the outer boundary.

In addition to the aforementioned requirements, these functions should provide single-valued stresses and displacements within the deformed region. In the following section the properties of the complex potential functions $\Omega(Z)$ and $\omega(Z)$ and the function χ_o, which will ensure meeting the criterion mentioned above are discussed.

4.6. Complex Functions $\Omega(Z)$ and $\omega(Z)$

If the complex function $\Omega(Z)$ is replaced by $\Omega(Z) + icZ + \alpha + i\beta$, and $\omega(Z)$ is replaced by $\omega(Z) + (\alpha' + i\beta')Z + \alpha'' + i\beta''$, where α, α', β, β', α'', β'' and c are real constants, then the stress system given by Eq. (4.27) is unaltered, but from (4.19) and (4.29), the displacements w and u + iv become

$$w = \text{original } w - (\alpha + \alpha' - i\beta + i\beta')Z - (\alpha + \alpha' + i\beta - i\beta')\bar{Z} - 2\alpha'' \tag{4.54}$$

and

$$u^i + v^i = \text{original } (u^i + v^i) + 2(\alpha + \alpha' + i\beta - i\beta') \, . \tag{4.55}$$

The additional displacement represents a rigid body motion of the whole plate. Excluding the terms which represent rigid-body motion, it is discovered that the constants c and β'' can be chosen arbitrarily since they do not affect the stresses and displacements. Usually these constants are considered to be zero.

From references [22] and [31] it is seen that any holomorphic function (a function that is analytic at every point of a region R is called a holomorphic function in R) is a solution of the Laplacian equation. Therefore, in nature numerous forms of the holomorphic function may be chosen. However, the selection of the function is based completely on the boundary conditions, loading conditions, and the geometric shape of the plate. If an infinite plate containing an unstressed hole bent by a uniform moment at infinity is considered, then the selected complex potential functions $\Omega(Z)$ and $\omega(Z)$, as suggested in references [22] and [31], are given in the following form:

$$\Omega(Z) = BZ + \frac{B_1 + iB_2}{D_{11}Z} + O(1/Z^2),$$

$$\omega(Z) = \frac{1}{2}(\alpha_2 + i\beta_2)Z^2 + K'\ln Z + \frac{\alpha_4 + i\beta_4}{D_{11}Z^2} + O(1/Z^3). \qquad (4.56)$$

In Eq. (4.56) the rigid-body motion has already been excluded. If M_1, M_2 are the applied principal stress couples at infinity and α is the angle between M_1 and the x-axis, then χ_0 and its derivatives vanish at infinity. From Eqs. (4.50b) and (4.51) at infinity, the constants B and $(\alpha_2 - i\beta_2)$ are obtained in the following form:

$$M_1 + M_2 = -8(D_{11} + D_{12})B,$$

$$(M_1 - M_2)e^{-2i\alpha} = -4(D_{11} - D_{12})(\alpha_2 - i\beta_2) . \qquad (4.57)$$

Thus, Eq. (4.56) becomes

$$\Omega(Z) = -\frac{(M_1 + M_2)}{8(D_{11} + D_{12})} Z + \frac{(B_1 + iB_2)}{D_{11} Z},$$

$$\omega(Z) = -\frac{(M_1 - M_2)e^{-2i\alpha}}{8(D_{11} - D_{12})} Z^2 + K\ln Z + \frac{(\alpha_4 + i\beta_4)}{D_{11}Z^2}. \qquad (4.58)$$

The remaining constants are determined from the inner boundary condition at the hole edge and are discussed later.

Examining Eq. (4.56), it is seen that the complex potential function consists of two parts: the first will provide the stresses at infinity through the terms BZ in $\Omega(Z)$ and $\frac{1}{2}(\alpha_2 + i\beta_2)Z^2$ in $\omega(Z)$,

and the others will provide zero stresses at infinity. The terms that will provide bounded stresses at infinity will be denoted by $\Omega_0(Z)$, $\omega_0(Z)$, respectively. Taking $\Omega(Z) = \Omega_0(Z)$ and $\omega(Z) = \omega_0(Z)$ and resubstituting these new functions into Eq. (4.27) a result is obtained that is the same as the plate under bending stresses without a hole. Therefore, functions $\Omega_0(Z)$ and $\omega_0(Z)$ are referred to as the bending state of stress of the plate. The remaining terms in Eq. (4.58) are referred to as the local stress state due to the presence of a hole of any shape in the plate.

Generally, in Eq. (4.58) terms to any high order may be used. However, from the function χ_0 and the boundary conditions, it is discovered that only the constants K', B_1, B_2, α_4, and β_4 have non-zero values. Therefore, the form given in Eq. (4.58) does not lose its generality.

4.7. Function χ_0

As mentioned in section 4.5, the function χ_0 is a solution of the Helmholtz equation. Upon examining the Helmholtz Eq. (4.16), it is seen that a different type of function χ_0 will be obtained for different coordinate systems. Therefore, the basic difficulty of this problem in comparison with the corresponding problem of the classical Kirchhoff theory, is the necessity of solving the Helmholtz equation in which the variables are separated for different coordinate systems. For the sake of convenience in analysis, the following three cases are considered: circular hole, elliptical hole, and an arbitrarily shaped hole.

V. SOLUTIONS FOR CIRCULAR AND ELLIPTICAL HOLES

5.1. Circular Hole Case

In this section, consider the case of a circular hole extending through a laminated, composite plate of infinite extent with the hole located at the origin of rectangular coordinates (xoy). A uniform bending moment is applied on the edge of the plate away from the hole. For the analysis in the vicinity of the circular hole a polar coordinate system (R, θ) is used. Its origin is chosen, as indicated in Figure 5, at the same origin as the rectangular coordinates - xoy. By using the conventional coordinate transformations Eq. (4.16) may be expressed in the polar coordinates in the following form:

$$\nabla^2 \chi_o - \frac{K}{P_{66}} \chi_o = 0, \text{ and } \nabla^2 = \frac{\partial^2}{\partial R^2} + \frac{\partial}{R\partial R} + \frac{\partial^2}{R^2 \partial \theta^2} . \qquad (5.1)$$

Eq. (5.1) is a second-order partial differential equation. Its solution is given as follows:

$$\chi_o = [(C_1' + iC_2')e^{2i\theta} + (c_1' - ic_2')e^{-2i\theta}][dK_2(\lambda R) + d'I_2(\lambda R)] \qquad (5.2)$$

where $\lambda = (K/P_{66})^{1/2}$, and C_1', C_2', d and d' all are real constants. $K_2(\lambda R)$ and $I_2(\lambda R)$ are modified Bessel functions of the second kind. $I_2(\lambda R)$ is bounded but $K_2(\lambda R)$ tends to be infinity as $R \to 0$. On the

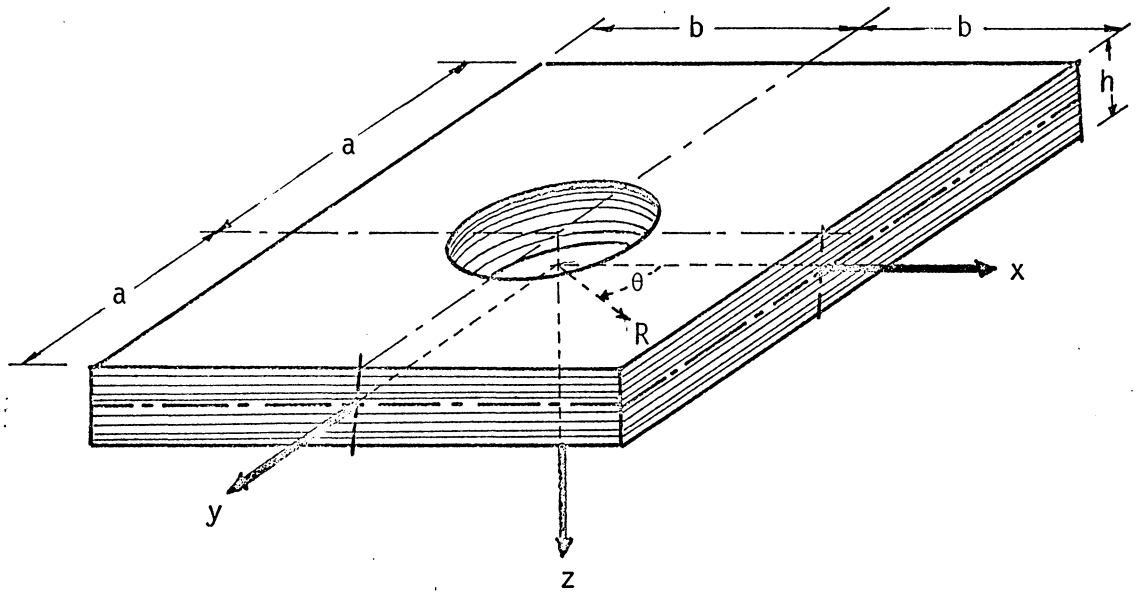

Figure 5. Configuration of Laminated Composite Plate With Circular Hole

other hand, $I_2(\lambda R)$ tends to be infinite and $K_2(\lambda R)$ tends to be zero as $R \to \infty$. In order to satisfy the boundary conditions at infinity, the function $I_2(\lambda R)$ must be dropped. This is done by choosing the constant d' to be zero. Eq. (5.2) then becomes

$$\chi_o = [(C_1 + iC_2)e^{2i\theta} + (C_1 - iC_2)e^{-2i\theta}]K_2(\lambda R) \quad (5.3)$$

where $c_1'd$ and $c_2'd$ are absorbed in new real constants C_1 and C_2, respectively. These two constants will be determined from the boundary conditions.

From Figure 5 the complex coordinates $(Z, \bar{Z})$ and polar coordinates (R, θ) are related by $Z = x + iy = Re^{i\theta}$, and $\bar{Z} = x - iy = Re^{-i\theta}$. Their differential operators, $\frac{\partial}{\partial \bar{Z}}$ and $\frac{\partial}{\partial Z}$, then have the following forms.

$$\frac{\partial}{\partial \bar{Z}} = \frac{1}{2}\left(\frac{\partial}{\partial R} + i\,\frac{\partial}{R\partial\theta}\right)e^{i}\ , \quad \frac{\partial}{\partial Z} = \frac{1}{2}\left(\frac{\partial}{\partial R} - i\,\frac{\partial}{R\partial\theta}\right)e^{-i\theta}. \quad (5.4)$$

In addition, the recurrence relations for $K_n(\lambda R)$ which will be used in later calculations are given as

$$K_n'(\lambda R) = -K_{n-1}(\lambda R) - \frac{n}{\lambda R} K_n(\lambda R)$$

where

$$K_n'(\lambda R) \quad \frac{dK_n(\lambda R)}{d(\lambda R)}\ . \quad (5.5)$$

Obviously, once the functions χ_o, $\Omega(Z)$ and $\omega(Z)$ are determined,

the problem is solved. Then there remains the task of determining the constants C_1, C_2, B_1, B_2, α_4, β_4, and K' from the boundary condition.

Substituting the function χ_0 as given in Eq. (5.3) and functions $\Omega(Z)$ and $\omega(Z)$ as given in Eq. (4.58) into the boundary conditions (4.52) and (4.53) at the hole edge (R = a), the following algebraic equations are obtained:

$$K_2(\lambda a)(C_1 + iC_2) - \frac{4i}{a^2K}(B_1 - iB_2) = 0, \qquad (5.6a)$$

$$(M_1 + M_2)a^2 + 4(D_{11} - D_{12})K' = 0, \qquad (5.6b)$$

$$- \frac{2(3D_{11} + D_{12})}{D_{11}a^2}(B_1 + iB_2) - \frac{(M_1 - M_2)}{2} e^{2i\alpha}$$

$$+ iK(C_1 - iC_2)[K_2(\lambda a) - K_0(\lambda a)] = 0, \qquad (5.6c)$$

$$- \frac{4(D_{11} - D_{12})}{KD_{11}a^4} (\alpha_4 - i\beta_4) + \left(\frac{32D_{11}}{\lambda^2 a^3} - \frac{4D_{66}}{D_{11}a}\right) \frac{B_1 - iB_2}{Ka}$$

$$+ i(C_1 + iC_2)\left[\frac{8}{\lambda^2 a^2} K_2(\lambda a) + K_2(\lambda a) - K_0(\lambda a)\right] = 0 \qquad (5.6d)$$

Replacing "i" in the expressions above with "-i", there arises three conjugate expressions for Eqs. (5.6a), (5.6b) and (5.6d),

respectively. Therefore the system of Eqs. (5.6) represent seven equations for seven constants - C_1, C_2, B_1, B_2, α_4, β_4, and K'. Solving these seven equations for the seven constants gives

$$K' = - \frac{M_1 + M_2}{4(D_{11} - D_{12})} a^2 ,$$

$$B_1 + iB_2 = - \frac{D_{11}(M_1 - M_2)a^2 e^{2i\alpha} K_2(\lambda a)}{4[(D_{11} + D_{12})K_2(\lambda a) + 2D_{11}K_0(\lambda a)]} ,$$

$$C_1 + iC_2 = - \frac{iD_{11}(M_1 - M_2)e^{-2i\alpha}}{K[(D_{11} + D_{12})K_2(\lambda a) + 2D_{11}K_0(\lambda a)]} ,$$

$$\alpha_4 + i\beta_4 = \frac{(M_1 - M_2)a^3 e^{-2i\alpha}}{2(D_{11} - D_{12})[(D_{11} + D_{12})K_2(\lambda a) + 2D_{11}K_0(\lambda a)]}$$

$$[8P_{66}D_{11}(1 + D_{11})K_2(\lambda a) - 4a^2K(D_{11} + D_{66})K_2(\lambda a) + 4KD_{11}a^2K_0(\lambda a)] \quad (5.7)$$

From Eqs. (4.41) and (4.29) with functions χ_0, $\Omega(Z)$, and $\omega(Z)$ given by Eqs. (4.58) and (5.3), and the constants given by Eqs. (5.7), the solutions for the displacements and stresses are sought. However, for this problem, of primary interest is the distribution of stresses around a hole edge. This information may be obtained directly from

Eqs. (4.27). That is, $T^{12} = M_x + M_y = M_R + M_\theta$. Since the quantity M_R at the hole edge is equal to zero, the only non-zero term is M_θ. Therefore, by calculating the T^{12} term and setting R = a, gives M_θ at a hole edge as follows:

$$M_\theta = (M_1 + M_2) - \frac{2(D_{11} + D_{12})(M_1 - M_2)K_2(\lambda a)}{(D_{11} + D_{12})K_2(\lambda a) + 2D_{11}K_o(\lambda a)} \cos 2(\theta - \alpha). \tag{5.8}$$

Also from Eqs. (4.27), the shear forces Q_R and Q_θ can be calculated. The results are given in the following form,

$$Q_R = \frac{4D_{11}(M_1 - M_2)}{[(D_{11} + D_{12})K_2(\lambda a) + 2D_{11}K_o(\lambda a)]} \left[\frac{a^2}{R^3} K_2(\lambda a) - \frac{1}{R} K_2(\lambda R)\right] \cos 2(\theta - \alpha) \tag{5.9}$$

and

$$Q_\theta = \frac{4D_{11}(M_1 - M_2)}{[(D_{11} + D_{12})K_2(\lambda a) + 2D_{11}K_o(\lambda a)]} \left[\frac{a^2}{R^3} K_2(\lambda a) - \frac{1}{R} K_2(\lambda R) - \frac{\lambda}{2} K_1(\lambda R)\right]$$

$$\sin 2(\theta - \alpha). \tag{5.10}$$

Setting R = a in Eq. (5.10) gives the shear force, Q_θ, distribution around the edge of a circular hole as

$$Q_\theta = - \frac{2D_{11}(M_1 - M_2)\, K_1(\lambda a)}{[(D_{11} + D_{11})K_2(\lambda a) + 2D_{11}K_o(\lambda a)]} \sin 2(\theta - \alpha) \tag{5.11}$$

By different combinations of bending moments M_1 and M_2 and angle α, several types of loading are specified. Several examples follow. (Case 1) - taking $\alpha = 0 = M_2 = 0$ and $M_1 = M_0$, gives the case of a uniform bending moment acting along the edge x = constant. (Case 2) - taking $\alpha = 0 = M_1 = 0$, $M_2 = M_0$ gives the case of uniform bending moment acting along the edge y = constant. (Case 3) - taking $\alpha = 0$, $M_1 = -M_0$, $M_2 = M_0$ gives the case of uniform twisting of the plate along rectangular edges. Here for brevity, case 1 is selected as an illustrative example. Letting $\alpha = M_2 = 0$, $M_2 = M_0$ in Eqs. (5.8) and (5.11) and defining M_θ/M_0 as SCF*, Q_θ/M_0 as SCQ**; yields the following for SCF and SCQ.

$$SCF = 1 - \frac{2(D_{11} + D_{12})K_2(\lambda a)}{(D_{11} + D_{12})K_2(\lambda a) + 2D_{11}K_0(\lambda a)} \cos 2\theta, \qquad (5.12a)$$

$$SCQ = - \frac{2D_{11}\lambda K_1(\lambda a)}{(D_{11} + D_{12})K_2(\lambda a) + 2D_{11}K_0(\lambda a)} \sin 2\theta. \qquad (5.12b)$$

Examining Eqs. (5.12) it is seen that the SCF will have a maximum value when the angle θ is 90°; however, the SCQ will have a maximum value when the angle θ is 45°. For future reference, the maximum values for SCF and SCQ are given as follows:

---

* SCF is a stress concentration factor for the bending moment.

**SCF is a stress concentration factor for the transverse shear force.

$$\frac{M_\theta(a, 90°)}{M_o} = 1 + \frac{2(D_{11} + D_{12})K_2(\lambda a)}{(D_{11} + D_{12})K_2(\lambda a) + 2D_{11}K_o(\lambda a)} \qquad (5.13)$$

and

$$\frac{Q_\theta\left(a, \frac{\pi}{4}\right)}{M_o} = - \frac{2D_{11}\lambda K_1(\lambda a)}{(D_{11} + D_{12})K_2(\lambda a) + 2D_{11}K_o(\lambda a)} \qquad (5.14)$$

To compare the results with Reissner's solutions, the laminated composite plate is degenerated to a single-layer plate. Thus, the values of D_{11}, D_{12}, and λ for this case may be evaluated from Eqs. (4.7), (4.8), (4.9) and (3.24). The final results are given as follows:

$$D_{11} = \frac{2Eh^3}{3(1 - \nu^2)}, \quad D_{12} = \frac{2\nu Eh^3}{3(1 - \nu^2)}, \quad \text{and } \lambda = \left(\frac{10}{h^2}\right)^{1/2} \qquad (5.15)$$

With the values of D_{11}, D_{12} and λ given in Eqs. (5.15) Eqs. (5.12) reduce to the following expressions:

$$SCF = 1 - \frac{2(1 + \nu)K_2\left(a\frac{\sqrt{10}}{h}\right)}{(1 + \nu)K_2\left(\frac{a}{h}\sqrt{10}\right) + 2K_o\left(\frac{a}{h}\sqrt{10}\right)}\cos 2\theta , \qquad (5.16)$$

$$SCQ = - \frac{\frac{a}{h}\ 10\ K_1\left(\frac{a}{h}\sqrt{10}\right)}{\frac{1 + \nu}{2}K_2\left(\frac{a}{h}\sqrt{10}\right) + K_o\left(\frac{a}{h}\sqrt{10}\right)} \sin 2\theta . \qquad (5.17)$$

Eqs. (5.16) and (5.17) are exactly the same as Reissner's solutions for a homogeneous isotropic plate including the effects of transverse shear deformation.

By examining the value of λ in Eqs. (5.15), it is seen that the dimension of λ is reciprocal of length. Upon examining the dimensions of P_{ij} and K in Eqs. (4.7) and (4.8), the same conclusion is obtained. However, the value of λ is not only a function of plate thickness but is also a function of the constitution of the material, stacking sequence, and volume fraction of laminated composite plate. Therefore, the constant λ can be expressed as $\lambda = \Lambda/h$, where Λ is a real number which is constant once the laminated composite plate is specified. Table I indicates the variation of Λ for a sandwich composite plate of 2-inch thickness with different volume fractions and stacking sequences. Now, upon specifying the stacking sequences and volume fractions of the composites, the constant Λ is specified. For the case of a thin plate ($h << a$), $\lambda a (= \frac{a}{h}\Lambda)$ becomes very large. Then Eq. (5.13) can be viewed as a thin plate solution by using the asymptotic expressions for $K_2(\lambda a)$ and $K_0(\lambda a)$ as given in reference [31]; that is,

$$K_n(\lambda a) \sim \sqrt{\frac{\pi}{2\lambda a}}\, e^{-\lambda a}\left(1 + \frac{4n^2 - 1}{8\lambda a}\right), \quad n = 0, 1, 2, \ldots . \qquad (5.18)$$

TABLE I. VALUES OF D_{12}/D_{11} AND λ FOR VARIOUS CONFIGURATIONS OF A LAMINATED PLATE

No. of layers (n)	Young's Modulus (E_n), 10^6 psi	Poisson's ratio (ν_n)	Thickness (h_n), in.	D_θ/D_h	λ, in.$^{-1}$	Λ
1	28	0.30	1.0	0.309	1.317	2.634
2	10	0.32	0.9			
1	28	0.30	1.0	0.301	1.086	2.172
2	10	0.32	0.5			
1	28	0.30	1.0	0.300	1.749	3.498
2	10	0.32	0.1			
1	10	0.32	1.0	0.302	1.724	3.448
2	28	0.30	0.5			
1	10	0.32	1.0	0.315	2.073	4.146
2	28	0.30	0.5			
1	10	0.32	1.0	0.319	1.857	3.714
2	28	0.30	0.1			

After some manipulation the final form of Eq. (5.13) for thin plates is

$$\frac{M_\theta\left(a, \frac{\pi}{2}\right)}{M_o} = \frac{3}{2} + \frac{1}{2}\frac{D_{11} + 3D_{12}}{D_{12} + 3D_{11}}, \quad \lambda a \to \infty \qquad (5.19)$$

Eq. (5.19), which is the same form as that derived from the classical plate theory by Lekhnitsky [21], is referred to as a thin plate solution. When the composite plate degenerates to a single layer, Eq. (5.19) is reduced to a familiar form; i.e.,

$$\frac{M_\theta\left(a, \frac{\pi}{2}\right)}{M_o} = \frac{3}{2} + \frac{1}{2}\frac{1 + 3\nu}{3 + \nu}, \quad \lambda a \to \infty . \qquad (5.20)$$

This solution is given in the well known book by Woinowsky-Kriger and Timoshenko [32] on plates and shells.

The other extreme case, which is opposite to the previous one, occurs when $\lambda a \to 0$. In this case the functions $K_2(\lambda a)$ and $K_o(\lambda a)$ approach infinity. However, the function $K_2(\lambda a)$ becomes infinite to a higher order than the function $K_o(\lambda a)$, and consequently Eq. (5.13) becomes

$$\frac{M_\theta\left(a, \frac{\pi}{2}\right)}{M_o} = 3, \quad \lambda a \to 0. \qquad (5.21)$$

This case corresponds to the limit of vanishing hole diameter. Eqs. (5.13) and (5.19) are plotted with respect to D/h (D is the diameter of the hole) for different material combinations as indicated in Figures 6, 7, and 8. It is clear that hole size does affect the stress concentration factor, and that the stress concentration factor increases as D/h decreases. When D/h goes to zero, the stress concentration factor converges to the value of 3. Figure 7 indicates that, even for a hole five times as wide as the plate thickness, the value of M_θ/M_o, according to the theory studied herein, is still more than 2% greater than the value obtained by application of the classical plate theory. Figures 6, 7, and 8 illustrate $M_\theta(a, \frac{\pi}{2})/M_o$ versus D/h for different material combinations. In Figures 6 and 8 it is seen that not only Poisson's ratio but also Young's modulus will influence the stress concentration factor. This phenomenon does not hold for a single-layer isotropic plate. The same results can also be found by comparing Eqs. (5.12) with (5.16) and (5.17) for the same Poisson's ratio. In computing the shear force, it is seen that when the value of λa ($= \frac{\Lambda}{h}a$) becomes very large, the first of the asymptotic expressions of $K_2(\lambda a)$ and $K_o(\lambda a)$ may be used. Therefore, Eq. (5.9) and (5.10) are reduced to

$$Q_R \simeq \frac{4D_{11}M_o}{R(D_{12} + 3D_{11})}\left[\left(\frac{a}{R}\right)^2 - \sqrt{\frac{a}{R}}\, e^{-\lambda a\left(\frac{R}{a} - 1\right)}\right] \cos 2\theta, \qquad (5.22)$$

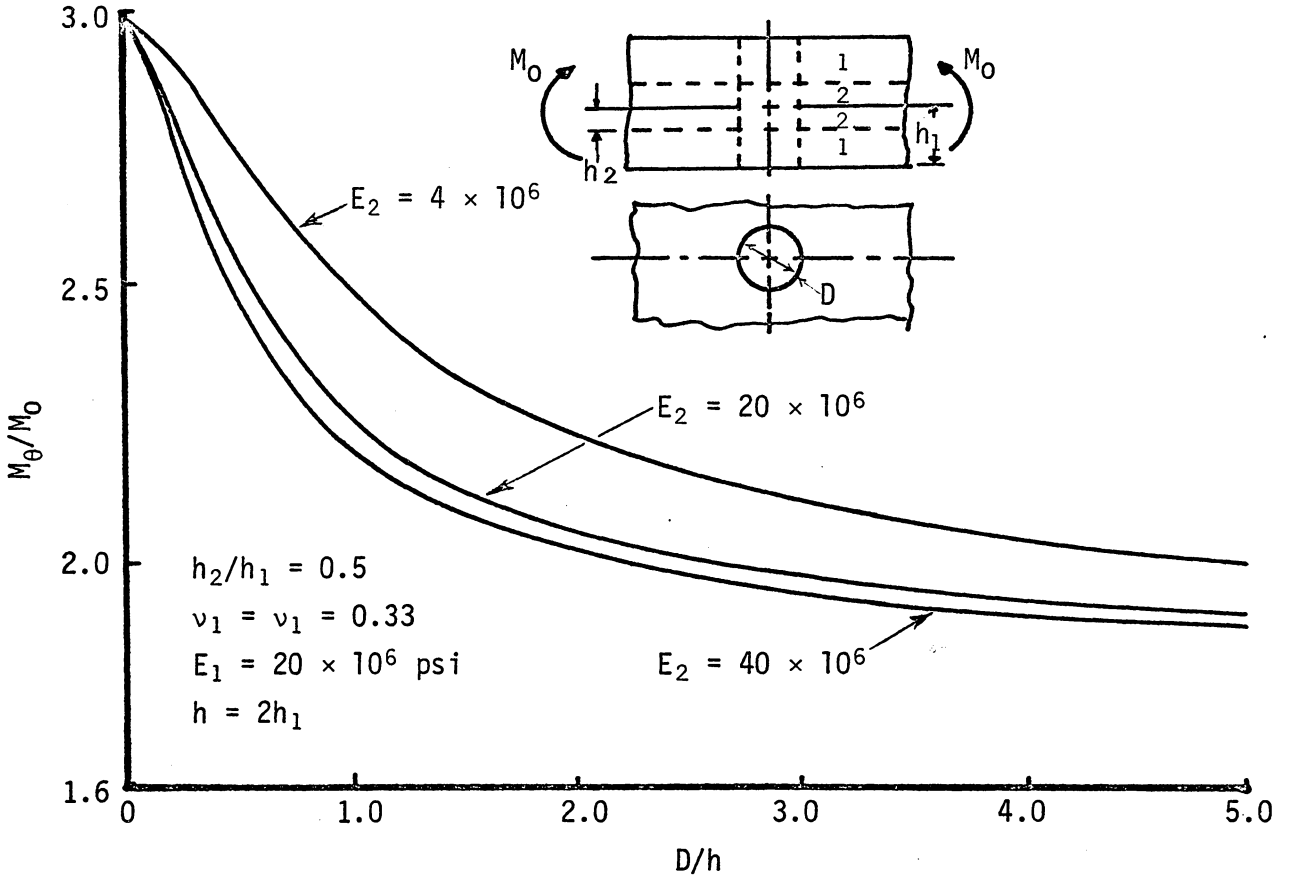

Figure 6. M_θ/M_o Vs D/h for Laminated Plate With Constant Poisson's Ratio

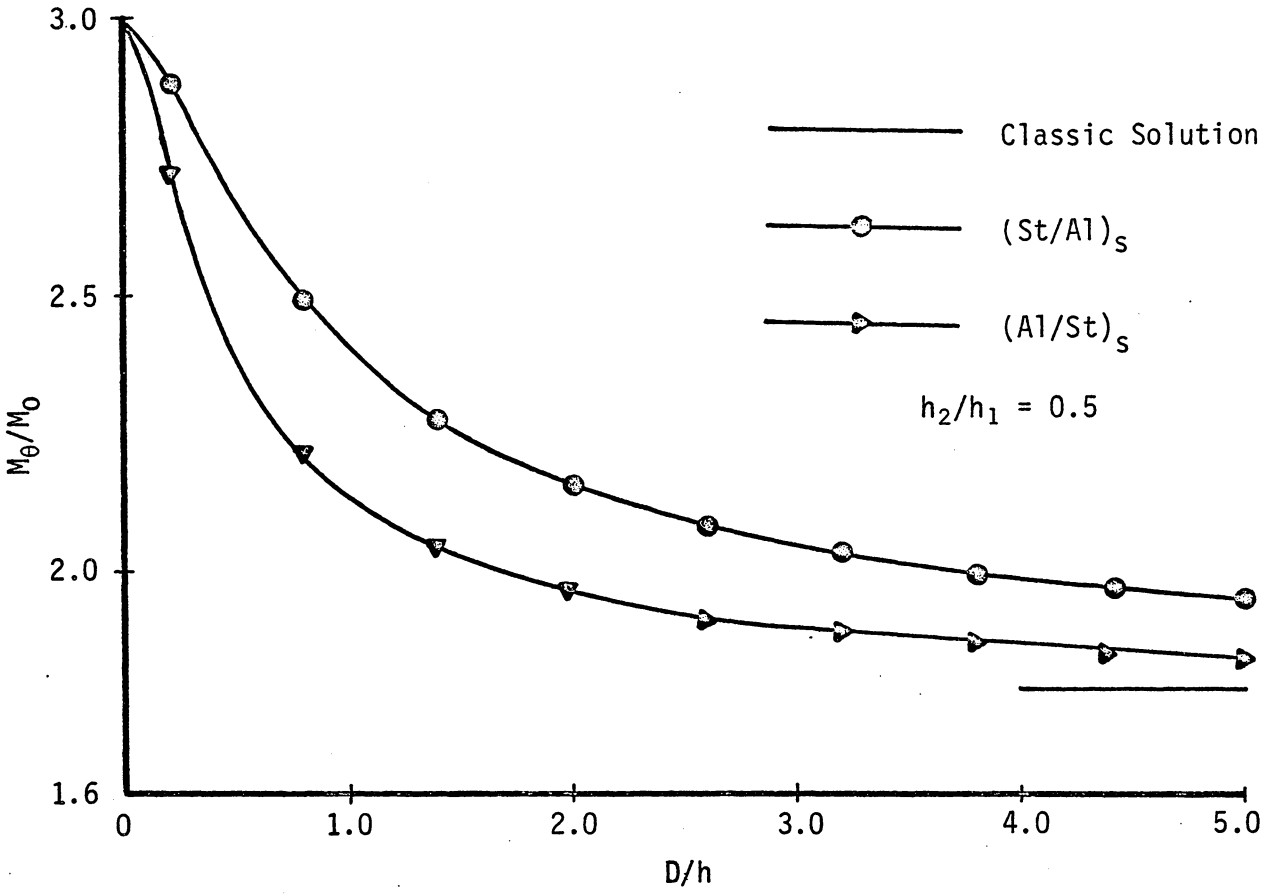

Figure 7. M_θ/M_o Vs D/h for $(St/Al)_s$ and $(Al/St)_s$ Laminated Composite Plate With Circular Hole

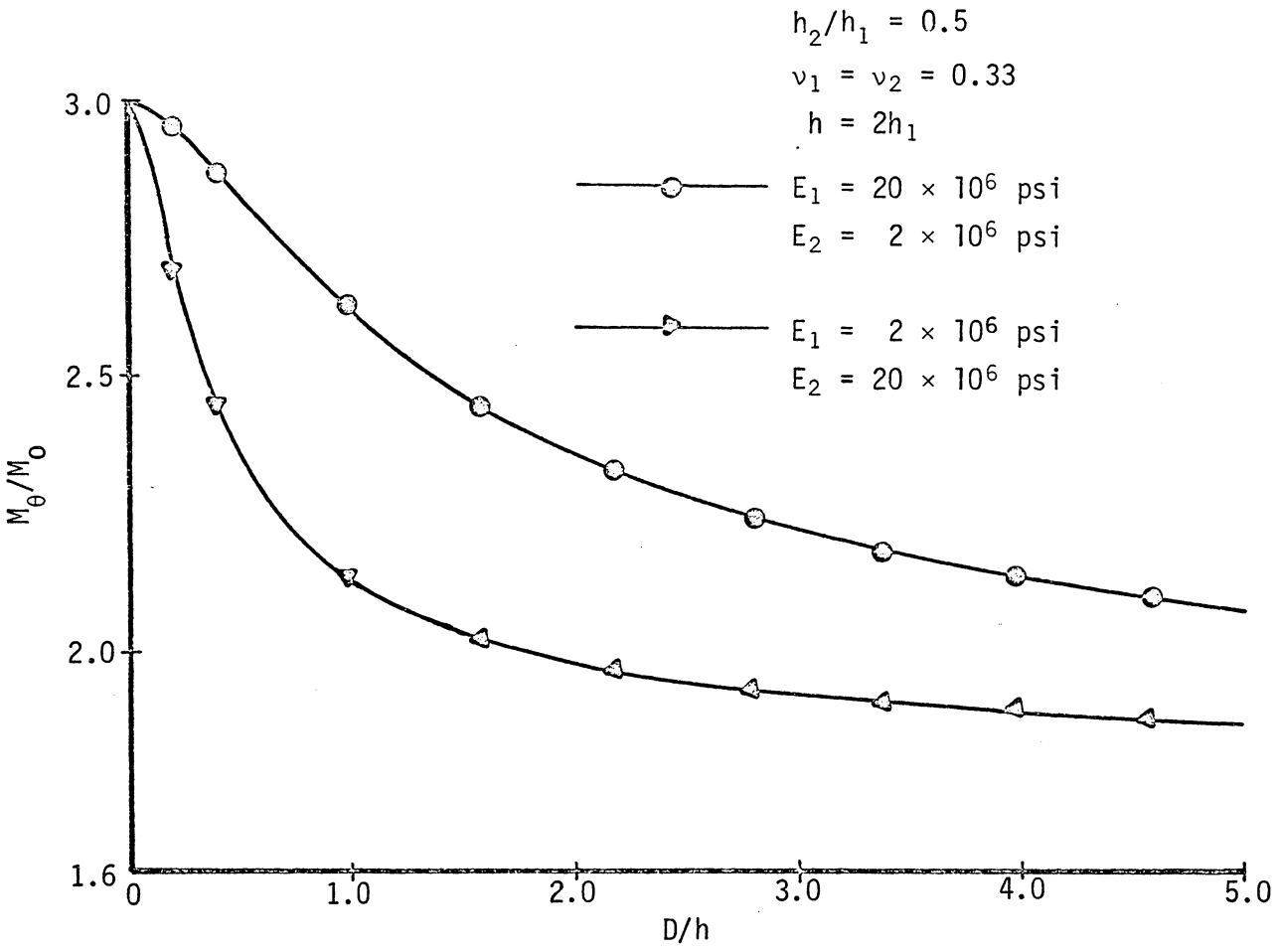

Figure 8. M_θ/M_o Vs D/h for Laminated Composite Plates With Constant Poisson's Ratios but Different Stacking Sequences

$$Q_\theta \simeq \frac{4D_{11}M_o}{R(D_{12} + 3D_{11})}\left[\left(\frac{a}{R}\right)^2 - \frac{a}{R}\left(1 + \frac{\lambda R}{2}\right)e^{-\lambda a\left(\frac{R}{a} + 1\right)}\right]\sin 2\theta. \qquad (5.23)$$

If we let $R = a + nh$ where n is a real constant, then the exponential, $-\lambda a\left(\frac{R}{a} - 1\right) = (-\Lambda n)$ is obtained. Thus it follows that for a very thin plate at a distance of the order of magnitude of the plate thickness away from the edge of the hole, the second terms in Eq. (5.22) and (5.23) vanish. Hence the shear resultants have the following form:

$$Q_\theta \simeq \frac{4D_{11}M_o}{R(D_{12} + 3D_{11})}\left(\frac{a}{R}\right)^2 \sin 2\theta,$$

$$Q_R \simeq \frac{4D_{11}M_o}{R(D_{12} + 3D_{11})}\left(\frac{a}{R}\right)^2 \cos 2\theta\ . \qquad (5.24)$$

Eqs. (5.24) are exactly those obtained by solving the classical thin plate theory. In comparing Eqs. (5.22) and (5.23) with Eqs. (5.24), it is seen that the resultant Q_R increases from its value of zero at the hole edge rapidly to the edge value of $\frac{4D_{11}M_o}{a(D_{12} + 3D_{11})}$ of thin plate theory. The case for $D/h \to \infty$ in Figure 9 corresponds to either a very thin plate or a very large hole. Figure 9 shows that classical lamination theory fails to apply in the region very close to the hole edge.

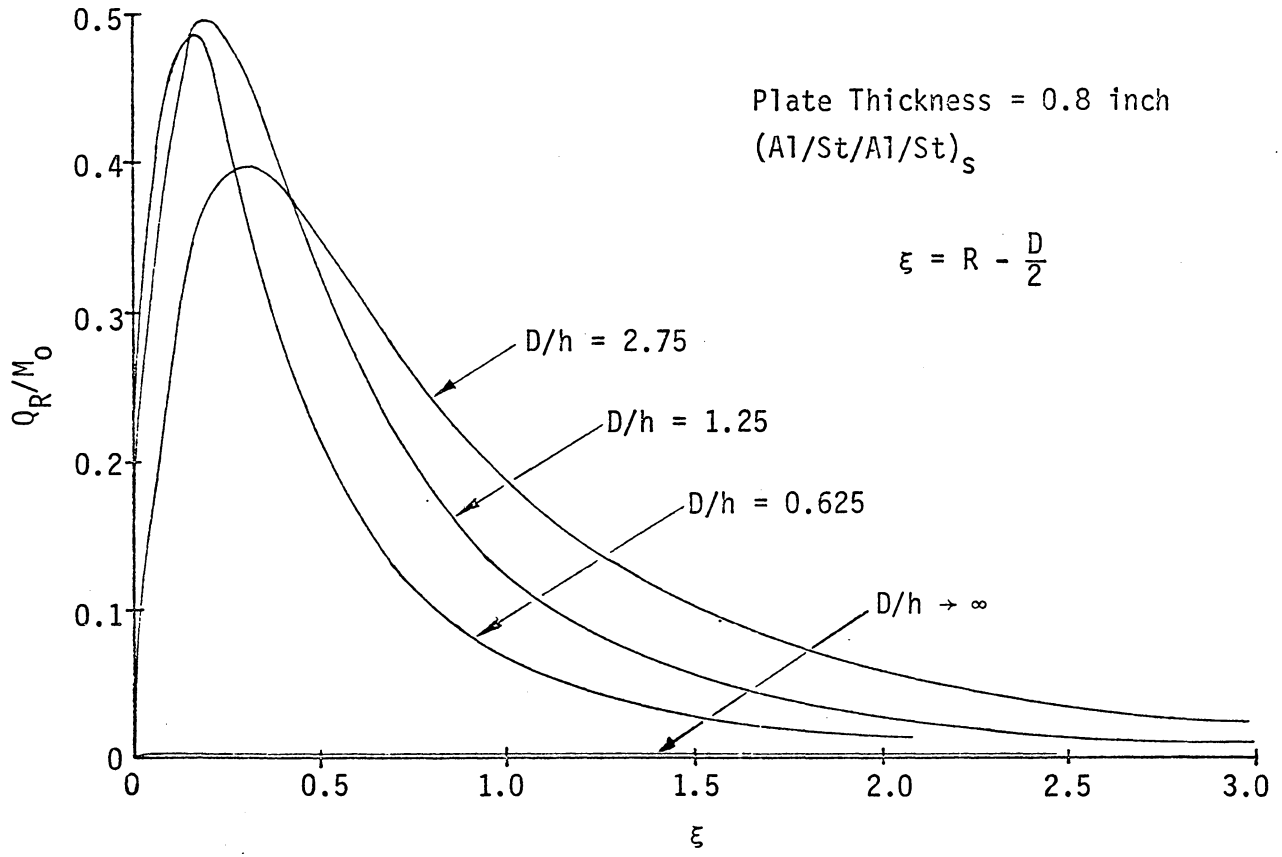

Figure 9. Length of Boundary Layer for Q_R/M_o Vs ξ Along $\theta = 0°$ for Circular Hole

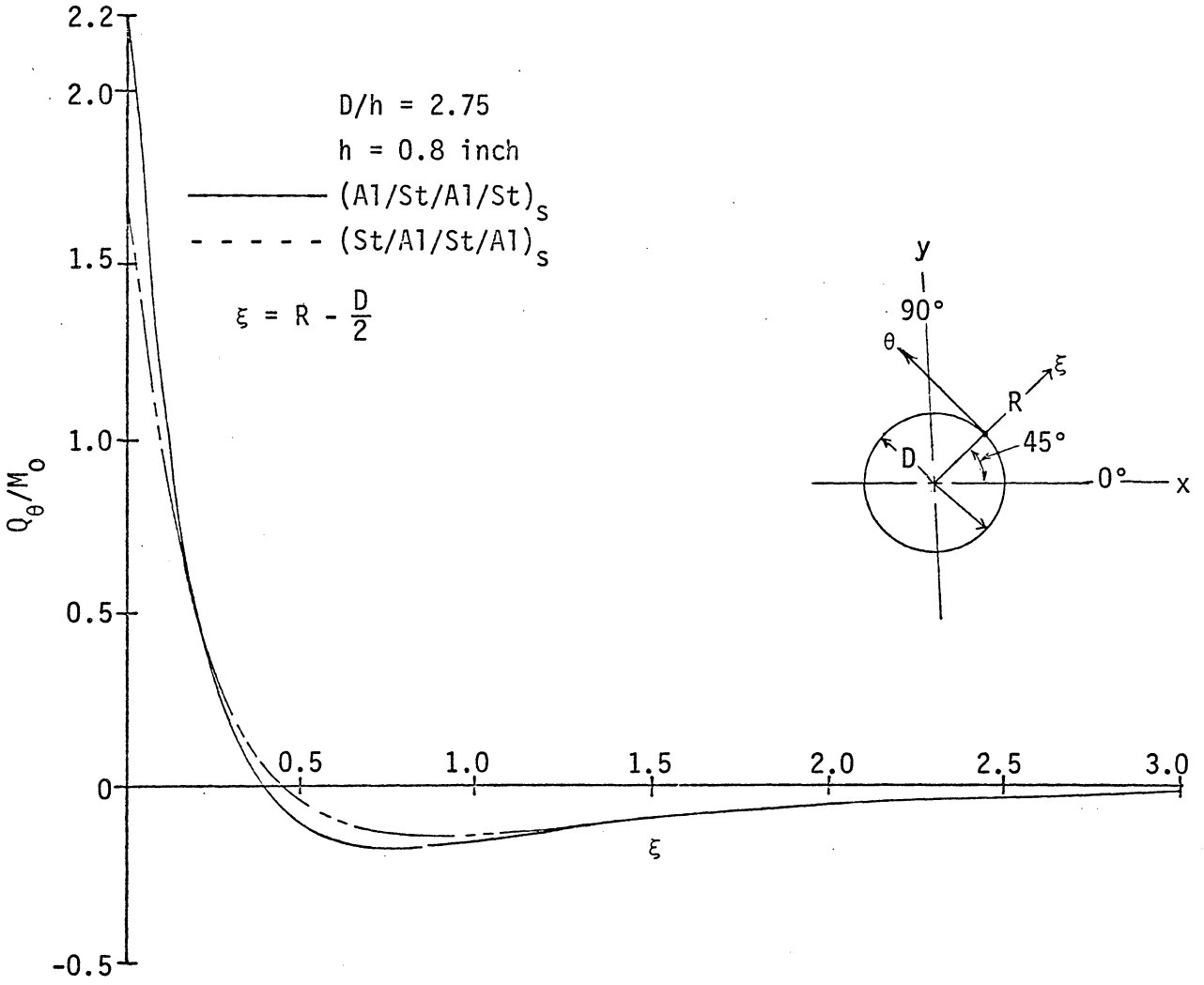

Figure 10. Variation of Q_θ/M_o Vs for Laminated Plate With 2.2-Inch-Diameter Hole

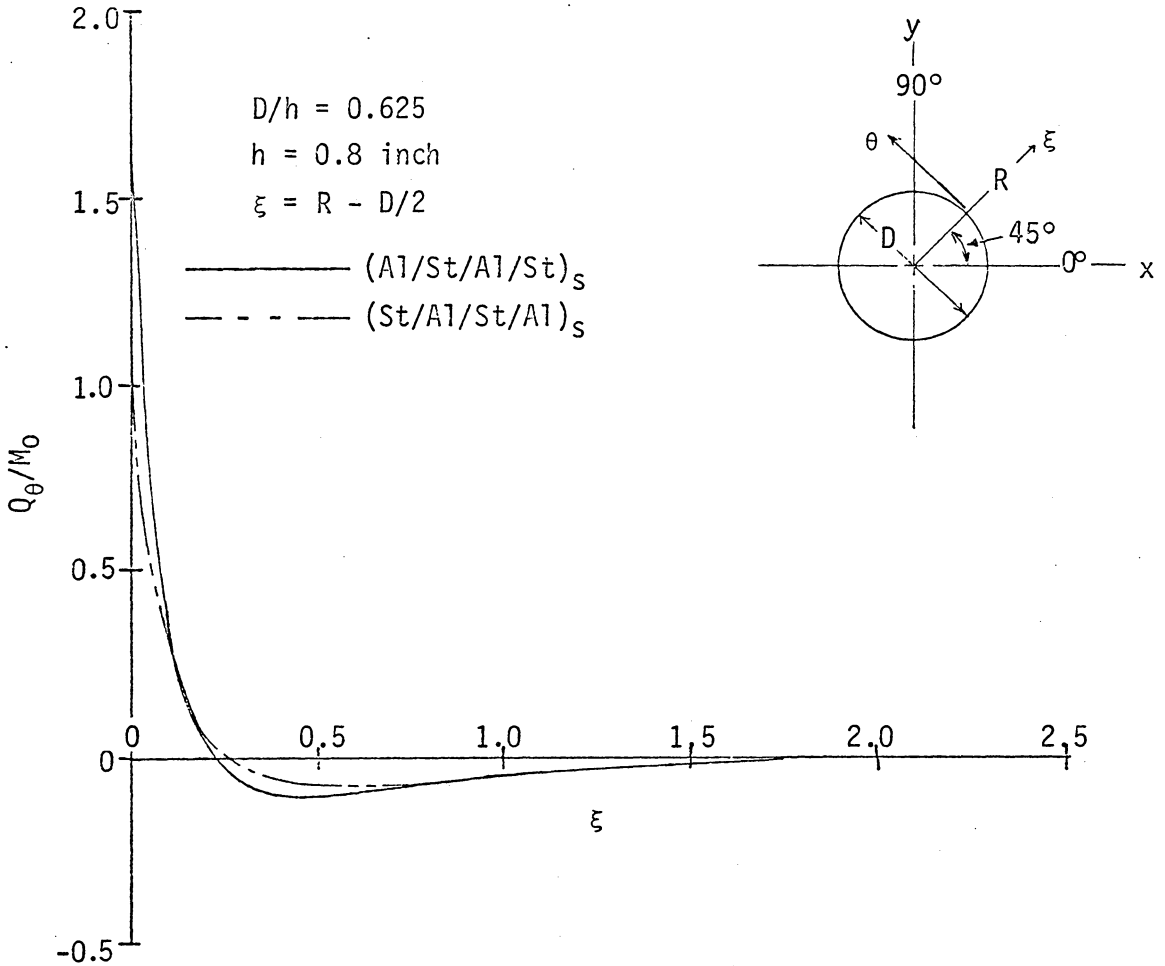

Figure 11. Variation of Q_θ/M_o Vs ξ for Laminated Composite Plate With 0.5-Inch-Diameter Hole

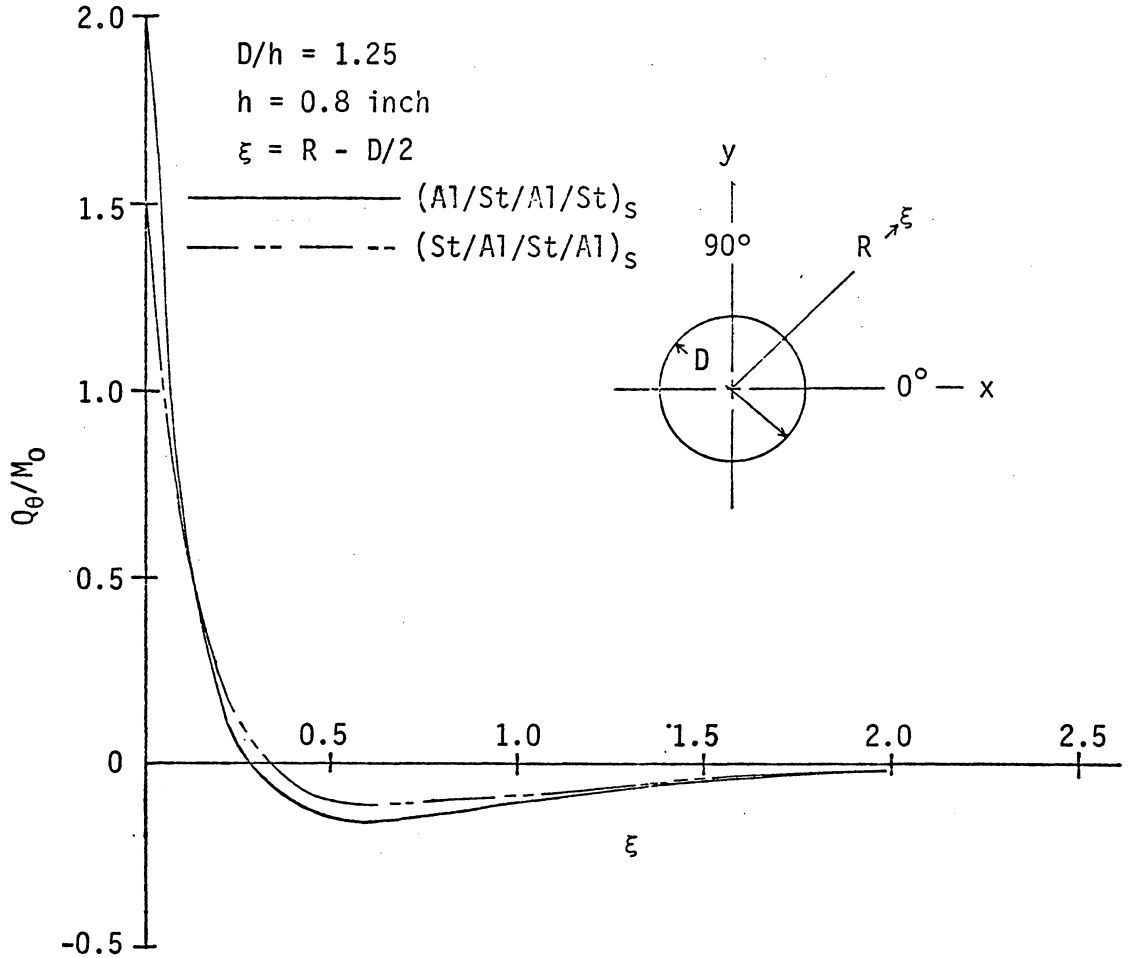

Figure 12. Variation of Q_θ/M_o Vs ξ for Laminated Composite Plate With 1.0-Inch-Diameter Hole

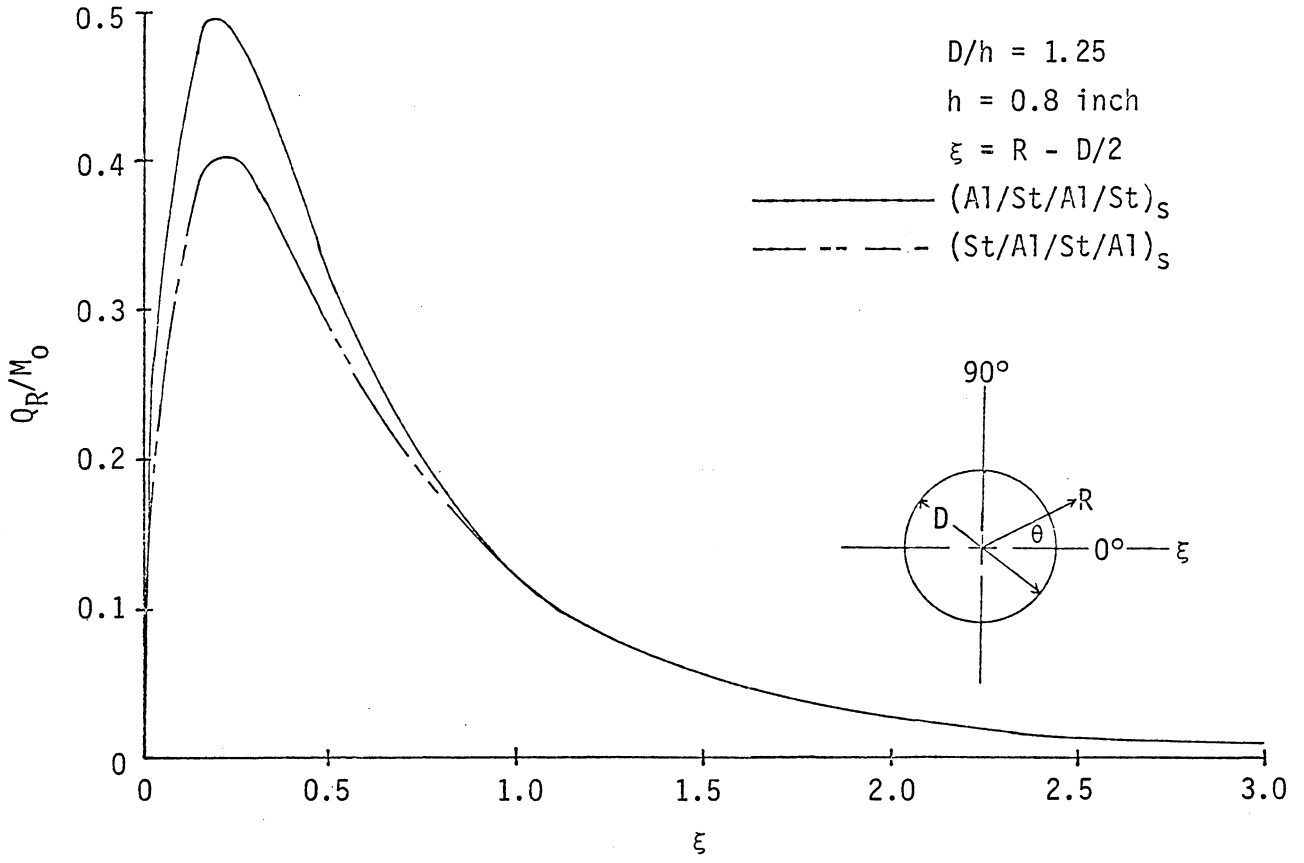

Figure 13. Variation of Q_R/M_o Vs ξ Along θ = 0° for Laminated Composite Plate With 1.0-Inch-Diameter Circular Hole

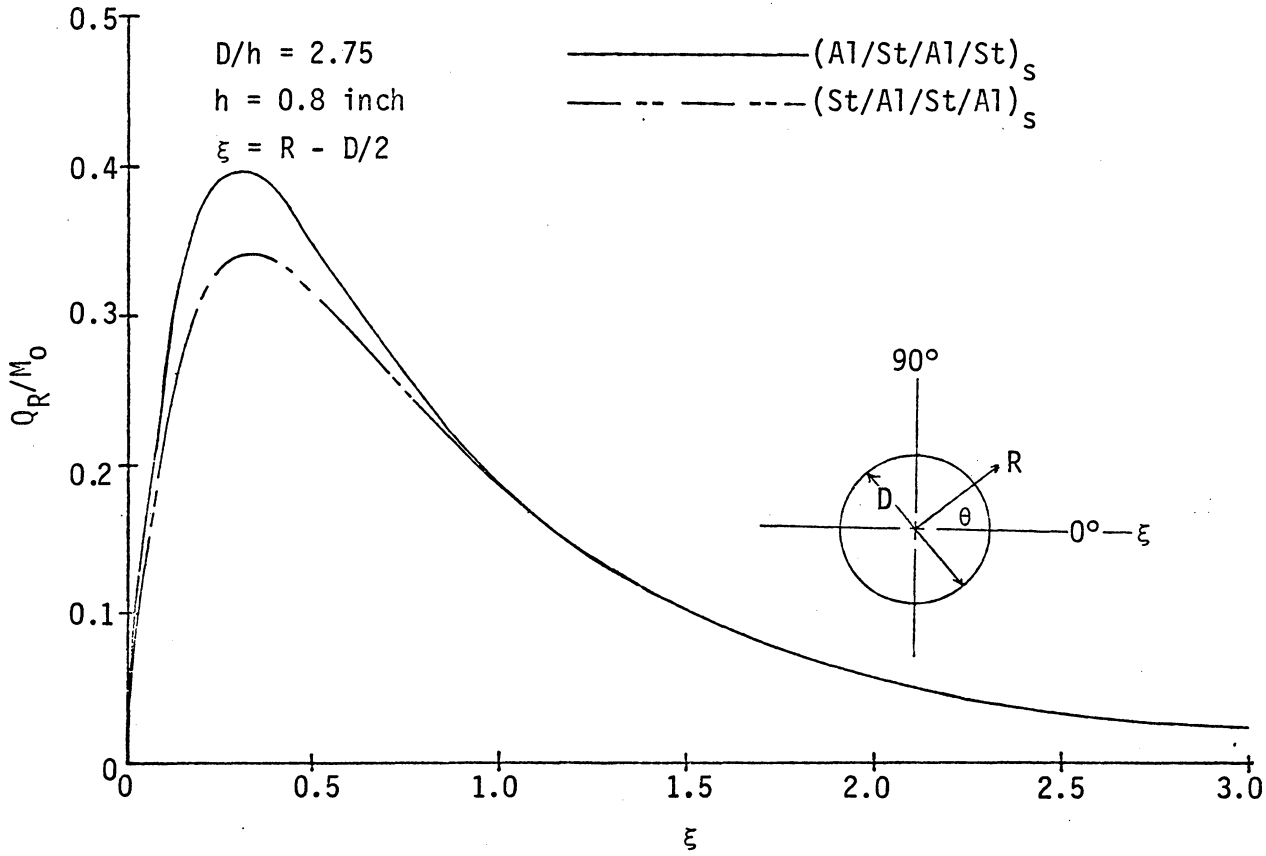

Figure 14. Variation of Q_R/M_o Vs ξ Along $\theta = 0°$ for Laminated Composite Plate With 2.2-Inch-Diameter Circular Hole

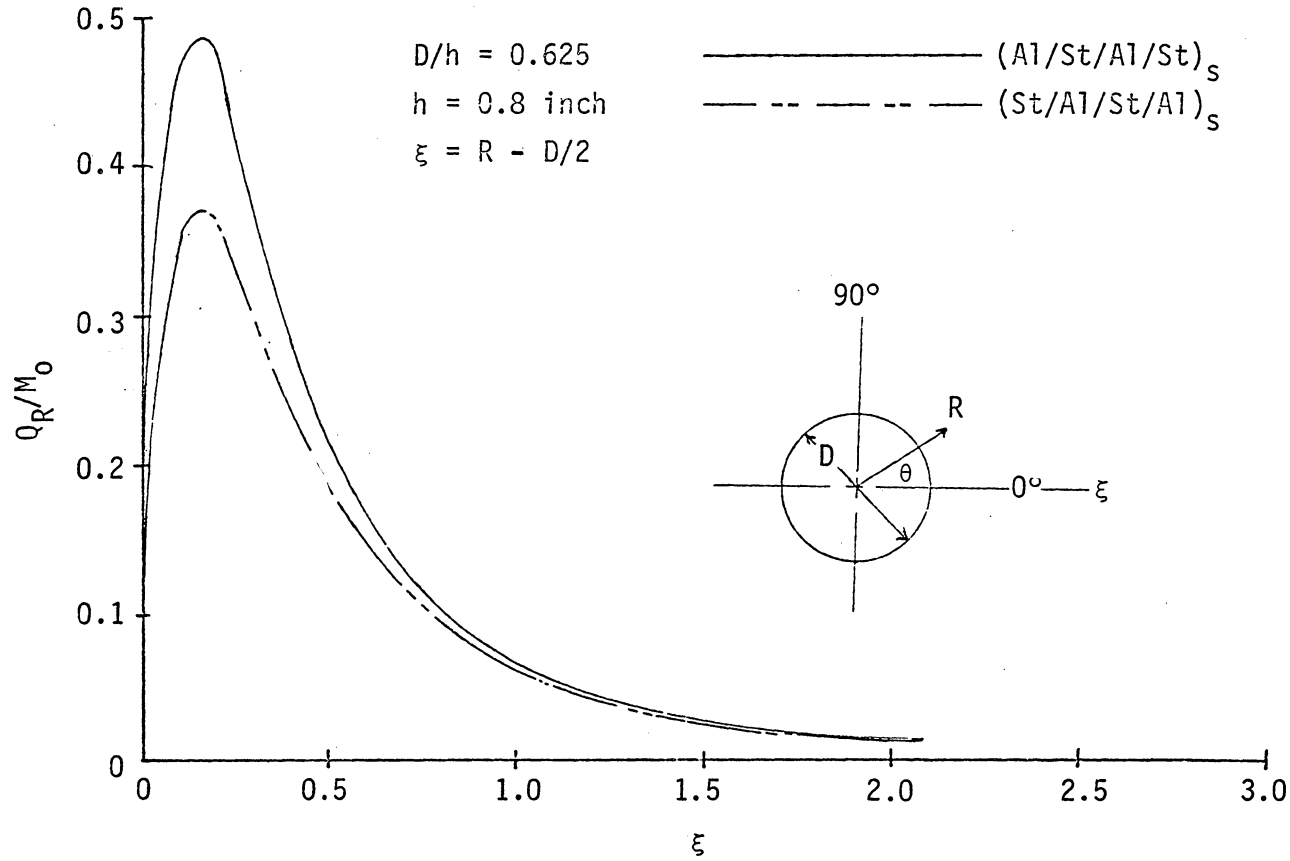

Figure 15. Variation of Q_R/M_o Vs ξ Along θ = 0° for Laminated Composite Plate With 0.5-Inch-Diameter Circular Hole

Also noteworthy is the behavior of the function representing Q_θ in Eq. (5.23). Upon examining the case for h << a in Eq. (5.23), the following expression arises:

$$Q_\theta \simeq - \frac{2D_{11}M_o\lambda}{(D_{12} + 3D_{11})} \sin 2\theta \qquad (5.25)$$

This shows that, for theory presented herein, the edge value of Q_θ is of opposite sign from the value according to Eq. (5.24). Therefore, for thin plates, Q_θ according to the theory of this study is of an entirely different order of magnitude than that given by the classical plate theory. For a given plate thickness, its value no longer decreases with increasing hole diameter. This shows that, with transverse-shearing deformation taken into account, there are portions of the plate where the transverse shear force is the same order of magnitude as the primary bending moment, no matter how thin the plate may be.

Therefore, a boundary layer phenomenon exists in the region near the hole edge. Figures 10, 11, and 12 give the variation of Q_θ/M_o versus ξ (=R - D/2) for $(Al/St/Al/St)_s$ and $(St/Al/St/Al)_s$ laminated composite plates with different hole diameters. Figures 13, 14 and 15 give the variation of Q_R/M_o versus ξ. They show that at the hole edge the value of Q_θ/M_o, as well as the boundary layer thickness, will increase with increasing D/h. Also, as can be seen in Table II, as D/h becomes very large with constant plate thickness, the value

TABLE II. BOUNDARY LAYER EFFECT IN $(AL/ST/AL/ST)_S$ LAMINATED COMPOSITE PLATES NEAR EDGE OF APPROXIMATELY ZERO CURVATURE

H=0.8in	D/h = 12,500		D/h = 1875		D/h = 1250	
ξ	Q_R	Q_Θ	Q_R	Q_Θ	Q_R	Q_Θ
0.000	0.0000	-2.4120	0.0000	-2.4120	0.0000	-2.4120
0.080	0.0000	-1.7631	0.0002	-1.7508	0.0003	-1.7507
0.160	0.0001	-1.2887	0.0004	-1.2696	0.0006	-1.2693
0.240	0.0001	-0.9273	0.0005	-0.9205	0.0007	-0.9202
0.320	0.0001	-0.6778	0.0006	-0.6680	0.0009	-0.6677
0.400	0.0001	-0.4877	0.0006	-0.4843	0.0010	-0.4839
0.480	0.0001	-0.3565	0.0007	-0.3510	0.0010	-0.3506
0.560	0.0001	-0.2565	0.0007	-0.2546	0.0011	-0.2542
0.640	0.0001	-0.1875	0.0007	-0.1844	0.0011	-0.1840
0.720	0.0001	-0.1349	0.0008	-0.1335	0.0011	-0.1331
0.800	0.0001	-0.0986	0.0008	-0.0967	0.0012	-0.0963
0.880	0.0001	-0.0709	0.0008	-0.0699	0.0012	-0.0695
0.960	0.0001	-0.0518	0.0008	-0.0505	0.0012	-0.0501
1.040	0.0001	-0.0372	0.0008	-0.0364	0.0012	-0.0360
1.120	0.0001	-0.0272	0.0008	-0.0262	0.0012	-0.0258
1.200	0.0001	-0.0195	0.0008	-0.0188	0.0012	-0.0184
1.280	0.0001	-0.0142	0.0008	-0.0134	0.0012	-0.0130
1.360	0.0001	-0.0102	0.0008	-0.0095	0.0012	-0.0091
1.440	0.0001	-0.0074	0.0008	-0.0067	0.0012	-0.0063
1.520	0.0001	-0.0053	0.0008	-0.0046	0.0012	-0.0042
1.600	0.0001	-0.0039	0.0008	-0.0031	0.0012	-0.0027
1.680	0.0001	-0.0027	0.0008	-0.0021	0.0012	-0.0017
1.760	0.0001	-0.0020	0.0008	-0.0013	0.0012	-0.0009
1.840	0.0001	-0.0014	0.0008	-0.0007	0.0012	-0.0003
1.920	0.0001	-0.0010	0.0008	-0.0003	0.0012	0.0001
2.000	0.0001	-0.0007	0.0008	0.0000	0.0012	0.0004
2.080	0.0001	-0.0005	0.0008	0.0002	0.0012	0.0006
2.160	0.0001	-0.0003	0.0008	0.0004	0.0012	0.0008
2.240	0.0001	-0.0002	0.0008	0.0005	0.0012	0.0009
2.320	0.0001	-0.0001	0.0008	0.0006	0.0012	0.0010
2.400	0.0001	-0.0000	0.0008	0.0006	0.0012	0.0010
2.480	0.0001	0.0000	0.0008	0.0007	0.0012	0.0011
2.560	0.0001	0.0000	0.0008	0.0007	0.0012	0.0011
2.640	0.0001	0.0001	0.0008	0.0007	0.0012	0.0011
2.720	0.0001	0.0001	0.0008	0.0008	0.0012	0.0011
2.800	0.0001	0.0001	0.0008	0.0008	0.0012	0.0012

of Q_θ/M_o at the hole edge will be a constant. For example, from Table II for a $(Al/St/Al/St)_s$ laminated composite plate, this constant at the hole edge has the value 2.4120. Therefore, as the curvature of the free edge becomes small and nears zero, the value of Q_θ/M_o for a specified laminated composite will be constant. This indicates a discrepancy in the singularity phenomena, which was found by Pipes and Pagano [38] [33] for a straight free edge. Figure 16 compares Q_θ/M_o versus ξ for a $(Al/St/Al/St)_s$ composite with hole diameters of 0.5, 1.0, 2.2, and infinity. The boundary layer thickness for very large D/h is approximately equal to the plate thickness. Figure 9 gives a similar plot for Q_R/M_o.

In comparing Eq. (5.12) with Reissner's solution given by Eq. (5.16), it is seen that for a homogeneous, single-layer plate the stress concentration factor is strongly influenced by Poisson's ratio and the ratio a/h; however, for a laminated composite plate, two parameters, D_{12}/D_{11} and λa, play essential roles instead of Poisson's ratio and a/h. Also, it should be kept in mind that D_{12}, D_{11}, and λ are functions of Poisson's ratio, Young's modulus, and the volume fraction of each layer of the laminated composite plate. Tables I and III give values of D_{12}/D_{11} and λ for different combinations of composite plates. Figure 7 gives values of M_θ/M_o for different D/h values for $(Al/St)_s$, and $(St/Al)_s$ sandwich plates. It shows that at the same values of D/h and volume fraction, the soft-core sandwich plate will produce a higher stress concentration factor than that of a hard-core sandwich plate. The values of

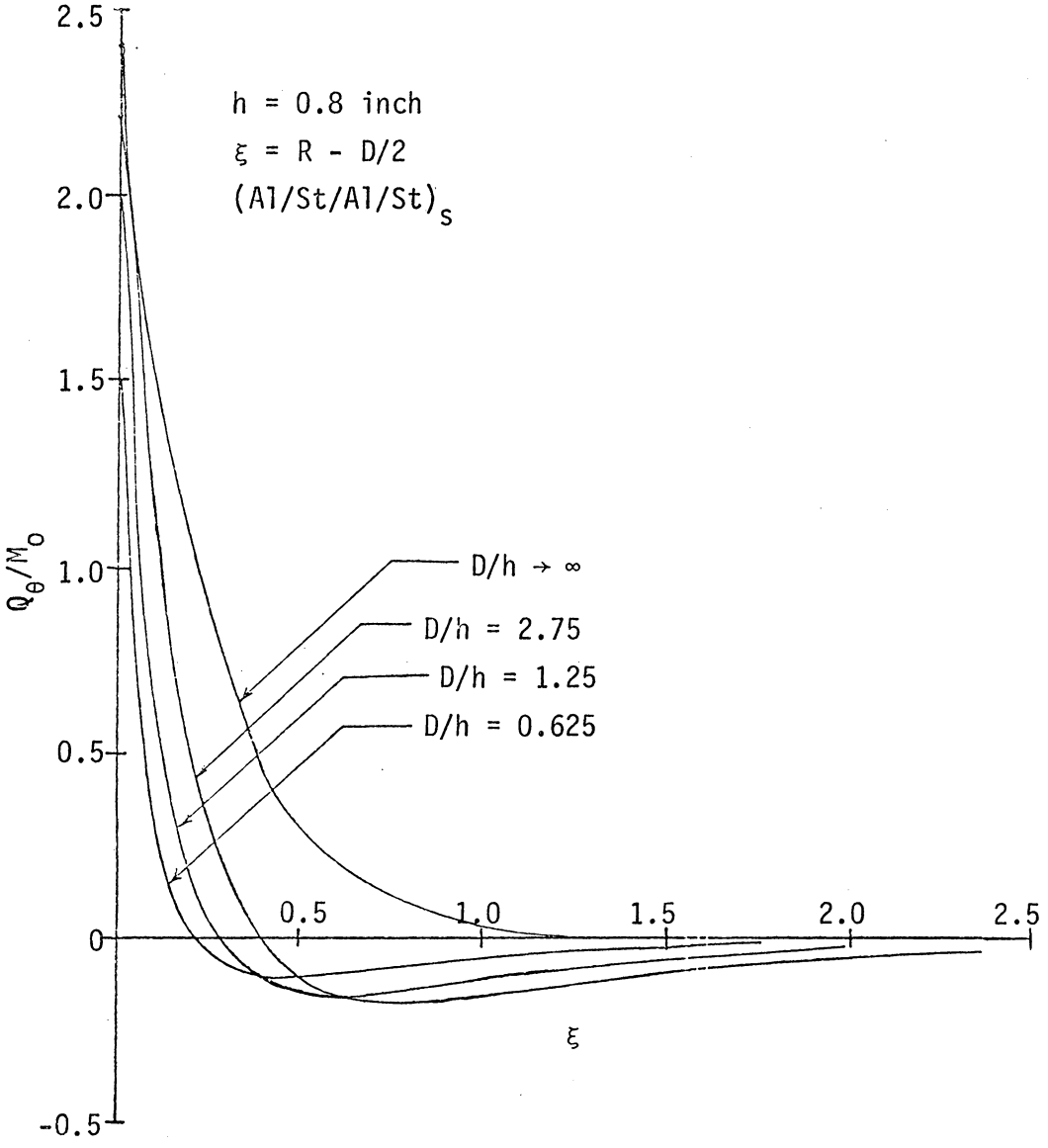

Figure 16. Length of Boundary Layer for Q_θ/M_o Along $\theta = 45°$ for Circular Hole

TABLE III. VALUES OF D_{12}/D_{11} AND λ FOR DIFFERENT THICKNESSES IN $(ST/AL)_s$ LAMINATED COMPOSITE PLATES WITH 0.5% VOL, 2.5-INCH-DIAMETER HOLE

h, in.	20	10	4	2	1.6	1.	0.4	0.2	0.02	0.002
D_{12}/D_{11}	0.329	0.330	0.328	0.329	0.331	0.330	0.328	0.329	0.329	0.329
λ	0.10	0.23	0.57	1.14	1.43	2.28	5.71	11.42	119.8	1142.
D/h	0.125	0.250	0.625	1.25	1.56	2.50	6.25	12.5	125.	1250.

$\Lambda = 2.284$

D_{12}/D_{11} and λ for $(St/Al)_s$ sandwich plates are 0.324 and 4.036, respectively; and for $(Al/St)_s$ sandwich plates are 0.329 and 2.282, respectively. Table III gives values for different thicknesses for $(St/Al)_s$ sandwich plates for a given hole diameter and volume fraction.

The distributions of M_θ/M_o and Q_θ/M_o around a hole are given in Figures 17 and 18 for different constituents, stacking sequences, and volume fractions. The pronounced influence of these factors on the stress distributions can be observed.

It is also worthwhile to examine the transfer of stress from one layer to another. By examining the stress distribution through the plate thickness, the mechanism for the transfer of stress can be understood. From Eqs. (3.21), (4.2), and (4.19),

$$\sigma_x^i + \sigma_y^i = -z \frac{4E^i}{1 - \nu^i} [\Omega'(Z) + \bar{\Omega}'(\bar{Z})] . \qquad (5.26)$$

Eq. (5.26) can also be rewritten in a polar coordinate system through the use of Eqs. (4.40). Obviously, from Eqs. (4.40), it should be noted that $\sigma_R^i + \sigma_\theta^i = \sigma_x^i + \sigma_y^i$. Therefore, the value of σ_θ/M_o at hole edge for the case of $M_1 = M_o$, $\alpha = 0$ is given as

$$\left(\frac{\sigma_\theta^i}{M_o}\right)_{R=a} = \frac{zE^i}{(1 - \nu^i)(D_{11} + D_{12})} - \frac{2E^i z K_2(\lambda a)\cos 2\theta}{(1 - \nu^i)[(D_{11} + D_{12})K_2(\lambda a) + 2D_{11}K_o(\lambda a)]} \qquad (5.27)$$

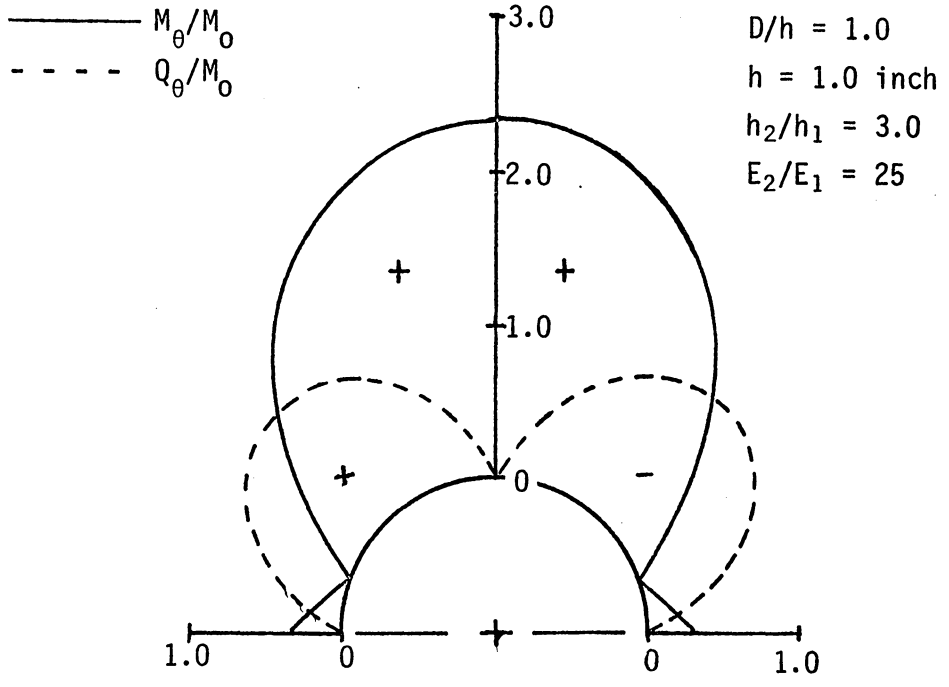

Figure 17. Distribution of M_θ/M_o and Q_θ/M_o Around Circular Hole Evaluated From Equations 5-16 and 5-17

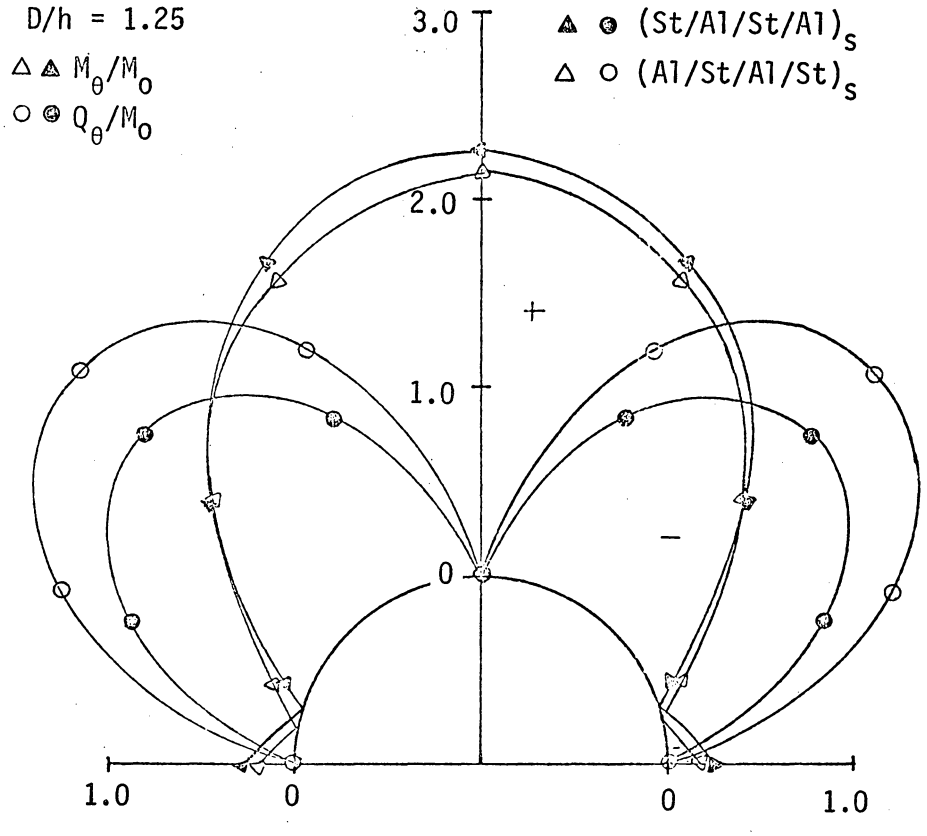

Figure 18. Distribution of M_θ/M_o and Q_θ/M_o Around Circular Hole for $(St/Al/St/Al)_s$ and $(Al/St/Al/St)_s$ Laminated Composite Plates

Similarly, shear stresses τ^{i}_{Rz} and $\tau^{i}_{\theta z}$ can be derived from Eqs. (4.40) and expressed in the following form:

$$\frac{\tau^{i}_{Rz}}{M_o} = \frac{4D_{11}\left[\frac{G^i}{2}\left(\frac{h^2}{4} - z^2\right) + A_j\right]}{K[(D_{11} + D_{12})K_2(\lambda a) + 2D_{11}K_o(\lambda a)]}\left[\frac{a^2}{R^3}K_2(\lambda a) - \frac{1}{R}K_2(\lambda R)\right]\cos 2\theta, \tag{5.28}$$

and

$$\frac{\tau^{i}_{\theta z}}{M_o} = \frac{4D_{11}\left[\frac{G^i}{2}\left(\frac{h^2}{4} - z^2\right) + A_j\right]}{K[(D_{11} + D_{12})K_2(\lambda a) + 2D_{11}K_o(\lambda a)}$$

$$\left[\frac{a^2}{R^3}K_2(\lambda a) - \frac{1}{R}K_2(\lambda R) - \frac{\lambda}{2}K_1(\lambda R)\right]\sin 2\theta. \tag{5.29}$$

At the hole edge, expressions for τ^{i}_{Rz}/M_o and $\tau^{i}_{\theta z}/M_o$ are obtained by substituting R = a in Eqs. (5.28) and (5.29) as follows.

$$\frac{\tau_{\theta z}(a,\Theta)}{M_o} = -\frac{2D_{11}\left[\frac{G^i}{2}\left(\frac{h^2}{4} - z^2\right) + A_j\right]\lambda}{K[(D_{11} + D_{12})K_2(\lambda a) + 2D_{11}K_o(\lambda a)]}K_1(\lambda a)\sin 2\theta. \tag{5.30}$$

Note that $\tau_{Rz}(a, \theta)/M_o$ vanishes at the hole edge.

Numerical examples for laminated composite plates of $(St/Al/St/Al)_s$ and $(Al/St/Al/St)_s$ stacking sequences are shown in Figures 19 and 20. Results for $(St/Al)_s$ and $(Al/St)_s$ sandwich composite plates are given in Figures 21 and 22. It should be

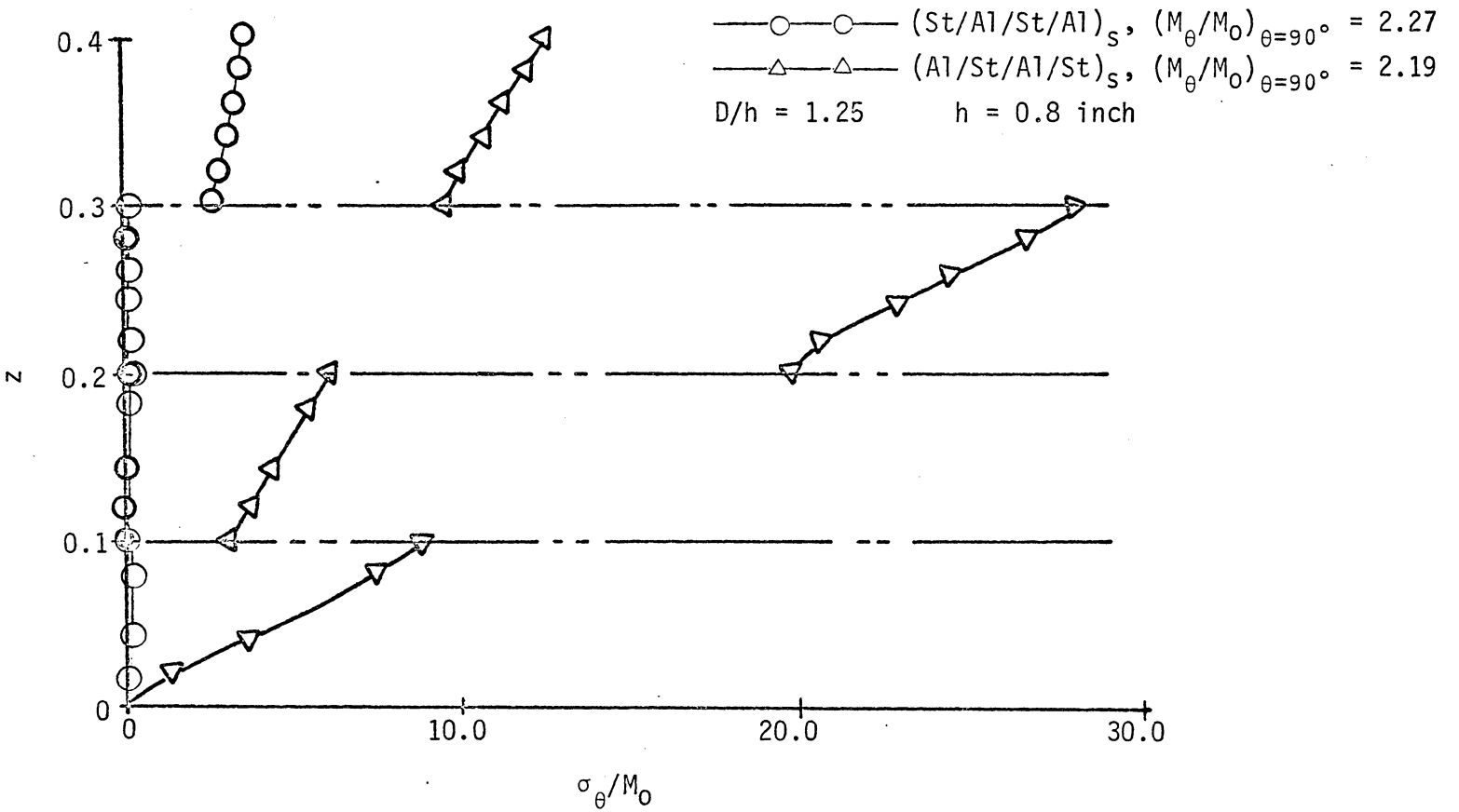

Figure 19. Normal Stress σ_θ/M_o Distribution Through Thickness for $(Al/St/Al/St)_s$ and $(St/Al/St/Al)_s$ Laminated Composite Plates

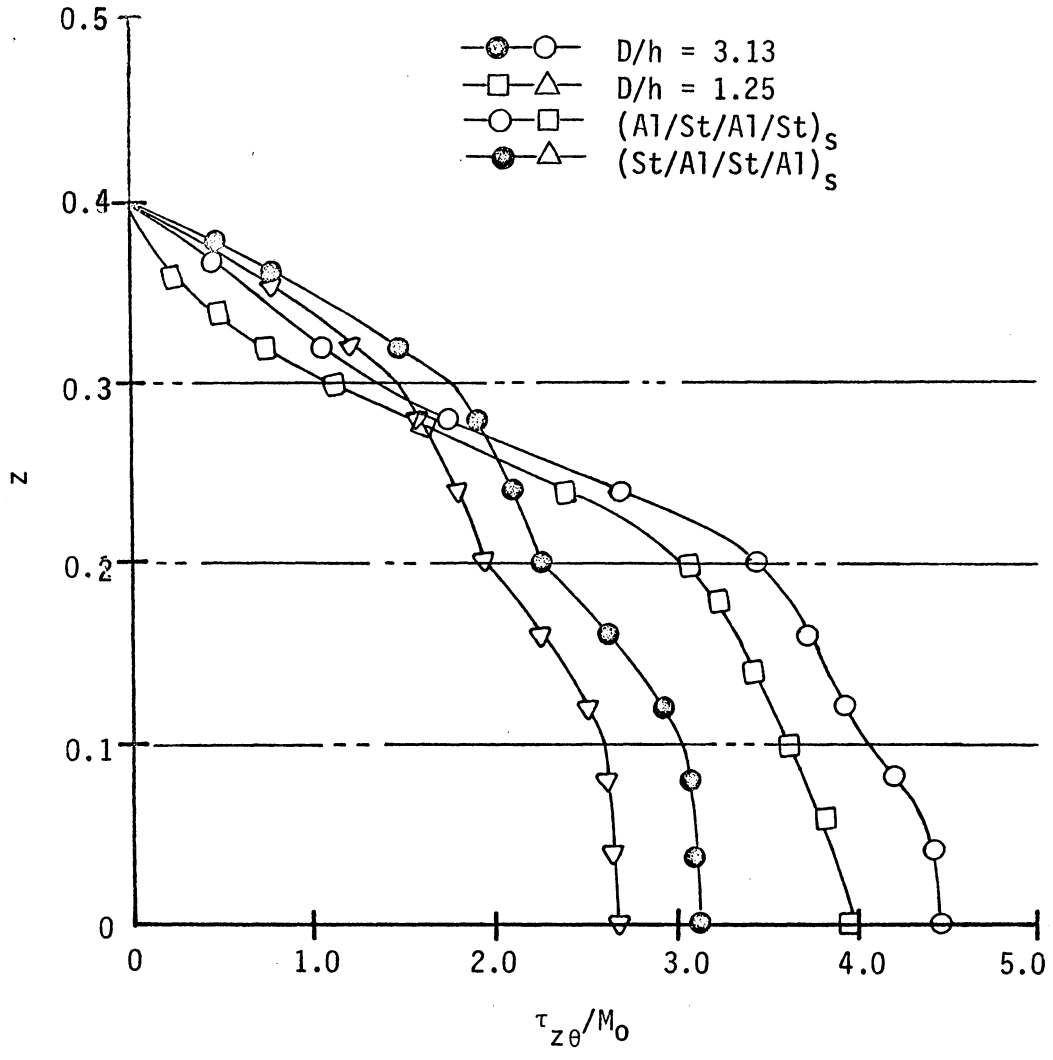

Figure 20. Shear Stress $\tau_{z\theta}/M_o$ Distribution Through Thickness for $(Al/St/Al/St)_s$ and $(St/Al/St/Al)_s$ Laminated Composite Plates

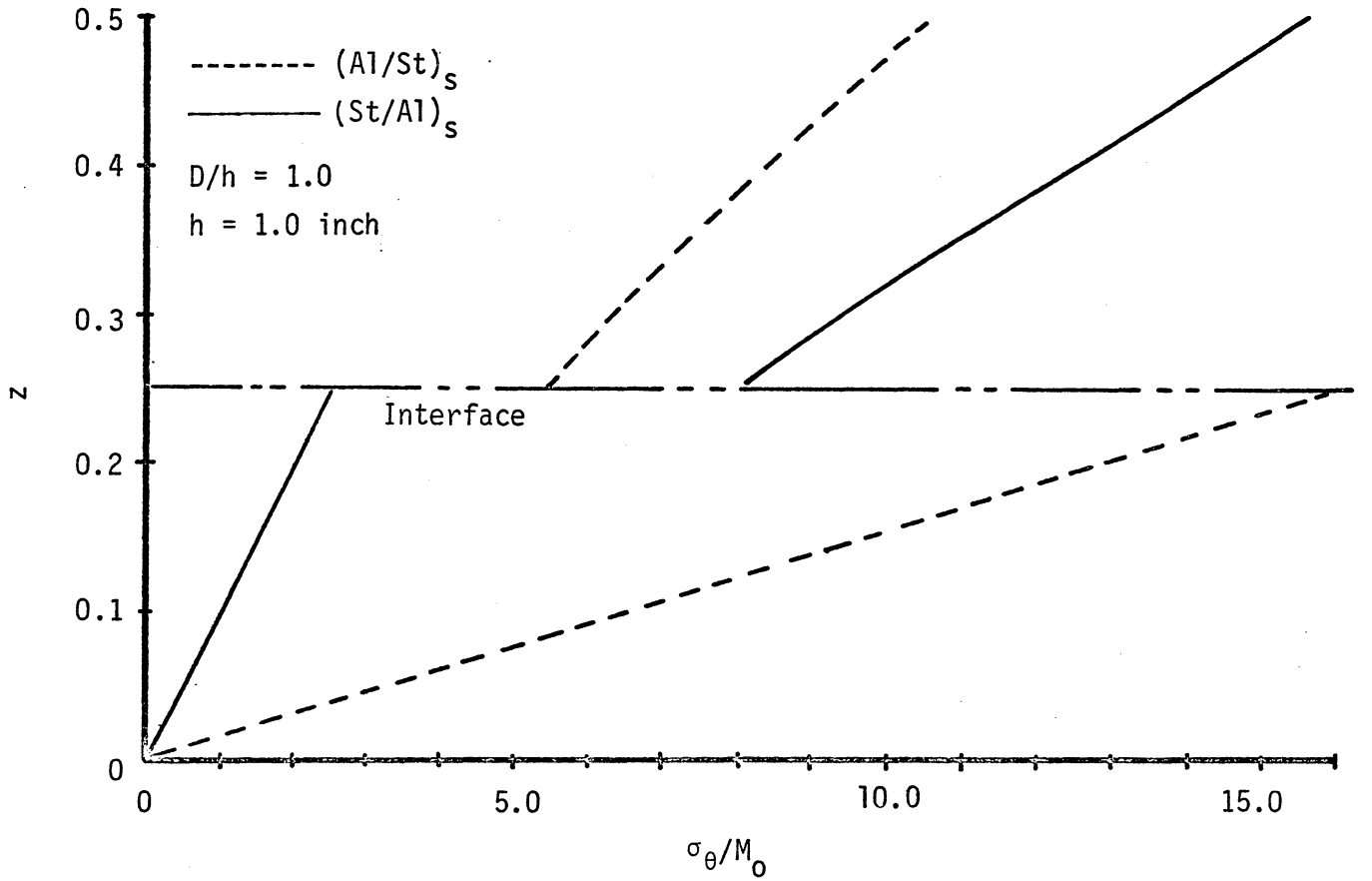

Figure 21. Normal Stress σ_θ/M_o Distribution Through Thickness for $(Al/St)_s$ and $(St/Al)_s$ Laminated Composite Plate

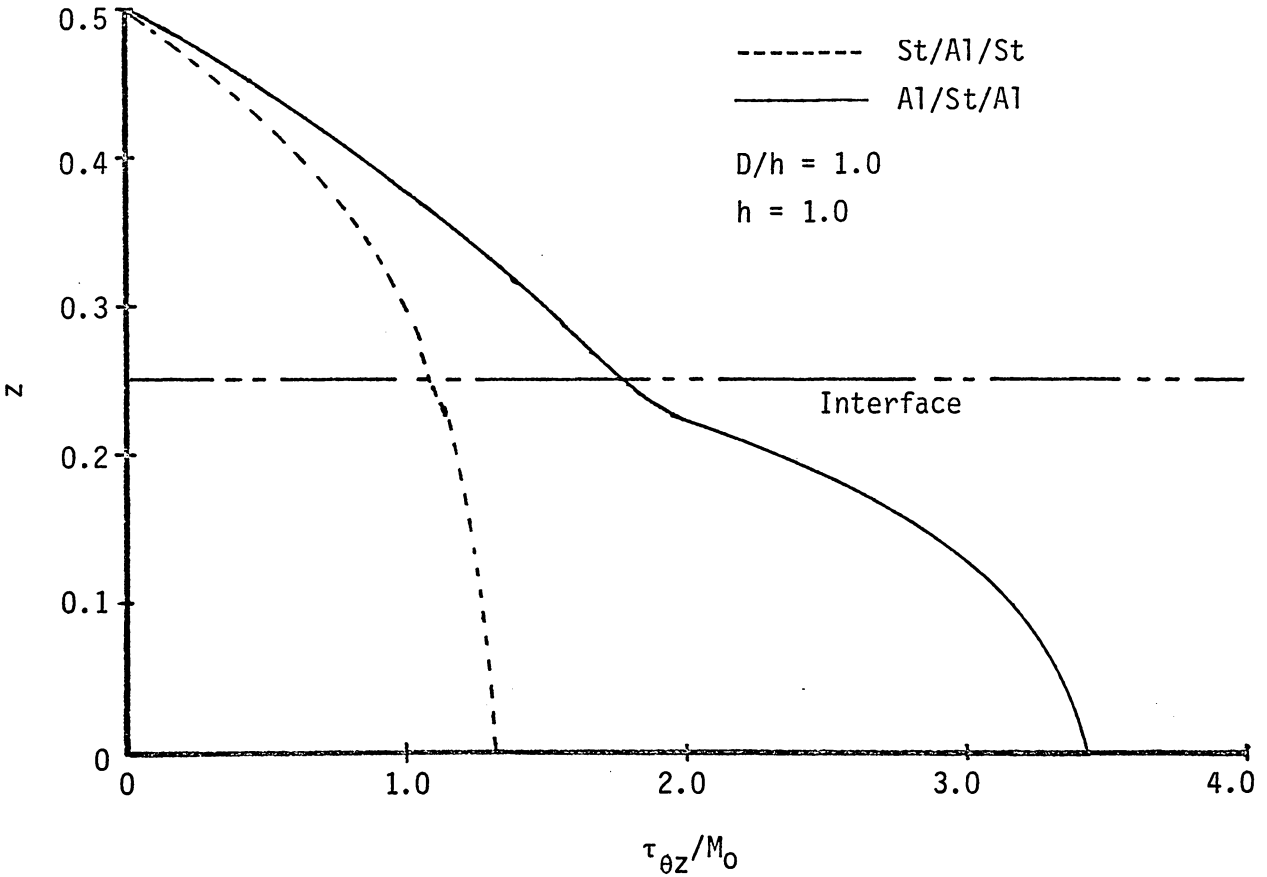

Figure 22. Shear Stress $\tau_{\theta z}/M_o$ Around Circular Hole for $(Al/St)_s$ and $(St/Al)_s$ Laminated Composite Plate

noted that the stress distribution patterns through the thickness are completely different for different stacking sequences and for different numbers of layers in a laminated composite plate.

5.2. Elliptical Hole Case

The previous section presented a study of the case of a circular hole. In this section a laminated, infinite composite plate containing an unstressed elliptical hole, under a uniform bending moment at infinity is considered. The origin of the coordinate system, for convenience in analysis, is located at the center of the elliptical hole as shown in Figure 23. The elliptical coordinate system (ξ, η, z), as shown in Figure 23, is the appropriate coordinate system for this study. The basic complex variable formulation given in the previous section can be extended to the transformed problem by choosing a proper conformal mapping function. This is

$$Z = F(\zeta) = Z \cosh \zeta \qquad (5.31)$$

where ζ is a complex variable defined as $\zeta = \xi + i\eta$. The function $F(\zeta)$ maps points in a region in the ζ-plane into points in a region in the Z-plane. As usual, it is assumed that the transformation between a region in the ζ-plane and a region in the Z-plane is one-to-one and invertible, so that by selecting a particular branch of the inverse transformation $\zeta = F^{-1}(Z)$, the corresponding one-to-one

Of = Focal Length

Oa = Major Axis for $\xi=r_0$

Ob = Minor Axis for $\xi=r_0$

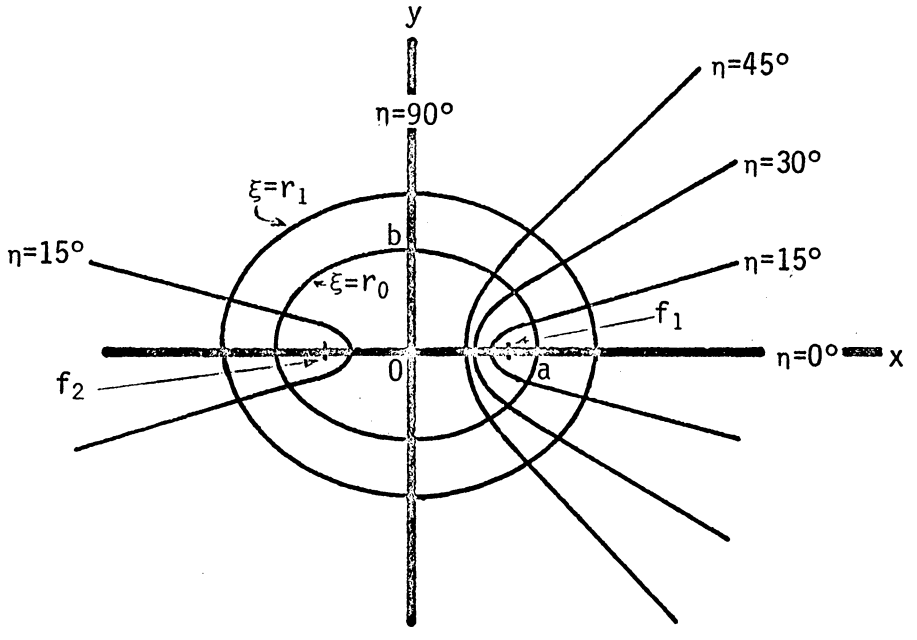

Figure 23. Elliptical Coordinates (ξ, η, z)

mapping from Z-plane to ζ-plane may be defined. Now, to preserve the basic complex variable formulation, it is assumed, in addition, that $F(\zeta)$ is holomorphic in the ζ-plane and that $F'(\zeta) \neq 0$ for all ζ belonging to regions in the ζ-plane.

Therefore, the new potential functions $\Omega(\zeta)$ and $\omega(\zeta)$, which are holomorphic, single valued in the region of interest in ζ, and give bounded stresses as $\zeta \to \infty$ can be chosen as shown below.

$$\Omega(\zeta) = \frac{C(M_1 + M_2)}{16(D_{11} + D_{12})}(e^{\zeta} + \bar{e}^{\zeta}) + \frac{2(\alpha_1 + i\beta_i)}{CD_{11}} \bar{e}^{\zeta}, \quad (5.32)$$

$$\omega(\zeta) = \frac{C^2(M_1 - M_2)}{32(D_{11} - D_{12})} e^{-2i\alpha}(e^{2\zeta} + \bar{e}^{2\zeta} + 2) + K'\zeta + \frac{4(\alpha_4 + i\beta_4)}{D_{11}C^2} \bar{e}^{2\zeta} \quad (5.33)$$

In these equations C is the focal length of the elliptical hole, which is used to mandate the size of the hole and α_1, β_1 K', α_4, and β_4 are constants which will be determined from boundary conditions.

Now one important problem still remaining.is finding a solution to the Helmholtz equation in elliptical coordinate system. The basic difficulty here is that the solution of the Helmholtz equation in a region of ζ-plane cannot be obtained from a region of Z-plane by the usual conformal mapping techniques. Therefore, it is necessary to solve the Helmholtz equation directly in the elliptical

coordinate system. From Eq. (5.31) it follows that

$$\frac{\partial}{\partial Z} = \frac{1}{2C \sin\zeta}\left(\frac{\partial}{\partial \zeta} - i\,\frac{\partial}{\partial \eta}\right), \frac{\partial}{\partial \bar{Z}} = \frac{1}{2C \sin\bar{\xi}}\left(\frac{\partial}{\partial \zeta} + i\,\frac{\partial}{\partial \eta}\right). \qquad (5.34)$$

Now the Helmholtz Eq. (4.16) can be expressed in terms of elliptical coordinates by using Eq. (5.34) and the mapping function of Eq. (5.31). After some manipulations, the final results expressed in the following form are obtained:

$$\frac{\partial \chi_o}{\partial \xi^2} + \frac{\partial^2 \chi_o}{\partial \eta^2} - 2q(\cosh 2\xi - \cos 2\eta)\chi_o = 0, \qquad (5.35)$$

where $q = \frac{KC^2}{4P_{66}}$. Eq. (5.35) can be solved by the technique of separation of variables in terms of Mathieu equations, which have the form

$$\frac{d^2\psi(\eta)}{d\eta^2} + (a + 2q\cos 2\eta)\psi(\eta) = 0, \qquad (5.36)$$

$$\frac{d^2\phi(\xi)}{d\xi^2} - (a + 2q\cosh 2\xi)\phi(\xi) = 0, \qquad (5.37)$$

and

$$\chi_o = \psi(\eta)\phi(\zeta) \; . \qquad (5.38)$$

The constant a in Eqs.(5.36) and (5.37) is often referred to as a separation constant; in general it is a function of q. For some

physically important solutions, the function $\psi(\eta)$ must be periodic, of period π or 2π. It can be shown that there exists a countably infinite set of characteristic values $a_r(q)$, which yield even periodic solutions to Eq. (5.36); and another countably infinite sequence of characteristic values $b_r(q)$ exists, which yield odd periodic solutions to Eq. (5.36). These characteristic values are of basic importance in obtaining the general solution of the differential equation for arbitrary parameters a and q.

Eq. (5.36) is called Mathieu's equation, and Eq. (5.37) is called the modified Mathieu's equation. Solutions for both equations can be derived as indicated in reference [35]. In the interest of brevity the theory of these differential equations and the procedures to derive their solutions are not presented. Instead, the final solution of Eq. (5.35) is given as

$$\chi_o = \sum_{n=0}^{\infty} \tilde{C}_n' F_e k_n(\xi, -q) C_{en}(\eta, -q) + \sum_{n=1}^{\infty} \tilde{C}_n G_e k_n(\xi, -q) S_{en}(\eta, -q) \quad (5.39)$$

where $\tilde{C}_n'$ and $\tilde{C}_n$ are arbitrary constants. The functions $C_{en}(\eta, -q)$ and $S_{en}(\eta, -q)$ are called Mathieu functions of the first kind akin to trigonometric cosine and sine functions. The functions $F_e k_n(\xi, -q)$ and $G_e k_n(\xi, -q)$ are called Mathieu functions of second kind and are akin to Bessel functions.

The functions $C_{en}(\eta, -q)$ and $S_{en}(\eta, -q)$ will decay to become $\cos(n\eta)$ and $\sin(n\eta)$, respectively, when q approaches zero. The

functions $F_e k_n(\xi, -q)$ and $G_e k_n(\xi, -q)$ become proportional to modified Bessel functions I_n and K_n, depending on whether q is positive or negative as ξ tends to infinity. However, when ξ becomes a small value, the functions $F_e k_n(\xi, -q)$ will remain finite, while $G_e k_n(\xi, -q)$ becomes infinite. For convenience in future analysis, Eq. (5.29) is rewritten as

$$\chi_o = \sum_0^\infty C'_{2n} \frac{F_e k_n(\xi, -q)}{F_e k_n(\xi_o, -q)} C_{en}(\eta, -q) + \sum_1^\infty C_{2n} \frac{G_e k_n(\xi, -q)}{G_e k_n(\xi_o, -q)} S_{en}(\eta, -q) \tag{5.40}$$

where ξ_o is the value of ξ at the edge of the hole. Again, C_{2n} and C'_{2n} are arbitrary real constants that are determined from the boundary conditions. Now the boundary conditions at the hole edge given in Eqs. (4.53) and (4.52) can be expressed in terms of the complex variable ζ as

$$\chi_o(\zeta) + i \frac{4D_{11}}{K}\left[\frac{\bar{\Omega}'(\bar{\zeta})}{\bar{F}'(\bar{\zeta})} - \frac{\Omega'(\zeta)}{F'(\zeta)}\right] = 0 \tag{5.41}$$

$$-2(3D_{11} + D_{12})\Omega(\zeta) + 4D_{66}\left[\frac{\bar{\omega}'(\bar{\zeta})}{\bar{F}'(\bar{\zeta})} + F(\zeta)\frac{\bar{\Omega}'(\bar{\zeta})}{\bar{F}'(\bar{\zeta})}\right] + \frac{16D_{11}P_{66}}{K[\bar{F}'(\bar{\zeta})]^3}$$

$$[\bar{F}'(\bar{\zeta})\bar{\Omega}''(\zeta) - \bar{\Omega}'(\bar{\zeta})\bar{F}''(\bar{\zeta})] - 4P_{66} i \frac{\partial \chi_o}{\partial \bar{\zeta}} \frac{1}{\bar{F}'(\bar{\zeta})} = 0. \tag{5.42}$$

By substituting as indicated into Eq. (5.41), the following algebraic equation is obtained:

$$C_2' C_{e2}(\eta, -q) + C_2 S_{e2}(\eta, -q) - \frac{32}{kC^2} \sum_{r=0}^{\infty} e^{-2r\xi_o} (\beta_1 \cos 2r\eta - \alpha_1 \sin 2r\eta) = 0. \tag{5.43}$$

As in reference [36], $S_{e2}(\eta, -q)$ and $C_{e2}(\eta, -q)$ are expressed as

$$S_{e2}(\eta, -q) = \sum_{r=0}^{\infty} (-1)^r B_{2r+2}^2 \sin(2r + 2)\eta,$$

$$C_{e2}(\eta, -q) = \sum_{r=0}^{\infty} (-1)^r A_{2r+2}^2 \cos(2r + 2)\eta \tag{5.44}$$

where B_{2r+2}^2 and A_{2r+2}^2 are called normalized Fourier coefficients in the series expansions of $S_{e2}(\eta, -q)$ and $C_{e2}(\eta, -q)$ in terms of the functions $\sin(2r + 2)\eta$ and $\cos(2r + 2)\eta$, respectively. Taking advantage of the orthogonality properties of $S_{e2}(\eta, -q)$ and $C_{e2}(\eta, -q)$, the coefficients C_2' and C_2 are obtained as follows:

$$C_2 = \frac{32\alpha_1 \sum_{r=0}^{\infty} (\lambda)^r e^{-(2r+2)\xi_o} B_{2r+2}}{kC^2 \sum_{r=0}^{\infty} \left(B_{2r+2}^2\right)^2},$$

$$C_2' = \frac{32\beta_1 \sum_{r=0}^{\infty} (\lambda)^r e^{-(2r+2)\xi_o} A_{2r+2}^2}{kC^2 \sum_{r=0}^{\infty} \left(A_{2r+2}^2\right)^2} \tag{5.45}$$

Or, upon simplifying, they become

$$C_2 = \frac{32e^{-2\xi_o} B_{2r+2}^2 \alpha_1}{kC^2 \sum_{r=0}^{\infty} (B_{2r+2}^2)^2},$$

$$C_2' = \frac{32e^{-2\xi_o} A_{2r+2}^2 \beta_1}{kC^2 \sum_{r=0}^{\infty} (A_{2r+2}^2)^2} \qquad (5.46)$$

Now the remaining constants α_1, β_1, α_4, β_4, and K' are determined from the boundary condition Eq. (5.42) by substituting Eqs. (5.32) and (5.33) and the mapping function given in Eq. (5.31) into Eq. (5.42). After some tedious manipulations and reductions, the values of these constants are finally obtained as

$$\alpha_1 = \frac{C^2}{32}\bar{\bar{A}}_2 = \frac{C^2 \frac{1}{2}\left[(M_1 + M_2) - (M_1 - M_2)e^{2\xi_o} e^{2i\alpha}\right]}{32\left[\frac{3D_{11} + D_{12}}{4D_{11}} + \frac{4P_{66}}{kC^2} e^{-2\xi_o}\left(2 + \frac{G_e k_2'}{G_e k_2}\right)\right]}, \quad \beta_1 = 0,$$

$$K' = -\frac{C^2(M_1 + M_2)}{8(D_{11} - D_{12})} \sinh 2\xi_o$$

$$- \frac{C^2(D_{11} + D_{12})\left[(M_1 + M_2)e^{-2\xi_o} - (M_1 - M_2)e^{2i\alpha}\right]}{16(D_{11} - D_{12})\left[(3D_{11} + D_{12}) + \frac{16D_{11}P_{66}}{kC^2} e^{-2\xi_o}\left(2 + \frac{G_e k_2'}{G_e k_2}\right)\right]},$$

$$\alpha_4 - i\beta_4 = \frac{D_{11}C^4}{128(D_{11} - D_{12})}\left[-(M_1 + M_2)e^{+2\xi_o} + (M_1 - M_2)e^{2i\alpha}\right]$$

$$- \left[\frac{C^4 e^{2\xi_o}}{256} + \frac{C^2 D_{11} P_{66}}{16k(D_{11} - D_{12})}\left(2 + \frac{G_e k_2'}{G_e k_2}\right)\right] = A_2 \qquad (5.47)$$

with

$$\frac{G_e k_2'}{G_e k_2} \equiv \frac{G_e k_2'(\xi_o, -q)}{G_e k_2(\xi_o, -q)} .$$

Now, with these constants given as stated in Eqs. (5.47), the function χ_o and complex potential functions $\Omega(\zeta)$ and $\omega(\zeta)$ for elliptical holes are determined. Then the stresses and displacements of the problem are found through Eqs. (4.41) and (4.29b) given in the previous chapter. However, for this problem, the stresses near the edge of the hole are more important than those elsewhere. As stated in Chapter IV the stress couple around the edge of the hole is given as

$$M_\eta = -4(D_{11} + D_{12})[\Omega'(\zeta)/F'(\zeta) + \bar{\Omega}'(\bar{\zeta})/\bar{F}'(\bar{\zeta})], \text{with } \xi = \xi_o \qquad (5.48)$$

With the known potential function $\Omega(\zeta)$ and mapping function $F(\zeta)$, Eq. (5.48) for this case can be expressed as follows:

$$M_\eta(\xi_o, \eta) = (M_1 + M_2) + \frac{D_{11} + D_{12}}{2D_{11}} \frac{\left(\frac{M_1 + M_2}{2} - \frac{M_1 - M_2}{2} e^{2\xi_o} e^{2i\alpha}\right)(\cos 2\eta - e^{-2\xi_o})}{\left[\frac{3D_{11} + D_{12}}{4D_{11}} + \frac{4P_{66}}{kC^2} e^{-2\xi_o}\left(2 + \frac{G_e k_2'}{G_e k_2}\right)\right](\cosh 2\xi_o - \cos 2\eta)} \tag{5.49}$$

Considering the case of $M_1 = M_o$, $M_2 = 0$, and $\alpha = 0$, the following is obtained:

$$\frac{M_\eta(\xi_o, \eta)}{M_o} = 1 + \frac{(D_{11} + D_{12})(\cos 2\eta - e^{-2\xi_o})\tilde{\tilde{A}}_2^*}{2D_{11}(\cosh 2\xi_o - \cos 2\eta)} \tag{5.50}$$

where $\tilde{\tilde{A}}_2^*$ is defined as

$$\tilde{\tilde{A}}_2^* \quad \frac{\frac{1}{2}\left(1 - e^{2\xi_o}\right)}{\frac{3D_{11} + D_{12}}{4D_{11}} + \frac{4P_{66}}{kC^2} e^{-2\xi_o}\left(2 + \frac{G_e k_2'}{G_e k_2}\right)} \; .$$

Eq. (5.50) gives the moment distribution around an elliptical hole in an infinite composite plate under pure bending along the edge of x = constant. When the laminated composite plate reduces to a single-layer of homogeneous material, the previous relation given in Eq. (5.15) holds. Consequently, for this case Eq. (5.50) becomes

$$\frac{M_\eta(\xi_o, \eta)}{M_o} = 1 + \frac{1+\nu}{2} \frac{\frac{1}{2}(1 - e^{2\xi_o})(\cos 2\eta - e^{-2\xi_o})}{\left[\frac{3+\nu}{4} + \frac{2h^2}{5C^2} e^{-2\xi_o}\left(2 + \frac{G_e k_2'}{G_e k_2}\right)\right](\cosh 2\xi_o - \cos 2\eta)} \tag{5.51}$$

Note that Eq. (5.51) is the solution given by Naghdi [34]. In comparing the solution for a single-layer plate with that for a laminated composite plate, it should be noted that the same results as stated in the previous section hold; the Young's modulus as well as the Poisson's ratio affect the stress distribution. The expressions for the shear forces, Q_η and Q_ξ can also be calculated from Eqs. (4.40) and (4.41). Around the perimeter of the hole edge, the shear force Q_η is more significant than Q_ξ; therefore, only the expression for Q_η is calculated. From Eqs. (5.47), (5.40), (5.32), and (5.33) and Eqs. (4.40) and (4.41), the final expression for Q_η is obtained as

$$\frac{Q_\eta}{M_o} = -\frac{\frac{1}{2}(1 - e^{2\xi_o})e^{-2\xi_o}\left(2 + \frac{G_e k_2'}{G_e k_2}\right)\sin 2\eta}{\left[\frac{3D_{11} + D_{12}}{4D_{11}} + \frac{4P_{66}}{kC^2} e^{-2\xi_o}\left(2 + \frac{G_e k_2'}{G_e k_2}\right)\right]J^{\frac{1}{2}}} \tag{5.52}$$

where J is defined as $C^2 \sinh\zeta \sinh\bar{\zeta}$.

Again, for a single-layer composite plate, the shear force Q_η around the hole edge is obtained by degenerating Eq. (5.52) through the use of Eq. (5.15). The final expression is

$$\frac{Q_\eta}{M_o} = -\frac{\frac{1}{2}(1 - e^{2\xi_o})e^{-2\xi_o}\left(2 + \frac{G_e k_2'}{G_e k_2}\right)\sin 2\eta}{\left[\frac{3+\nu}{4} + \frac{2h^2}{5C^2}e^{-2\xi_o}\left(2 + \frac{G_e k_2'}{G_e k_2}\right)\right]J^{\frac{1}{2}}} \qquad (5.53)$$

Again, this agrees with the solution given by Naghdi [34].

For the following discussion and comparative study, Eqs. (5.50) and (5.52) are rewritten in terms of the parameters of the major and minor axes of the elliptical hole. Suppose that α and β are the ratios of h/a and b/a, respectively; where a is a semi-major axis and b is a semi-minor axis. They are related to the parameter ξ_o through

$$a = C \cosh \xi_o, \quad b = C \sinh \xi_o . \qquad (5.54)$$

Then Eqs. (5.50) and (5.52) can be expressed in terms of α and β as follows:

$$\frac{M_\eta}{M_o} = 1 + \frac{\left(\frac{D_{11}+D_{12}}{2D_{11}}\right)\beta[(1-\beta) - (1+\beta)\cos 2\eta]}{\left[\frac{3D_{11}+D_{12}}{4D_{11}} + \left(\frac{4P_{66}}{kA^2}\right)\frac{1}{(1+\beta)^2}\left(2 + \frac{G_e k_2'}{G_e k_2}\right)\right][(1+\beta^2) - (1-\beta^2)\cos 2\eta]} \qquad (5.55)$$

$$\frac{Q_\eta}{\frac{M_o}{a}} = \frac{\sqrt{2\beta}\left(2 + \frac{G_e k_2'}{G_e k_2}\right)\sin 2\eta}{\left[\frac{3D_{11}+D_{12}}{4D_{11}} + \frac{4P_{66}}{ka^2(1+\beta)^2}\left(2 + \frac{G_e k_2'}{G_e k_2}\right)\right](1+\beta)[(1+\beta^2) - (1-\beta^2)\cos 2\eta]^{\frac{1}{2}}} \qquad (5.56)$$

Eqs. (5.55) and (5.56) are much more convenient than Eqs. (5.50) and (5.52) for studying the following special cases:

Case a - the case where $\xi_0 \to \infty$, that is, the case where the elliptical hole tends to be a circular hole (see Figure 23). From reference [39], the functions below behave as indicated:

$$G_e k_2(\xi, -q) \to \frac{S_2'}{\pi} K_2(qe^{\xi}) = \frac{S_2'}{\pi} K_2(\lambda r)$$

$$G_e k_2'(\xi, -q) \to \frac{S_2'}{\pi} qe^{\xi} K_2'(qe^{\xi}) = \frac{S_2'}{\pi} \lambda r K_2'(\lambda r) \text{ as } \xi \to \infty,$$

where S_2' is a constant defined in references [36] and [35]. Now for this case, $a = \frac{c}{2}(e^{\xi_0} + e^{-\xi_0}) \to r_0$, $b = \frac{c}{2}(e^{\xi_0} - e^{-\xi_0}) \to r_0$ as $\xi_0 \to \infty$. Therefore,

$$\frac{G_e k_2'(\xi_0, -q)}{G_e k_2(\xi_0, -q)} \to \lambda r_0 \frac{K_2'(\lambda r_0)}{K_2(\lambda r_0)}$$

where K_2 is a modified Bessel function of second kind, and K_2' is the derivative of K_2 with respect to its argument. For this case, the value of β is equal to one. Then Eqs. (5.55) and (5.56) become

$$\frac{M_\eta}{M_0} = 1 + \frac{(D_{11} + D_{12})K_2(\lambda r_0)}{(D_{11} + D_{12})K_2(\lambda r_0) + 2D_{11}K_0(\lambda r_0)} \cos 2\eta$$

$$\frac{Q_\eta}{\left(\frac{M_0}{r_0}\right)} = -\frac{2D_{11}\lambda r_0 K_1(\lambda r_0)}{(D_{11} + D_{12})K_2(\lambda r_0) + 2D_{11}K_0(\lambda r_0)} \sin 2\eta \quad (5.57)$$

Recalling Eq. (5.12), it can be seen that Eq. (5.57) is exactly the same expression as (5.12).

Case b - the classical laminated composite plate solution can also be derived from Eqs. (5.55) and (5.56). From Table III note that the value of λ(i.e., ka^2/P_{66}) increases in magnitude of order (2/h) with decreasing plate thickness. Therefore, if the hole dimension is specified for the case of $h << 1$, then the term P_{66}/ka^2 in Eq. (5.55) and (5.56) will approach zero. For this case, Eq. (5.55) then becomes

$$\frac{M_\eta}{M_o} = 1 + \frac{2(D_{11} + D_{12})\beta[(1 - \beta) - (1 + \beta)\cos 2\eta]}{(3D_{11} + D_{12})[(1 + \beta^2) - (1 - \beta^2)\cos 2\eta]} \quad (5.58)$$

Eq. (5.58) is a solution of classical lamination theory. In order to make a comparison with the solution for a homogeneous single-layer classical plate given in reference [20](page 231), a new parameter ε is introduced, defined as

$$\varepsilon = \frac{a - b}{a + b} = \frac{\cosh \xi_o - \sinh \xi_o}{\cosh \xi_o + \sinh \xi_o} = e^{-2\xi_o} = \frac{1 - \beta}{1 + \beta} \quad (5.59)$$

Introducing the parameter ε and the relationship in Eq. (5.15) for a single-layer composite plate, Eq. (5.58) becomes

$$\frac{M_\eta}{M_o} = 1 + \frac{2(1 + \nu)(1 - \varepsilon)(\varepsilon - \cos 2\eta)}{(3 + \nu)(\varepsilon^2 - 2\varepsilon \cos 2\eta + 1)} \quad (5.60)$$

This solution was given by Savin [20] for a single-layer classical plate. Notice from either Eq. (5.58) or (5.60) that the effects of the plate thickness are not included. Hence, as long as the eccentricity of the ellipse is specified, the stress distribution given by classical lamination theory is not influenced by the size of the hole. Figure 24 compares the deviation between the classical lamination theory and the present theory. Unlike the circular hole case, for the elliptical hole the limiting case of vanishing hole size is not provided. This case is difficult to obtain from the expression presented because of the lack of information in the recurrence relation on the Mathieu function $G_e k_2$.

Figure 24 shows $M_\eta(\xi_o, \pi/2)/M_o$ versus a/h for St/Al/St and Al/St/Al laminated composite plates. The result is the same as that for the circular hole case - that is, the hard-core sandwich plate has a lower stress concentration factor than the soft-core sandwich. This figure also presents the solution by classical lamination theory for a Al/St/Al sandwich plate. Note that the deviation of Eq. (5.50) from Eq. (5.58) is vast since the value of a/h is less than one. Figures 25 through 30 present the distributions of $M_\eta(\xi_o, \eta)/M_o$ around a hole with the same eccentricity but of different hole sizes. The solid line is for a (St/Al/St) sandwich plate, and the broken line is for a (Al/St/Al) sandwich plate. The applied moment in Figures 25 through 26 is along the edge which is perpendicular to the major axis of the elliptical hole, whereas for Figures 29 through 30 it is along the edge that

is parallel to the major axis of the hole. It is also noteworthy to examine the stress distribution through the plate thickness. It provides information on the mechanism for transferring stress from layer to layer. Using the procedure employed for the case of the circular hole, the normal and shear stresses at the hole edge are calculated as

$$\left(\frac{\sigma_\eta^i}{M_o}\right)_{\xi_o} = \frac{z\, E^i}{1 - \nu^i}\left[\frac{M_1 + M_2}{D_{11} + D_{12}} + \frac{\approx{A}_2^*}{2D_{11}}\,\frac{\cos 2\eta - e^{-2\xi_o}}{\cosh 2\xi_o - \cos 2\eta}\right] \quad (5.61)$$

and

$$\left(\frac{\tau_{\eta z}}{M_o}\right)_{\xi_o} = -\frac{\approx{A}_2^* e^{-2\xi_o}}{J^{1/2}k}\left[\frac{G^i}{2}\left(\frac{h^2}{4} - z^2\right) + A_i\right]\left(2 + \frac{G_e k_2'}{G_e k_2}\right)\sin 2\eta. \quad (5.62)$$

The numerical results of Eq. (5.61) for a (St/Al/St) laminated composite plate with a 0.5% volume fraction are given in Figure 31. The ratio of the major axis to the minor axis is 1.22. The stress was computed at the point $\eta = 90°$. It may be noted that the finite element solution and analytical results agree.

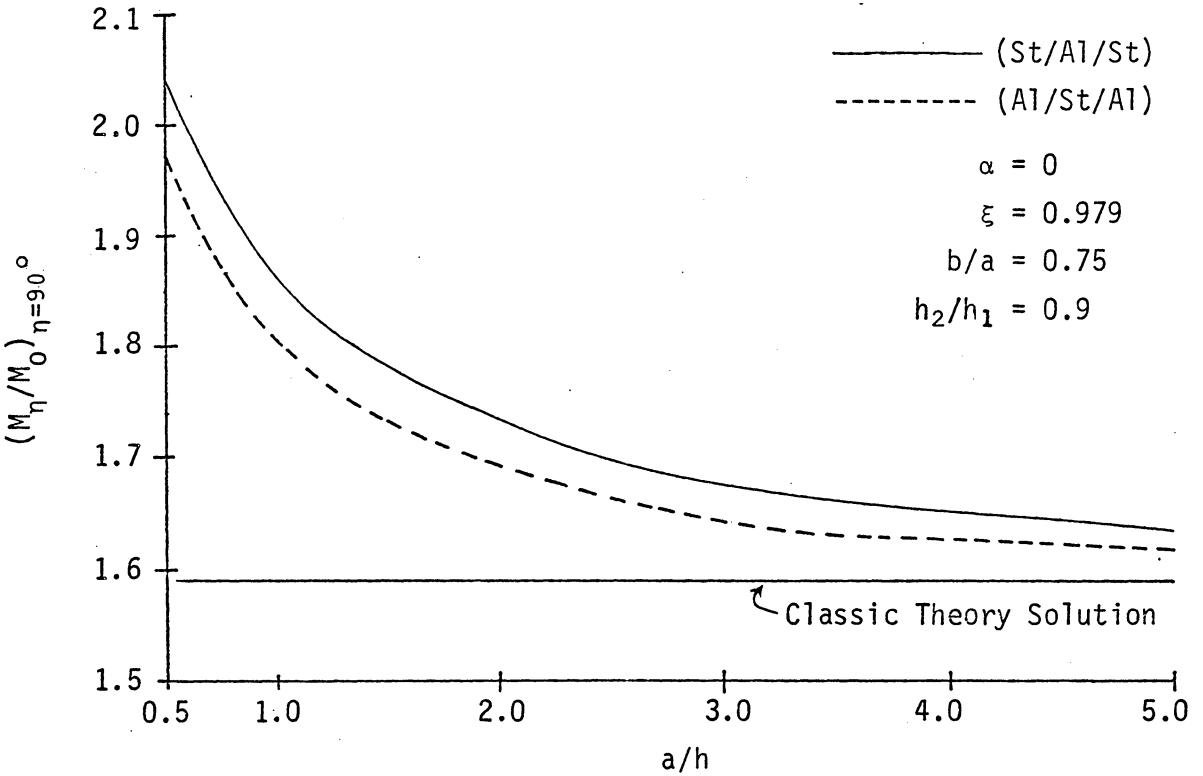

Figure 24. Variation of M_η/M_o Vs a/h for Elliptical Hole in Sandwich Plate

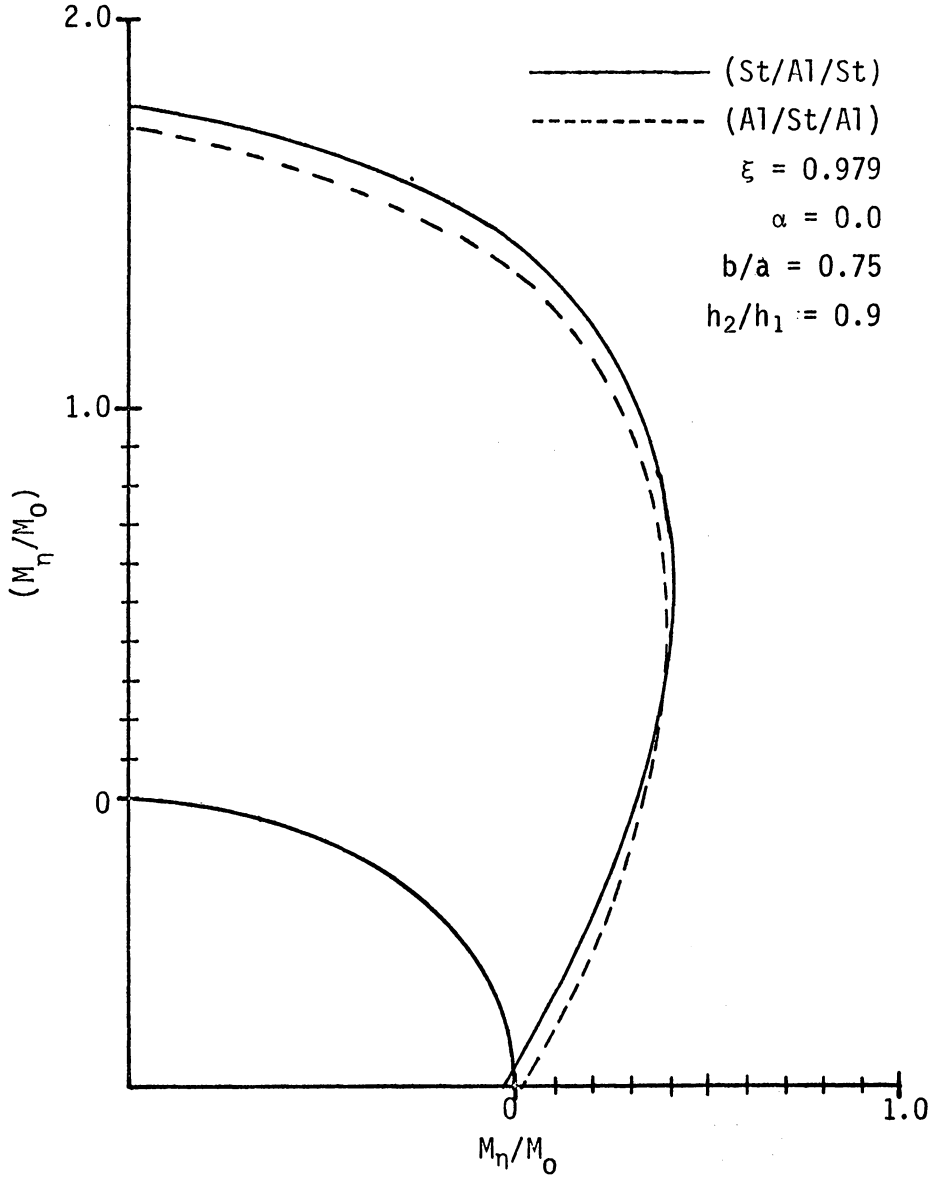

Figure 25. Variation of M_η/M_o Around Elliptical Hole in Sandwich Plate With a/h = 0.759

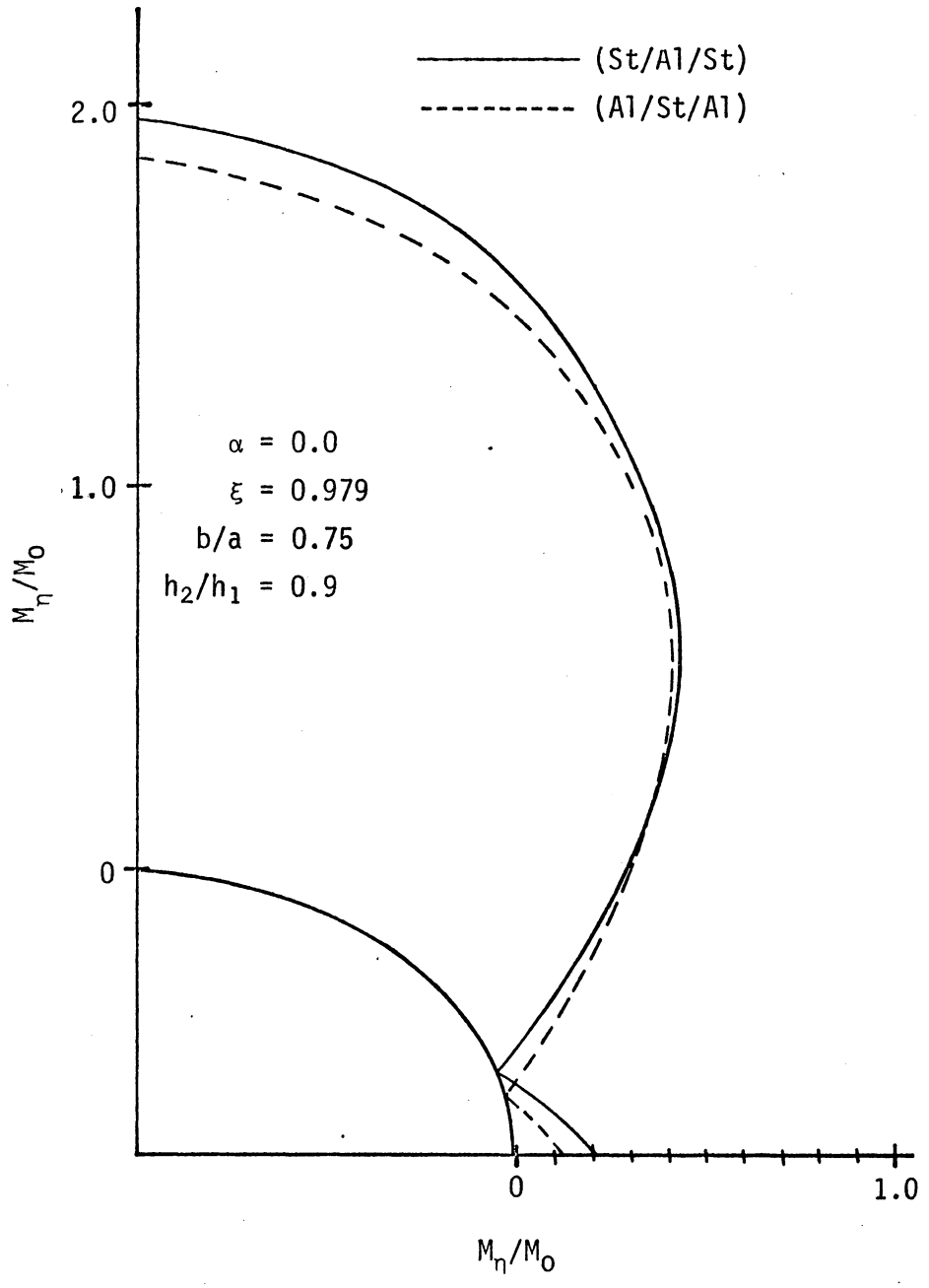

Figure 26. Variation of M_η/M_o Around Elliptical Hole in Sandwich Plate With a/h = 0.759

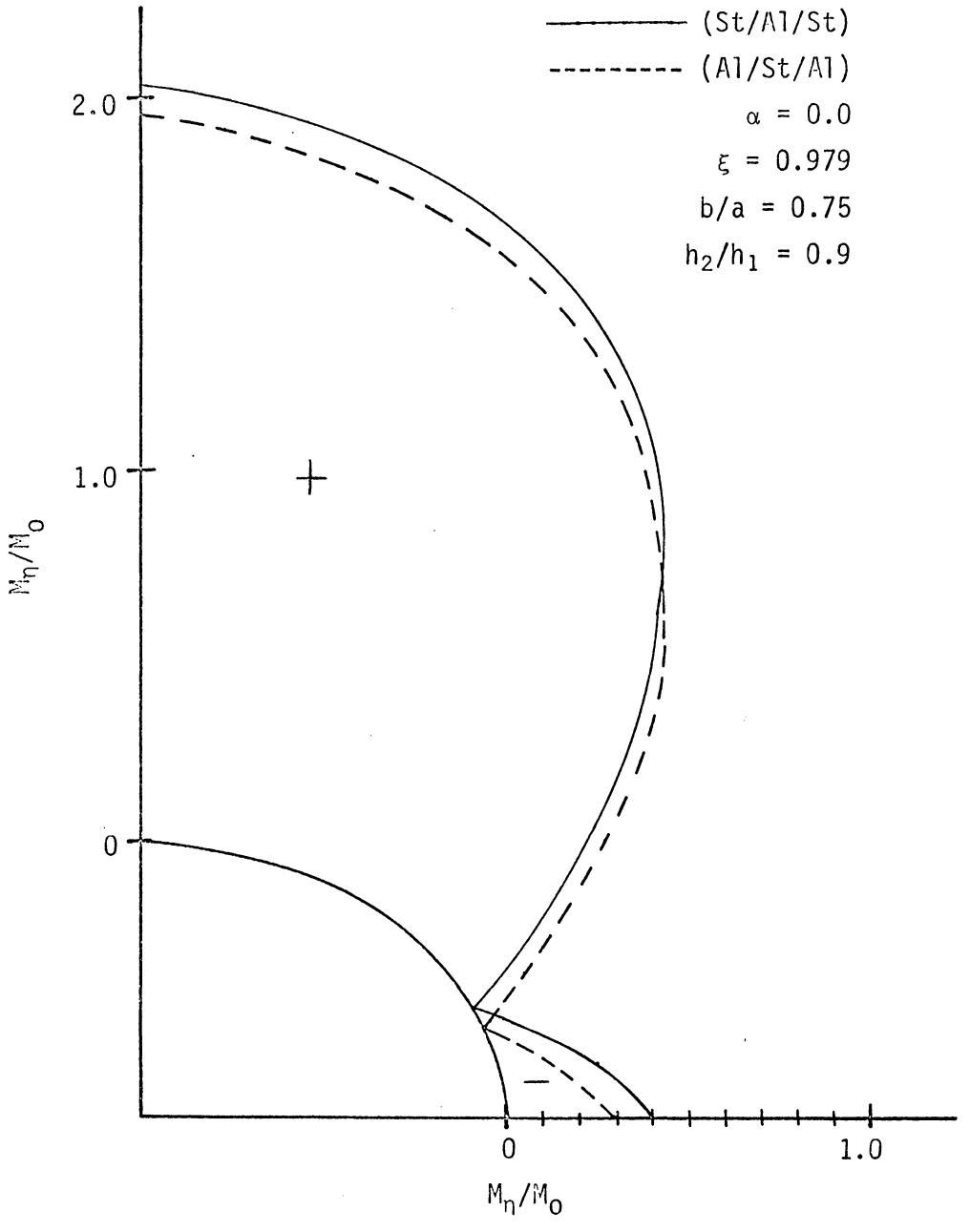

Figure 27. Variation of M_η/M_o Around Elliptical Hole in Sandwich Plate With a/h = 0.5

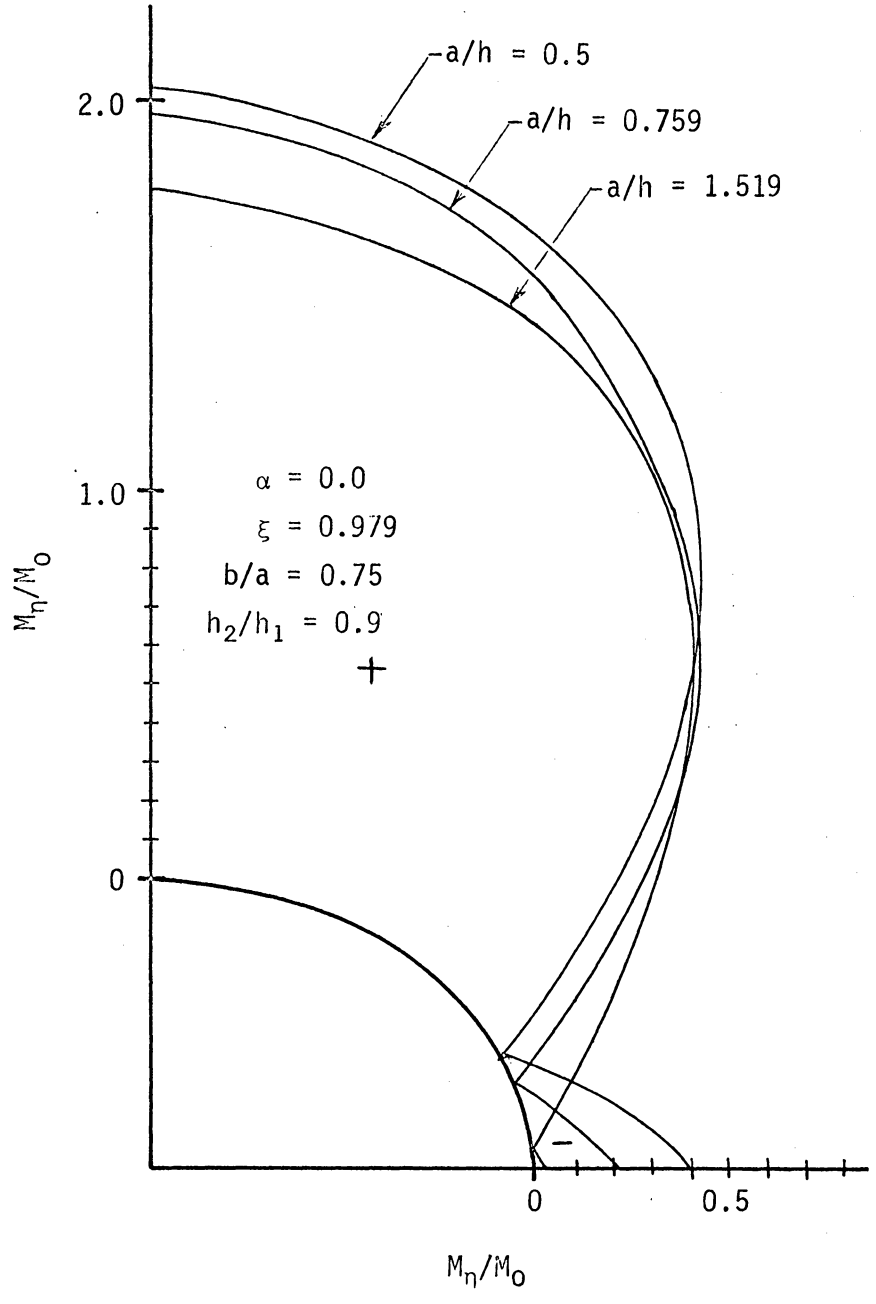

Figure 28. Variation of M_η/M_o Around Elliptical Hole in $(St/Al)_s$ Laminated Composite Plate With Different a/h Ratios

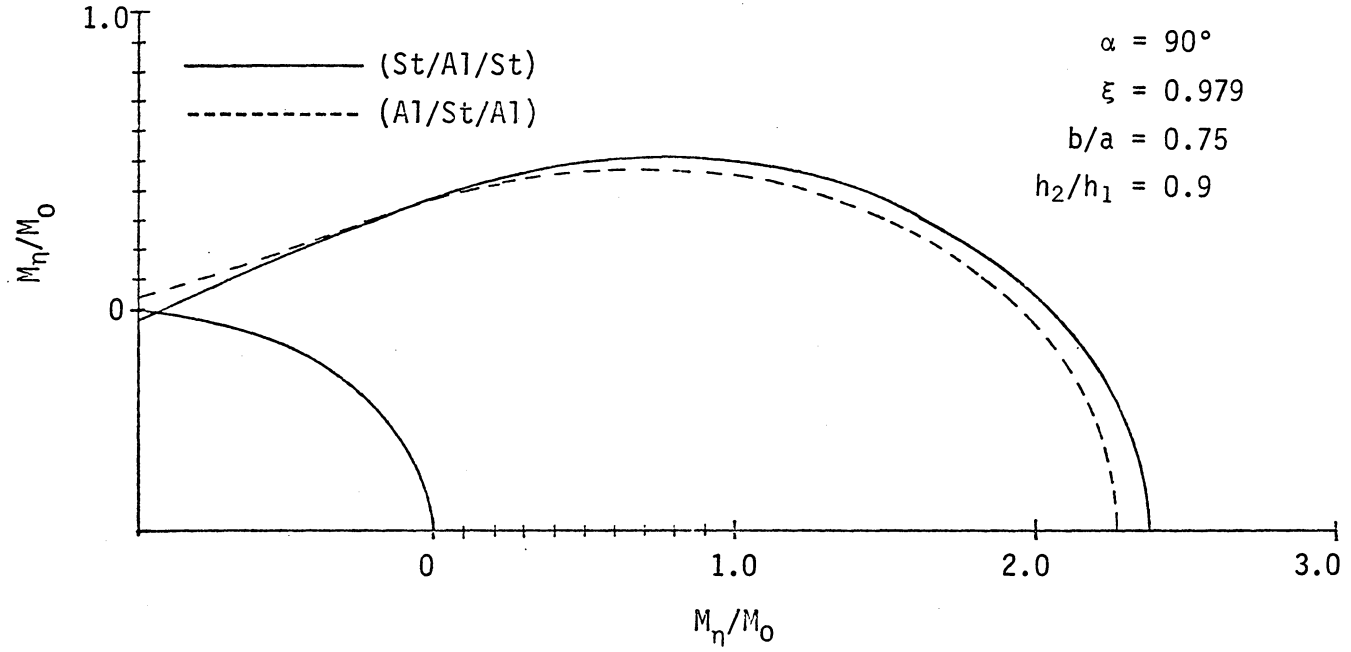

Figure 29. Distribution of M_η/M_o Around Elliptical Hole in Sandwich Plate With a/h = 1.519 With Moment Applied on Edges of Constant y

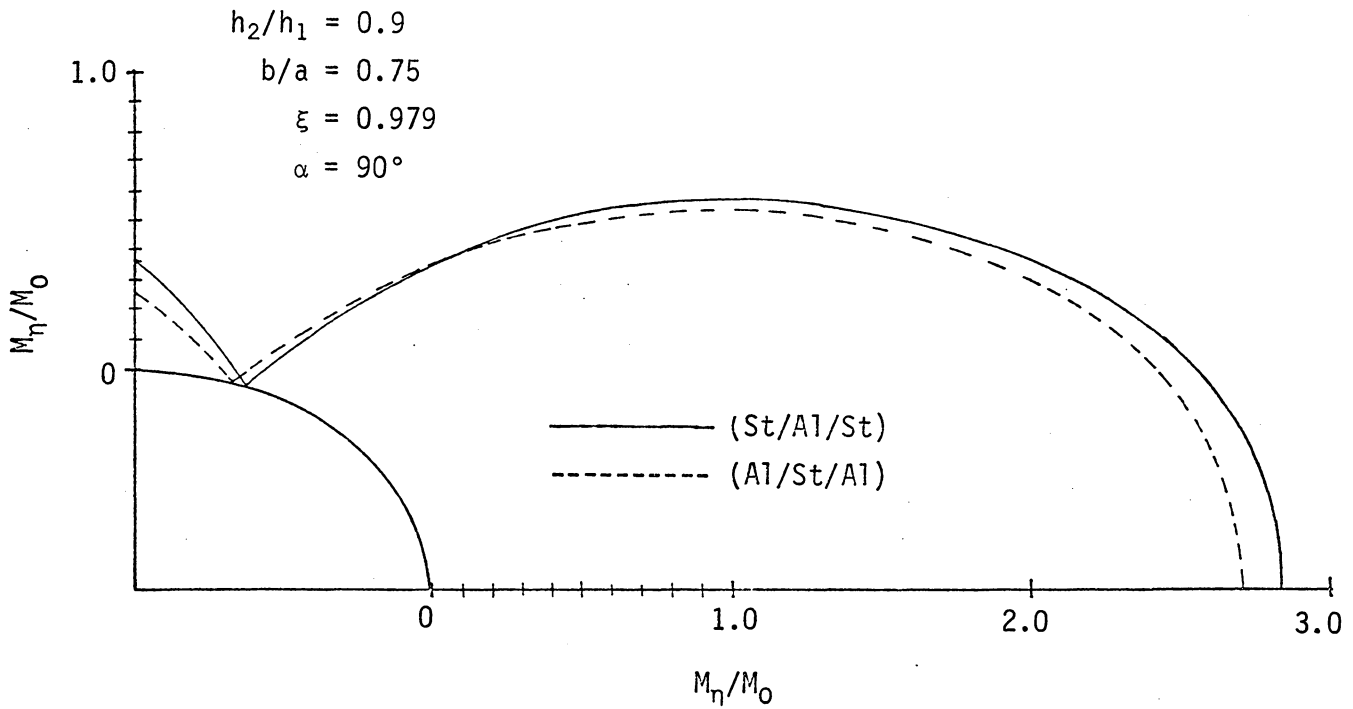

Figure 30. Distribution of M_η/M_o Around Elliptical Hole in Sandwich Plate With a/h = 0.5 With Moment Applied on Edges of Constant y

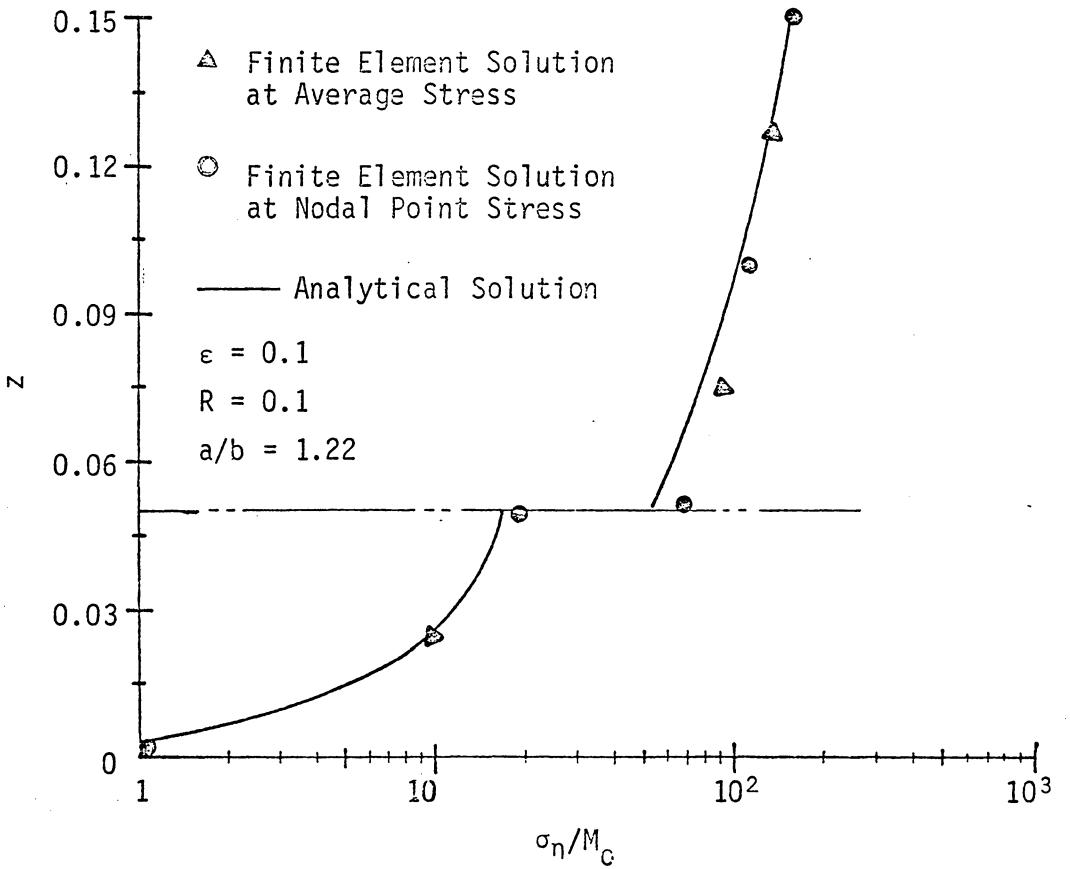

Figure 31. Distribution of σ_η/M_0 Through Plate Thickness at Elliptical Hole in $(St/Al)_S$ Sandwich Plate for Finite Element and Analytical Solutions

VI. CURVILINEAR HOLE CASE

6.1. Introduction

It is obvious from Chapter V that the solution of the Helmholtz equation depends on the coordinate system selected. For the case of a circular hole, a polar coordinate system was used, and the Helmholtz equation in the polar coordinates was transformed to a modified Bessel equation. This equation, its solution, and properties are well known and have been widely reported. However, for the case of an elliptical hole, an elliptical coordinate system was used because of its convenience; and the Helmholtz equation in this coordinate system was separated into Mathieu and modified Mathieu functions as shown in Eqs. (5.95) and (5.96). Therefore, the basic difficulty in using theory presented herein compared to the corresponding classical Kirchhoff theory, is the necessity of solving the Helmholtz equation by the method of separation of variables for different coordinate systems.

In view of this, for a simply connected region the solution of Eqs. (4.14) can be obtained only for circular and elliptical holes. However, in the latter case an infinite system of algebraic equations arise and it is necessary to expand the Mathieu functions in terms of trigonometric functions in order to match the solution of the biharmonic equation on the boundary. Therefore,

it is more profitable, when solving Eqs. (4.14) for curvilinear holes, including elliptical holes, to use the method of "boundary shape perturbation." This method was proposed earlier by Lekhnitky [21] and was continuously extended by Savin [20],[37]. The method to be used here will be the same as that used by Savin on the stress concentrations near an arbitrary hole whose contours have no angular points.

By using the boundary shape perturbation method, the difficulty mentioned above can be avoided. The solution of the system of Eqs. (4.14) for a curvilinear hole can be obtained approximately by the series of solutions for circular holes by selecting an appropriate mapping function.

6.2. Methods of Analysis

Next, a mapping function (transformation equation) is introduced that will conformally map the exterior of the unit circle into a region representing the exterior of the hole under consideration. This mapping function is given in the form

$$Z = \Omega(\zeta) \tag{6.1}$$

with $Z = Re^{i\theta}$, $Z = x + iy$, and $\zeta = \rho e^{i\theta}$. For convenience in later analysis, a dimensionless quantity is introduced as follows:

$$z_o = \frac{Z}{r_o} = x_o + iy_o = re^{i\theta} \tag{6.2a}$$

and

$$z_0 = \omega(\zeta) = \zeta + \varepsilon f(\zeta) \tag{6.2b}$$

where $r = R/r_0$, The function $\omega(\zeta)$ was given by Savin [38] and Muskelishnili [31]. The function $f(\zeta)$ is a holonomic function at infinity. The parameter ε is assumed to be a real constant; its value is within the range $0 < \varepsilon << 1$, and it is designed to characterize the degree of deviation of the examined hole from a circular hole. Using the equations above, Eq. (6.2) can be rewritten in the parametric form as

$$\begin{aligned} x_0 &= \cos\theta + \frac{\varepsilon}{2}(f + \overline{f}), \\ y_0 &= \sin\theta - i\,\frac{\varepsilon}{2}(f - \overline{f}) \end{aligned} \tag{6.3}$$

where $\overline{f}$ is the conjugate function of $f(\zeta)$. Eqs. (6.3) represent a curvilinear, orthogonal coordinate system with coordinate curves of ρ = constant and θ = constant, as shown in Figure 32. The angle θ can be found from Eq. (6.3), expressed as

$$\theta = \tan^{-1}\frac{y_0}{x_0} = \tan^{-1}\frac{\sin\theta - \frac{i\varepsilon}{2\rho}(f - \overline{f})}{\cos\theta + \frac{\varepsilon}{2\rho}(f + \overline{f})} \tag{6.4}$$

As for the angle α shown in Figure 32, it is found by the following

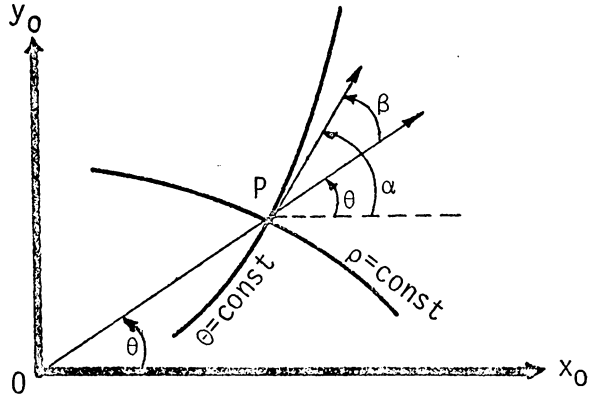

Figure 32. Curvilinear Coordinates (ρ, Θ, z)

procedure. First, differentiate Eq. (6.2) along the curve Θ = constant; thus, an expression for dz_0 is obtained as

$$dz_0 = \omega'(\zeta)e^{i\Theta}d\rho. \tag{6.5}$$

Then, from the relation $dz_0 = |dz_0|e^{i\alpha}$, with the value of dz_0 given by Eq. (6.5), the following expression of $e^{i\alpha}$ is obtained:

$$e^{i\alpha} = \frac{\zeta\omega'(\zeta)}{\rho|\omega'(\zeta)|} \tag{6.6}$$

where the $|\omega'(\zeta)|$ is the absolute value of the function $\omega'(\zeta)$, which is equal to $[\omega'(\zeta)\overline{\omega'(\zeta)}]^{1/2}$. Obviously, the expression for the angle β may now be obtained. It is written as

$$e^{i\beta} = \frac{\zeta\omega'(\zeta)\overline{\omega(\zeta)}}{\rho[\bar{\omega}'(\zeta)\omega'(\zeta)]^{1/2}} \tag{6.7}$$

6.3. Perturbation Expansion

So far the angles α, β, and θ have been presented in terms of a mapping function. It can be inferred from these results that all magnitudes which depend on r and θ can be expanded in powers of the small parameter ε. Before proceeding with the analysis, the coordinates r and θ must be expressed in terms of the small parameter ε. From Eq. (6.3), by taking the square root of the sum of x^2 and y^2, an expression for γ may be obtained in the form

$$\gamma = [\rho^2 + \varepsilon(\bar{\zeta}f + \zeta\bar{f}) + \varepsilon^2 f\bar{f}]^{1/2} \qquad (6.8)$$

By expanding the right-hand side of Eq. (6.8) in a binomial series and collecting terms which have the same power of ε, the following expression for γ is obtained:

$$\gamma = \rho[1 + \gamma_1\varepsilon + \gamma_2\varepsilon^2 + O(\varepsilon^3)] \qquad (6.9a)$$

For the θ coordinate, by expanding the right-hand side of Eq. (6.4) and using the properties of the trigonometric functions given in the Appendix (page 188) an expression for θ is obtained in the form

$$\theta = \Theta + \varepsilon\theta_1 + \varepsilon^2\theta_2 + O(\varepsilon^3). \qquad (6.9b)$$

The various quantities in Eqs. (6.9) are defined as follows:

$$\gamma_1 = \frac{1}{2\rho^2}(\bar{\zeta}f + \zeta\bar{f}), \quad \gamma_2 = -\frac{1}{8\rho^4}(\bar{\zeta}f - \zeta\bar{f})^2,$$

$$\theta_1 = \frac{-1}{2\rho}[(f + \bar{f})\sin\Theta + i(f - \bar{f})\cos\Theta],$$

$$\theta_2 = \frac{1}{4\rho^2}[(f^2 + \bar{f}^2)\sin 2\Theta + i(f^2 - \bar{f}^2)\cos\Theta]. \qquad (6.10)$$

Since cos β and sin β will be used later, their expansions are also presented here for convenience. From Eq. (6.7) it is known that $e^{i\beta}$ can be expressed in terms of ζ, $f(\zeta)$, and ε by substituting $\omega(\zeta)$ and $\omega'(\zeta)$ from Eq. (6.2). The resultant expression has the following form:

$$e^{i\beta} = 1 + \varepsilon\beta_1 + \varepsilon^2\beta_2 + O(\varepsilon^2) \tag{6.11}$$

where

$$\beta_1 = \frac{1}{2\rho^2}\left[\zeta\bar{f} - \bar{\zeta}f + \zeta\bar{\zeta}(f' - \bar{f}')\right],$$

$$\beta_2 = -\frac{1}{8}\left(2\frac{f\bar{f}}{\zeta\bar{\zeta}} + \frac{\bar{f}^2}{\bar{\zeta}^2} + 2\bar{f}'\frac{f}{\zeta} + f'^2 + 2f'\bar{f}' - 3\bar{f}'^2 - 2\bar{f}'\frac{f}{\zeta} - 2\frac{\bar{f}}{\zeta}f'\right). \tag{6.12}$$

Then expansions for sin β and cos β are obtained by using Euler's formula and Eq. (6.11):

$$\cos\beta = 1 + \frac{\varepsilon^2}{8\zeta^2\bar{\zeta}^2}\left[(\bar{\zeta}f - \zeta\bar{f})^2 + \zeta^2\bar{\zeta}^2(f'-\bar{f}')^2 - 2\zeta\bar{\zeta}(\zeta\bar{f}-\bar{\zeta}f)(\bar{f}'-f')\right] + O(\varepsilon^3),$$

$$i\sin\beta = \varepsilon\beta_1 - \frac{\varepsilon^2}{8\zeta^2\bar{\zeta}^2}\left[2(\zeta^2\bar{f}^2 - \bar{\zeta}^2f^2) + 2\zeta^2\bar{\zeta}^2(f'^2 - \bar{f}'^2)\right] + O(\varepsilon^3). \tag{6.13}$$

It can now be shown that all of the pertinent quantities and functions depend on r, Θ and β can be expanded in powers of a small parameter ε. For example, the general arbitrary function $G(r, \theta, \varepsilon)$ can also be rewritten as

$$G\left\{\rho[1 + \varepsilon r_1 + \varepsilon^2 r_2 + O(\varepsilon^3)],\ [\theta + \varepsilon\theta_1 + \varepsilon^2\theta_2 + O(\varepsilon^3)]\right\},$$

When $\varepsilon = 0$, the function G becomes $G(\rho, \theta)$. Therefore, the function $G(r, \theta, \varepsilon)$ can be expanded in Taylor series around the function $G(\rho, \theta)$ as follows:

$$G(r,\theta,\varepsilon) = G(\rho,\theta) + \left[\rho(\varepsilon r_1 + \varepsilon^2 r_2 + \ldots)\frac{\partial G}{\partial \rho} + (\varepsilon\theta_1 + \varepsilon^2\theta_2 + \ldots)\frac{\partial G}{\partial \theta}\right]$$

$$+ \frac{1}{2!}\left[\rho^2(\varepsilon\gamma_1 + \varepsilon^2\gamma_2 + \ldots)^2 \frac{\partial^2 G}{\partial \rho^2} + 2\rho(\varepsilon\gamma_1 + \theta^2\gamma_2 + \ldots)\right.$$

$$\left.(\varepsilon\gamma_1 + \varepsilon^2\gamma_2 + \ldots)\frac{\partial^2 G}{\partial\rho\partial\theta} + (\varepsilon\theta_1 + \varepsilon^2\theta_2 + \ldots)^2 \frac{\partial^2 G}{\partial\theta^2}\right] + \ldots \tag{6.14}$$

Substituting Eq. (6.10) into (6.14), and then collecting terms that have the same power of ε, the following expression is obtained:

$$G(r, \theta, \varepsilon) = G(\rho, \theta) + \varepsilon\left(I_1 \frac{\partial}{\partial\rho} + I_2 \frac{\partial}{\partial\theta}\right)G(\rho, \theta)$$

$$+ \frac{\varepsilon^2}{2!}\left(I_3 \frac{\partial^2}{\partial\rho^2} + 2I_4 \frac{\partial^2}{\partial\theta\partial\rho} + I_5 \frac{\partial^2}{\partial\theta^2} + I_6 \frac{\partial}{\partial\rho} + I_7 \frac{\partial}{\partial\theta}\right)G(\rho, \theta) + \ldots \tag{6.15}$$

where the quantities $I_m (m = 1, 2, 3, \ldots, 7)$ are defined as

$$I_1 = \frac{1}{2\rho}(\bar{\zeta}f + \zeta\bar{f}), \quad I_3 = \frac{1}{4\rho^2}(\bar{\zeta}f + \zeta\bar{f})^2 ,$$

$$I_2 = \frac{1}{2\rho}[i(\bar{f} - f)\cos\Theta - (f + \bar{f})\sin\Theta], \quad I_6 = \frac{-1}{4\rho^3}(\bar{\zeta}f - \zeta\bar{f})^2,$$

$$I_4 = \frac{\bar{\zeta}f + \zeta\bar{f}}{4\rho^2} - [i(\bar{f} - f)\cos\Theta - (f + \bar{f})\sin\Theta],$$

$$I_5 = \frac{1}{4\rho^2}[(f^2 + \bar{f}^2)\cos 2\Theta - 2f\bar{f} - i(f^2 - \bar{f}^2)\sin 2\Theta],$$

$$I_7 = \frac{1}{2\zeta\bar{\zeta}}[(f^2 + \bar{f}^2)\sin 2\Theta + i(f^2 - \bar{f}^2)\cos 2\Theta] .$$

The pattern of Eq. (6.15) may also extend to derivatives. For example, $\partial^2 G/\partial\gamma^2$ may be expanded in the same form as shown in Eq. (6.15) by replacing $G(\rho, \Theta)$ with $\frac{\partial^2 G(\rho,\Theta)}{\partial\gamma^2}$. The stress resultants and couples given in Chapter IV may be expanded in terms of the small parameter ε also. However, the coordinates employed in this section are dimensionless quantities. For consistency, Eqs. (4.5) and (4.6) are rewritten in terms of the dimensionless polar coordinate (r, θ):

$$M_r = -D\frac{\partial^2 w}{\partial\gamma^2} - D_{12}\left(\frac{\partial^2 w}{r^2\partial\theta^2} + \frac{\partial w}{r\partial r}\right) + 2P_{66}\left(\frac{\partial^2\chi}{r\partial r\partial\theta} - \frac{\partial\chi}{r^2\partial\theta}\right)$$

$$M_\theta = -D\left(\frac{\partial^2 w}{r^2\partial\theta^2} + \frac{\partial w}{r\partial r}\right) - D_{12}\frac{\partial^2 w}{\partial r^2} - 2P_{66}\left(\frac{\partial^2\chi}{r\partial r\partial\theta} - \frac{\partial\chi}{r^2\partial\theta}\right)$$

$$M_{r\theta} = -2D_{66}\left(\frac{\partial^2 w}{r\partial r\partial\theta} - \frac{\partial w}{r^2\partial\theta}\right) + P_{66}\left(\frac{\partial^2\chi}{r^2\partial\theta^2} - \frac{\partial^2\chi}{\partial r^2} + \frac{\partial\chi}{r\partial r}\right)$$

$$Q_r = k\,\frac{\partial\chi}{r\partial\theta}, \quad Q_\theta = -k\,\frac{\partial\chi}{\partial r} \tag{6.17}$$

where M_r, M_θ, $M_{r\theta}$, and Q_θ are related to M_R, M_Ξ, $M_{R\Xi}$, Q_R, and $Q_{R\Xi}$ in the following way:

$$(M_R, M_\Xi, M_{R\Xi}) = \frac{1}{r_o^2}(Q_r, Q_\theta), \quad (Q_R, Q_\Xi) = \frac{1}{r_o}(Q_r, Q_\theta). \tag{6.18}$$

In Eqs. (6.17), each term such as $\partial^2 w/\partial r^2$, $\partial^2 w/r^2\partial\theta^2$, $\partial w/r\partial r$, $\partial^2\chi/r\partial r\partial\theta$, $\partial^2\chi/r\partial r\partial\theta$, $\partial^2\chi/\partial r^2$, and $\partial\chi/r\partial r$ may be expanded in a Taylor series in the same way as indicated in Eq. (6.15). Using the relations stated in Eq. (6.18) the final form can be expressed as

$$\begin{pmatrix} M_R \\ M_\Xi \\ M_{R\Xi} \\ Q_R \\ Q_\Xi \end{pmatrix} = \left[1 + \varepsilon\left(I_1\frac{\partial}{\partial\rho} + I_2\frac{\partial}{\partial\Theta}\right) + \frac{\varepsilon}{2}\left(I_3\frac{\partial}{\partial\rho^2} + 2I_4\frac{\partial^2}{\partial\rho\partial\Theta} + I_5\frac{\partial^2}{\partial\Theta^2}\right.\right.$$

$$\left.\left. + I_6\frac{\partial}{\partial\rho} + I_7\frac{\partial}{\partial\Theta}\right)\right] \begin{pmatrix} \tilde{M}_\rho \\ \tilde{M}_\Theta \\ \tilde{M}_{\rho\Theta} \\ \tilde{Q}_\rho \\ Q_\Theta \end{pmatrix} \tag{6.19}$$

where

$$\tilde{Q}_\rho = \frac{K}{\gamma_o}\frac{\partial \chi}{\rho \partial \Theta}, \quad \tilde{Q}_\Theta = -\frac{K}{\gamma_o}\frac{\partial \chi}{\partial \rho},$$

$$\tilde{M}_\rho = \frac{1}{r_o^2}\left[-D\frac{\partial^2 w}{\partial \rho^2} - D_{12}\left(\frac{\partial^2 w}{\rho^2 \partial \Theta^2} + \frac{\partial w}{\rho \partial \rho}\right) + 2P_{66}\left(\frac{\partial^2 \chi}{\rho \partial \rho \partial \Theta} - \frac{\partial^2 \chi}{\rho^2 \partial \Theta}\right)\right],$$

$$\tilde{M}_\Theta = \frac{1}{r_o^2}\left[-D\left(\frac{\partial^2 w}{\rho^2 \partial \Theta^2} + \frac{\partial w}{\rho \partial \rho}\right) - D_{12}\frac{\partial^2 w}{\partial \rho^2} - 2P_{66}\left(\frac{\partial^2 \chi}{\rho \partial \rho \partial \Theta} - \frac{\partial \chi}{\rho^2 \partial \Theta}\right)\right],$$

$$\tilde{M}_{\rho\Theta} = \frac{1}{r_o^2}\left[-2D_{66}\left(\frac{\partial^2 w}{\rho \partial \rho \partial \Theta} - \frac{\partial w}{\rho \partial \Theta}\right) + P_{66}\left(\frac{\partial^2 \chi}{\rho^2 \partial \Theta^2} - \frac{\partial^2 \chi}{\partial \rho^2} + \frac{\partial \chi}{\rho \partial \rho}\right)\right]. \tag{6.20}$$

The components of the stress resultants and couples in curvilinear coordinates (ρ, Θ) may be derived from the stress resultants and couples in the polar coordinates (R, Ξ) by the stress tensor transformation law mentioned in Chapter IV. For simplicity, the transformation equations are written in the form:

$$M_\rho = M_R \cos^2\beta + M_\Xi \sin^2\beta + M_{R\Xi} \sin\beta \cos\beta,$$

$$M_{\rho\Theta} = M_R \sin^2\beta + M_\Xi \cos^2\beta - M_{R\Xi} \sin\beta \cos\beta,$$

$$M_{\rho\Theta} = (M_\Xi - M_R)\sin\beta \cos\beta + M_{R\Xi}(\cos^2\beta - \sin^2\beta),$$

$$Q_\rho = Q_R \cos\beta + Q_\Xi \sin\beta, \quad Q_\Theta = -Q_R \sin\beta + Q_\Xi \cos\beta. \tag{6.21}$$

The deflection function W and stress function χ may also be expanded in terms of the small parameter ε,

$$W = \sum_{i=0}^{\infty} \varepsilon^i W_i, \quad \text{and } \chi = \sum_{i=0}^{\infty} \varepsilon^i \chi_i. \tag{6.22}$$

Equations (6.22) indicate that, when i = 0, the terms W_0 and χ_0 provide the solution for the circular hole case. In addition, the higher order terms provide the solution for the hole which deviates from circular hole. Substitution of Eqs. (6.19), (6.20), (6.22), and (6.13) into Eq. (6.21) yields a highly complicated set of expressions for the stress resultants and couples. In the interest of brevity, the intermediate steps are not presented. Instead, the final expression is written in the form:

$$(M_\rho, M_\theta, M_{\rho\theta}, Q_\rho, Q_\theta) = \sum_{i=0}^{\infty} \varepsilon \left[M_{\rho(i)}, M_{\Theta(i)}, M_{\rho\Theta(i)}, Q_{\rho(i)}, Q_{\Theta(i)} \right] \tag{6.23}$$

where

$$M_{\rho(i)} = \tilde{M}_\rho^i + \sum_{m=0}^{i-1} \left[L_1^{i-m} \tilde{M}_\rho^m + L_2^{i-m} (\tilde{M}_\rho^m - \tilde{M}_\theta^m) + L_3^{i-m} \tilde{M}_{\rho\Theta}^m \right],$$

$$M_{\theta(i)} = \tilde{M}_{\theta}^{i} + \sum_{m=0}^{i-1}[L_1^{i-m}\tilde{M}_{\theta}^{m} - L_2^{i-m}(\tilde{M}_{\rho}^{m} - \tilde{M}_{\theta}^{m}) - L_3^{i-m}\tilde{M}_{\rho\theta}^{m}],$$

$$M_{\rho\theta(i)} = \tilde{M}_{\rho\theta}^{i} + \sum_{m=0}^{i-1}[L_1^{i-m}\tilde{M}_{\rho\theta}^{m} + 2L_2^{i-m}\tilde{M}_{\rho\theta}^{m} + L_3^{i-m}(\tilde{M}_{\theta}^{m} - \tilde{M}_{\rho}^{m})],$$

$$Q_{\theta(i)} = \tilde{Q}_{\theta}^{i} + \sum_{m=0}^{i-1}(L_1^{i-m}\tilde{Q}_{\theta}^{m} + \tfrac{1}{2}L_2^{i-m}\tilde{Q}_{\theta}^{m} - L_3^{i-m}\tilde{Q}_{\theta}^{m})$$

$$Q_{\rho(i)} = \tilde{Q}_{\rho}^{i} + \sum_{m=0}^{i-1}(L_1^{i-m}\tilde{Q}_{\rho}^{m} + \frac{1}{2}L_2^{i-m}\tilde{Q}_{\rho}^{m} + L_3^{i-m}\tilde{Q}_{\rho}^{m}). \quad (6.24)$$

The quantities $L_n^m (n = 1, 2, 3)$ are differential operators. The zero, first and second order operators L_n^m are given as

$$L_1^0 = L_2^0 = L_3^0 = 0 ,$$

$$L_1^1 = \frac{1}{2}(\bar{\zeta}f + \zeta\bar{f})\frac{\partial}{\rho\partial\rho} - \frac{1}{2}[i(f - \bar{f})\cos\theta + (f + \bar{f})\sin\theta]\frac{\partial}{\rho\partial\theta},$$

$$L_2^1 = 0, \quad L_3^1 = \frac{1}{2i\zeta\bar{\zeta}}[\zeta\bar{\zeta}(f' - \bar{f}') + \zeta\bar{f} - \bar{\zeta}f],$$

$$L_1^2 = J_3\frac{\partial^2}{\partial\rho^2} + J_4\frac{\partial^2}{\partial\rho\partial\theta} + J_5\frac{\partial^2}{\partial\theta^2} + J_6\frac{\partial}{\partial\rho} + J_7\frac{\partial}{\partial\theta},$$

$$L_2^2 = \frac{1}{4\zeta^2\bar{\zeta}^2}[(\bar{\zeta}f - \zeta\bar{f})^2 + \zeta^2\bar{\zeta}^2(f' - \bar{f}')^2 + 2\zeta\bar{\zeta}(\zeta\bar{f} - \bar{\zeta}f)(\bar{f}' - f')],$$

$$L_3^2 = \frac{1}{4i\zeta^2\bar{\zeta}^2}[\bar{\zeta}^2f^2 - \zeta^2\bar{f}^2 + \zeta^2\bar{\zeta}^2(\bar{f}'^2 - f'^2)] + J_1\frac{\partial}{\partial\rho} + J_2\frac{\partial}{\partial\theta} . \quad (6.25)$$

The notations J_1, J_2, J_3, J_4, J_5, J_6, and J_7 are given in the following form:

$$J_1 = \frac{1}{4i\zeta^2\bar{\zeta}^2}[\zeta\bar{f} - \bar{\zeta}f + \zeta\bar{\zeta}(f' - \bar{f}')](\bar{\zeta}f + \zeta\bar{f}),$$

$$J_2 = \frac{1}{4i\zeta^2\bar{\zeta}^2}[\zeta\bar{f} - \bar{\zeta}f + \zeta\bar{\zeta}(f' - \bar{f}')][i(f' - f)\cos\Theta - (f + \bar{f})\sin\Theta],$$

$$J_3 = \frac{1}{8\zeta\bar{\zeta}}(\bar{\zeta}f + \zeta\bar{f})^2,$$

$$J_4 = \frac{1}{4\zeta\bar{\zeta}}(\bar{\zeta}f + \zeta\bar{f})[i(\bar{f} - f)\cos\Theta - (f + \bar{f})\sin\Theta],$$

$$J_5 = \frac{1}{8i\zeta\bar{\zeta}}[2if\bar{f} - i(f^2 + \bar{f}^2)\cos 2\Theta - (f^2 - \bar{f}^2)\sin 2\Theta],$$

$$J_6 = \frac{1}{8\zeta\bar{\zeta}\rho}(\bar{\zeta}f - \zeta\bar{f})^2,$$

$$J_7 = \frac{1}{4\zeta\bar{\zeta}}(f^2 + \bar{f}^2)\sin 2\Theta + \frac{i}{4\zeta\bar{\zeta}}(f^2 - \bar{f}^2)\cos 2\Theta.$$

Expressions for $\tilde{M}^i_\rho$, $\tilde{M}^i_\Theta$, $\tilde{M}^i_{\rho\Theta}$, $\tilde{Q}^i_\rho$, and $\tilde{Q}^i_\Theta$ in Eq. (6.24) have the same form as in Eq. (6.20), but W and χ are replaced by W_i and χ_i, respectively. For future reference, expressions of $\tilde{M}^i_\rho$, $\tilde{M}^i_\Theta$, $\tilde{M}^i_{\rho\Theta}$, $\tilde{Q}^i_\rho$, and $\tilde{Q}^i_\Theta$ are stated in the form

$$\tilde{M}_{\rho}^{i} = \frac{1}{\gamma_o^2}\left[-D\frac{\partial^2 w}{\partial\rho^2} - D_{12}\left(\frac{\partial^2 w_i}{\rho^2\partial\theta^2} + \frac{\partial w_i}{\rho\partial\rho}\right) + 2P_{66}\left(\frac{\partial^2\chi_i}{\rho\partial\rho\partial\theta} - \frac{\partial\chi_i}{\rho^2\partial\theta}\right)\right],$$

$$\tilde{M}^{i} = \frac{1}{\gamma_o^2}\left[-D\left(\frac{\partial^2 w_i}{\rho^2\partial\theta^2} + \frac{\partial^2 w_i}{\rho\partial\rho}\right) - D_{12}\frac{\partial^2 w_i}{\partial\rho^2} - 2P_{66}\left(\frac{\partial^2\chi_i}{\rho\partial\rho\partial\theta} - \frac{\partial\chi_i}{\rho^2\partial\theta}\right)\right],$$

$$\tilde{M}_{\rho\theta}^{i} = \frac{1}{\gamma_o^2}\left[-2D_{66}\left(\frac{\partial^2 w_i}{\rho\partial\rho\partial\theta} - \frac{\partial w_i}{\rho^2\partial\rho}\right) + P_{66}\left(\frac{\partial\chi_i}{\rho^2\partial\theta^2} - \frac{\partial\chi_i}{\partial\rho^2} + \frac{\partial\chi_i}{\rho\partial\theta}\right)\right],$$

$$\tilde{Q}_{\rho}^{i} = \frac{1}{\gamma_o} k \frac{\partial\chi_i}{\rho\partial\theta},$$

$$\tilde{Q}_{\theta}^{i} = \frac{1}{\gamma_o} k \frac{\partial\chi_i}{\partial\rho}. \qquad (6.27)$$

6.4. Conformal Transformation

Some properties of conformal transformation have already been mentioned in Chapter V. This section treats some detailed properties and ways to choose the appropriate mapping function for the problem under study. Recall Eq. (6.1), the conformal mapping function $Z = \Omega(\zeta)$ is a single-valued analytic function relating every point ζ of Σ plane to some definite point Z in the Z plane. These latter points will cover some region S in the Z plane. Conversely, let it be assumed that each point Z of S, by the Eq. (6.1), corresponds to some definite point of Σ. It may then be noted that Eq. (6.1) determines an inevitable single-valued conformal transformation of the region S into the region Σ (or the converse).

The transformation is called conformal because, under the transformation $Z = \Omega(\zeta)$, the angle between any two curves passing through any point Z at which $dZ/d\zeta \neq 0$ is preserved, and its sense remains unchanged. As is well known, a transformation from Σ to Z is conformal when $\Omega(\zeta)$ is holomorphic and $dz/d\zeta \neq 0$ for all ζ in Σ. In light of these considerations, a holomorphic function is the function being sought.

The regions Σ and S may be finite or infinite (and, in particular, one of them may be finite while the other is infinite). If, for example, the region Σ is finite and S is infinite, the function $\Omega(\zeta)$ must become infinite at some point of Σ (since otherwise there would be no point of Σ corresponding to the point at infinity in S). Thus, it can be easily proved that $\Omega(\zeta)$ must have a simple pole at that point; i.e., assuming for simplicity that $Z = \infty$ corresponds to $\zeta = 0$, then

$$\Omega(\zeta) = \frac{C}{\zeta} + \text{holomorphic function} \qquad (6.28)$$

where C is a constant. No other singularities can occur in Σ; otherwise the transformation would not be reversible and single-valued. If Σ and S are both infinite and the points at infinity correspond to each other, the function $\Omega(\zeta)$ must, for the same reason, have the form

$$\omega(\zeta) = R\zeta + \text{a holomorphic function} \qquad (6.29)$$

where R is a constant. Recall that a function, holomorphic in an infinite region, is understood to be one that is holomorphic in any finite part of this region and which, for sufficiently large $|\zeta|$, may be represented by a series of the form

$$a_0 + a_1/\zeta + a_2/\zeta^2 + \ldots . \qquad (6.30)$$

Further, it may be shown that the derivative $\Omega'(\zeta)$ cannot become zero in Σ; otherwise, the transformation would not be reversible and single-valued.

Consider now the case where two regions are simply connected and bounded by simple contours. The transformation of Eq. (6.1) maps the exterior of the circle onto the exterior of an examined hole. In light of the preceding arguments, the function $\Omega(\zeta)$ is assumed in the form

$$\Omega(\zeta) = R\zeta + \frac{a_1}{\zeta} + \frac{a_2}{\zeta^2} + \ldots . \qquad (6.31)$$

Generally, Eq. (6.31) can be used to transfer any shape of contour in the z plane to a circular contour in the ζ plane by choosing proper values of R and a_i (i = 1, 2, 3, ...). Obviously, if only a finite number of terms of the series in Eq. (6.31) is considered,

the shape of the hole that will be obtained is not the precise one examined but will be a hole with curvilinear sides and rounded-off angles. The degree of deviation of the contour may serve as a criterion for the accuracy of the function constructed.

Muskhelishvili [31] and Savin [20] gave a function of the two terms for mapping elliptical, rectangular, and equilateral triangle contours. They showed that mapping functions are very accurate. Because of its simplicity this is clearly practical. For this study the simple mapping function, which is given in the form below, will be selected

$$\Omega(\zeta) = r_0(\zeta + \varepsilon/\zeta^N)$$

or

$$\omega(\zeta) = \zeta + \varepsilon\zeta^{-N} \ . \qquad (6.32)$$

By properly selecting the values of ε and N, mapping functions for different holes are obtained: (a) for elliptical holes, $\varepsilon = a - b/(a + b)$, $N = 1$, and $r_0 = (a + b)/2$, where a and b are the semi-axis of an elliptical hole, respectively, along the x and y axes. When $\varepsilon > 0$, the major axis of the ellipse is on the x-axis, while when $\varepsilon < 0$, the ellipse rotates 90°, and its major axis is then on the y axis. Since the $|\varepsilon| \ll 1$, the elliptical hole is very close to a circular hole. (b) For an equilateral triangular hole, $N = 2$, and the value of $\varepsilon = \pm 1/3$ or $\pm 1/4$. (c) For a square hole, $N = 3$, and the value of $\varepsilon = \pm 1/6$ or $\pm 1/9$. The

magnitude, or the size, of the hole depends on the value of r_o.

An understanding of the criterion for choosing the type of function $f(\zeta)$ given in Eq. (6.2) was presented in the previous paragraph. As noted earlier, in this analysis the function $f(\zeta)$ is chosen to be ζ^{-N}. As a summary of all derivations presented in this section, it is clear that as long as the function $f(\zeta)$ is obtained, the perturbation expansions of the problem are accomplished by substituting $f(\zeta) = \zeta^{-N}$ into Eqs. (6.21), (6.24), (6.25), and (6.26). The remaining tasks are those of repeating the steps of Chapter V and computing the highly complicated set of algebraic expressions. In general, any desired order of solution may be obtained. However, for brevity, only the zero and first-order solutions are presented. For reference, Eq. (6.25) for $f(\zeta) = \zeta^{-N}$ is expressed in the following form:

$$L_1^0 = L_2^0 = L_3^0 = 0,$$

$$L_1^1 = \rho^{-N}\left[\cos(1+N)\theta\,\frac{\partial}{\partial\rho} - \sin(1+N)\theta\,\frac{\partial}{\rho\partial\theta}\right],$$

$$L_3^1 = \frac{N+1}{\rho^{N+1}}\sin(1+N)\theta, \quad L_2^1 = 0,$$

$$L_1^2 = \frac{1}{2\rho^{2N}}\left[\cos^2(1+N)\theta\,\frac{\partial^2}{\partial\rho^2} - \sin 2(1+N)\theta\,\frac{\partial^2}{\partial\rho\partial\theta}\left(\frac{1}{\rho}\right)\right.$$

$$\left. + \frac{\sin^2(1+N)\theta}{\rho^2}\left(\frac{\partial^2}{\partial\theta^2} + \rho\,\frac{\partial}{\partial\rho}\right)\right],$$

$$L_2^2 = -\rho^{-2(N+1)}(1+N)^2 \sin^2(1+N)\theta,$$

$$L_3^2 = \frac{(N^2-1)\sin 2(1+N)\theta}{2\rho^{2N+2}} + \frac{(N+1)\sin 2(1+N)}{2\rho^{2N+1}}\frac{\partial}{\partial\rho}$$

$$- \frac{(N+1)^2 \sin^2(1+N)\theta}{\rho^{2N+2}}\frac{\partial}{\partial\theta}. \qquad (6.33)$$

The zero and first-order solutions for the stress resultants and couples associated with the function $f(\zeta) = \zeta^{-N}$ may be obtained from Eq. (6.24). They are expressed in the form

$$O(\varepsilon^0)$$

$$\left\{M_{\rho(0)}, M_{\theta(0)}, M_{\rho\theta(0)}, Q_{\rho(0)}, Q_{\theta(0)}\right\} = \{\tilde{M}_\rho^{(0)}, \tilde{M}_\theta^{(0)}, \tilde{M}_{\rho\theta}^{(0)}, \tilde{Q}_\rho^{(0)}, \tilde{Q}_\theta^{(0)}\},$$

$$O(\varepsilon)$$

$$\begin{Bmatrix} M_{\rho(1)} \\ M_{\theta(1)} \\ M_{\rho\theta(1)} \\ Q_{\rho(1)} \\ Q_{\theta(1)} \end{Bmatrix} = \begin{Bmatrix} \tilde{M}_\rho^1 \\ \tilde{M}_\theta^1 \\ \tilde{M}_{\rho\theta}^1 \\ \tilde{Q}_\rho^1 \\ \tilde{Q}_\theta^1 \end{Bmatrix} + \frac{1}{\rho N}\left[\cos(1+N)\theta\frac{\partial}{\partial\rho} - \sin(1+N)\theta\frac{\partial}{\rho\partial\theta}\right]$$

$$\begin{Bmatrix} \tilde{M}^{o}_{\rho} \\ \tilde{M}^{o}_{\theta} \\ \tilde{M}^{o}_{\rho\theta} \\ \tilde{Q}^{o}_{\rho} \\ \tilde{Q}^{o}_{\theta} \end{Bmatrix} + \frac{N+1}{\rho^{N+1}} \sin (1+N)\theta \begin{Bmatrix} \tilde{M}^{o}_{\rho\theta} \\ -\tilde{M}^{o}_{\rho\theta} \\ (\tilde{M}^{o}_{\theta} - \tilde{M}^{o}_{\rho}) \\ \tilde{Q}^{o}_{\theta} \\ -\tilde{Q}^{o}_{\rho} \end{Bmatrix} \quad (6.35)$$

Equation (6.35) is a general expression. $\tilde{M}^{o}_{\rho}$, $\tilde{M}^{o}_{\theta}$, $\tilde{M}_{\rho\theta}$, $\tilde{Q}^{o}_{\rho}$ and $\tilde{Q}^{o}_{\theta}$ are the stress resultants and couples corresponding to the circular hole case. The terms M^{1}_{ρ}, M^{1}_{θ}, $M^{1}_{\rho\theta}$, Q^{1}_{θ} and Q^{1} are calculated from Eq. (6.27), and they also relate to the circular hole solution. Therefore, as long as the solution for the circular hole is provided, the perturbation solution for any hole shape may be obtained. Note that the expressions obtained in Chapter V are not convenient for the analysis in this section. The work of Chapter V will not be repeated in Section 6.5; instead, Eq. (4.14) is solved directly to obtain the appropriate expressions for the displacement function W and stress function χ in terms of dimensionless quantities.

6.5. Functions W and χ

The system of Eqs. (4.14) in the dimensionless polar coordinates (r, θ) can be expressed as

$$\tilde{\nabla}^2\tilde{\nabla}^2 W = 0,$$

$$\tilde{\nabla}^2(\tilde{\nabla}^2 - \tilde{\lambda}^2)\chi = 0, \tag{6.36}$$

or as

$$\frac{\partial}{\partial r}(\tilde{\nabla}^2 DW) = -\frac{\partial}{r\partial\theta}(r_o^2 k\chi - P_{66}\tilde{\nabla}^2\chi),$$

$$\frac{\partial}{r\partial\theta}(\tilde{\nabla}^2 DW) = \frac{\partial}{\partial r}(r_o^2 k\chi - P_{66}\tilde{\nabla}^2\chi) \tag{6.37}$$

where $\tilde{\nabla}^2$ is a dimensionless Laplacian operator defined as $\frac{\partial^2}{\partial r^2} + \frac{\partial}{r\partial r} + \frac{\partial^2}{r^2\partial\theta^2}$, and $\tilde{\lambda}^2$ is defined as $r_o^2\lambda^2 = \left(\frac{r_o^2 k}{P_{66}}\right)$. The solution of the system Eqs. (6.36) and (6.37) can be taken from Chapter V. They are given in the following form:

$$W(r, \theta) = A_o \ln r + \sum_{n=1}^{\infty}\left[r_o^{-n}r^{-n}\begin{pmatrix}A_n\\B_n\end{pmatrix} + r_o^{-n+2}r^{-n+2}\begin{pmatrix}C_n\\D_n\end{pmatrix}\right]\begin{matrix}\cos n\theta\\ \sin n\theta\end{matrix} \tag{6.38}$$

$$\chi(r, \theta) = F_o K_o(\tilde{\lambda}r) + \sum_{n=1}^{\infty}\left[K_n(\tilde{\lambda}r)\begin{pmatrix}E_n\\F_n\end{pmatrix} \pm \frac{4D(1-n)}{kr_o^n r^n}\begin{pmatrix}C_n\\D_n\end{pmatrix}\right]\begin{matrix}\sin n\theta\\ \cos n\theta\end{matrix} \tag{6.39}$$

where A_o, F_o, A_n, B_n, C_n, D_n, E_n, and F_n are all constants and will be determined from the boundary conditions. The functions $W(\rho, \Theta)$ and $\chi(\rho, \Theta)$ can be calculated directly from Eqs. (6.38) and (6.39) by changing (r, θ) to (ρ, Θ). Referring to Eq. (5.22), $W_i(\rho, \Theta)$ and $\chi_i(\rho, \Theta)$ are obtained and expressed as follows:

$$W_i(\rho, \Theta) = A_o^i \ln \rho + \sum_{n=1}^{\infty} \left[r_o^{-n} \rho^{-n} \begin{pmatrix} A_n^i \\ B_n^i \end{pmatrix} + r_o^{-n+2} \begin{pmatrix} C_n^i \\ D_n^i \end{pmatrix} \right] \begin{matrix} \cos n\Theta \\ \sin n\Theta \end{matrix},$$

$$\chi_i(\rho, \Theta) = F_o^i K_o(\tilde{\lambda}\rho) + \sum_{n=1}^{\infty} \left[K_n(\tilde{\lambda}\rho) \begin{pmatrix} E_n^i \\ F_n^i \end{pmatrix} \pm \frac{4D(1 - n)}{k r_o^n \rho^n} \begin{pmatrix} C_n^i \\ D_n^i \end{pmatrix} \right] \begin{matrix} \sin n\Theta \\ \cos n\Theta \end{matrix} \tag{6.40}$$

where $K_n(\tilde{\lambda}\rho)$ is a modified Bessel function. Substituting Eq. (6.40) into (6.27) yields a complicated set of algebraic expressions. After simplification and combination, the final expression for Eq. (6.27) becomes

$$\tilde{M}_\rho^i = \frac{D_{11} - D_{12}}{r_o^2 \rho^2} A^i + \frac{1}{r_o^2} \sum_{n=1}^{\infty} \left[- \frac{2D_{66} n(n + 1)}{r_o^n \rho^{n+2}} \right.$$

$$\left. \begin{pmatrix} A_n^i \\ B_n^i \end{pmatrix} + \left(\frac{t_2^-}{r_o^{n-2} \rho^n} - \frac{t_3}{r_o^n \rho^{n+2}} \right) \begin{pmatrix} C_n^i \\ D_n^i \end{pmatrix} \pm 2p^* n N_n^1 \begin{pmatrix} E_n^i \\ F_n^i \end{pmatrix} \right] \begin{matrix} \cos n\Theta \\ \sin n\Theta \end{matrix},$$

$$\tilde{M}^i_\Theta = -\frac{D - D_{12}}{r_o^2\rho^2} A^i_o + \frac{1}{r_o^2}\sum_{n=1}^{\infty}\left[\frac{2D_{66}n(n+1)}{r_o^n\rho^{n+2}}\right.$$

$$\left.\begin{pmatrix} A^i_n \\ B^i_n \end{pmatrix} + \left(\frac{t_2^+}{r_o^{n-2}\rho^n} + \frac{t_3}{r_o^n\rho^{n+2}}\right)\begin{pmatrix} C^i_n \\ D^i_n \end{pmatrix} \mp 2p^*N^1_n \begin{pmatrix} E^i_n \\ F^i_n \end{pmatrix}\right]\begin{matrix}\cos n\Theta \\ \sin n\Theta\end{matrix},$$

$$\tilde{M}^i_{\rho\Theta} = \frac{p^*}{r_o^2} N^3_o F^i_o + \frac{1}{r_o^2}\sum_{n=1}^{\infty}\left[\mp\frac{2D_{66}n(n+1)}{r_o^n\rho^{n+2}}\right.$$

$$\left.\begin{pmatrix} A^i_n \\ B^i_n \end{pmatrix} \mp \left(\frac{2t_4}{r_o^{n-2}\rho^n} + \frac{t_3}{r_o^n\rho^{n+2}}\right)\begin{pmatrix} C^i_n \\ D^i_n \end{pmatrix} + p^*N^3_n \begin{pmatrix} E^i_n \\ F^i_n \end{pmatrix}\right]\begin{matrix}\sin n\Theta \\ \cos n\Theta\end{matrix},$$

$$\tilde{Q}^i_\rho = \sum_{n=1}^{\infty}\left[\mp\frac{kn}{r_o} K_n(\tilde{\lambda}\rho)\begin{pmatrix} E^i_n \\ F^i_n \end{pmatrix} + \frac{4Dn(1-n)}{r_o^{n+1}\rho^{n+1}}\begin{pmatrix} C^i_n \\ D^i_n \end{pmatrix}\right]\begin{matrix}\cos n\Theta \\ \sin n\Theta\end{matrix},$$

$$\tilde{Q}_\Theta = -\frac{k}{r_o}\tilde{\lambda}K'_o(\tilde{\lambda}\rho)F^i_o - \sum_{n=1}^{\infty}\left[\frac{\tilde{\lambda}k}{r_o} K'_n(\tilde{\lambda}\rho)\begin{pmatrix} E^i_n \\ F^i_n \end{pmatrix} \mp \frac{4Dn(1-n)}{r_o^{n+1}\rho^{n+1}}\begin{pmatrix} C^i_n \\ i \\ n \end{pmatrix}\right]\begin{matrix}\sin n\Theta \\ \cos n\Theta\end{matrix}$$

(6.41)

where $t_2^{\pm} = 2(n-1)[(D_{11} + D_{12}) \mp nD_{66}]$,

$$t_3 = \frac{8P_{66}D_{11}}{k} n(1 - n^2), \quad P^* = P_{66}$$

$$t_4 = D_{66}n(n-1), \quad D = D_{11}$$

$$N_3^1 = \frac{\tilde{\lambda}}{\rho} K_n'(\tilde{\lambda}\rho) - \frac{1}{\rho^2} K_n(\tilde{\lambda}\rho),$$

$$N_n^3 = \tilde{\lambda}^2[K_n(\tilde{\lambda}\rho) - 2K_n''(\tilde{\lambda}\rho)]. \tag{6.42}$$

$K_n'(\tilde{\lambda}\rho)$ is defined as the derivative of the modified Bessel with respect to its argument, i.e., $K_n'(\tilde{\lambda}\rho) \equiv \dfrac{dK_n(\tilde{\lambda}\rho)}{d(\tilde{\lambda}\rho)}$.

In Eq. (6.41), by letting the superscript i equal zero, expressions for $\tilde{M}_\rho^o$, $\tilde{M}_\theta^o$, $\tilde{M}_{\rho\theta}^o$, $\tilde{Q}_\rho^o$, and $\tilde{Q}_\theta^o$ are obtained. When i is set equal to 1, expressions for $\tilde{M}_\rho^1$, $\tilde{M}_\theta^1$, $\tilde{M}_{\rho\theta}^1$, $\tilde{Q}_\rho^1$, and $\tilde{Q}_\theta^1$ are obtained in a similar way. To avoid the tedious work of writing them, the expressions for these quantities are not presented in this dissertation. With expressions obtained for $\tilde{M}_\rho^o$, $\tilde{M}_\theta^o$, $\tilde{M}_{\rho\theta}^o$, $\tilde{Q}_\rho^o$, $\tilde{Q}_\theta^o$, $\tilde{M}_\rho^1$, $\tilde{M}_\theta^1$, $\tilde{M}_{\rho\theta}^1$, $\tilde{Q}_\rho^1$, and $\tilde{Q}_\theta^1$, the zero and first-order expressions for the stress resultants and couples are obtained and given below:

$$M_\rho(0) = \frac{D - D_{12}}{r_o^2\rho^2} A_o^o + \sum_{n=1}^{\infty} \left[\frac{2D_{66}n(n+1)}{r_o^{n+2}\rho^{n+2}} \begin{pmatrix} A_n^o \\ B_n^o \end{pmatrix} \right.$$

$$\left. \mp \left(\frac{t_2}{r_o^n \rho^n} - \frac{t_3}{r_o^{n+2}\rho^{n+2}} \right) \begin{pmatrix} C_n^o \\ D_n^o \end{pmatrix} \mp \frac{2np^*}{r_o^2} N_n^1 \begin{pmatrix} E_n^o \\ F_n^o \end{pmatrix} \right] \begin{matrix} \cos n\theta \\ \sin n\theta \end{matrix} \tag{6.43a}$$

$$M_{\theta(0)} = -\frac{D - D_{12}}{r_o^2 \rho^2} A_o^o + \sum_{n=1}^{\infty} \left[\frac{2D_{66} n(n+1)}{r_o^{n+2} \rho^{n+2}} \begin{pmatrix} A_n^o \\ B_n^o \end{pmatrix} \right.$$

$$\left. + \left(\frac{t_2^+}{r_o^n \rho_o^n} + \frac{t_3}{r_o^{n+2} \rho^{n+2}} \right) \begin{pmatrix} C_n^o \\ D_n^o \end{pmatrix} \mp \frac{2np^*}{r_o^2} N_n^1 \begin{pmatrix} E_n^o \\ F_n^o \end{pmatrix} \right] \begin{matrix} \cos n\theta \\ \sin n\theta \end{matrix} \qquad (6.43b)$$

$$M_{\rho\theta(0)} = \frac{N_o p^*}{r_o^2} F_o^o + \sum_{n=1}^{\infty} \left[\mp \frac{2D_{66} n(n+1)}{r_o^{n+2} \rho^{n+2}} \begin{pmatrix} A_n^o \\ B_n^o \end{pmatrix} \right.$$

$$\left. \mp \left(\frac{2t_4}{r_o^n \rho_o^n} + \frac{t_3}{r_o^{n+2} \rho^{n+2}} \right) \begin{pmatrix} C_n^o \\ D_n^o \end{pmatrix} + \frac{p^* N_n^3}{r_o^2} \begin{pmatrix} E_n^o \\ F_n^o \end{pmatrix} \right] \begin{matrix} \sin n\theta \\ \cos n\theta \end{matrix}, \qquad (6.43c)$$

$$Q_{\rho(0)} = -\frac{k\tilde{\lambda}}{r_o} K_o'(\tilde{\lambda}\rho) F_o^o - \sum_{n=1}^{\infty} \left[\frac{\tilde{\lambda} k}{r_o} K_n'(\tilde{\lambda}\rho) \begin{pmatrix} E_n^o \\ F_n^o \end{pmatrix} \mp \frac{4Dn(1-n)}{r_o^{n+1} \rho^{n+1}} \begin{pmatrix} C_n^o \\ D_n^o \end{pmatrix} \right] \begin{matrix} \sin n\theta \\ \cos n\theta \end{matrix}, \qquad (6.43d)$$

$$Q_{\theta(0)} = \frac{k\tilde{\lambda}}{r_o} K_o'(\tilde{\lambda}\rho) F_o^o - \sum_{n=1}^{\infty} \left[\frac{\tilde{\lambda} k}{r_o} K_n'(\tilde{\lambda}\rho) \begin{pmatrix} E_n^o \\ F_n^o \end{pmatrix} \mp \frac{4Dn(1-n)}{r_o^{n+1} \rho^{n+1}} \begin{pmatrix} C_n^o \\ D_n^o \end{pmatrix} \right] \begin{matrix} \sin n\theta \\ \cos n\theta \end{matrix} \qquad (6.43e)$$

In $O(\varepsilon)$ form, they are

$$M_{\rho(0)} = \tilde{M}_\rho^1 - \frac{2(D - D_{12})}{r_o^2 \rho^{N+3}} A_o^o \cos(1+N)\theta + \frac{p^*(N+1) N_o^3}{r_o^2 \rho^{N+1}} F_o^o \sin(1+N)\theta$$

$$+ \frac{1}{2} \sum_{n=1}^{\infty} \left\{ \frac{(1-N)t_1}{r_o^{n+2} \rho^{n+N+3}} \begin{pmatrix} A_n^o \\ B_n^o \end{pmatrix} + \frac{-2(1+N)t_4}{r_o^n \rho^{n+N+1}} + \frac{(1-N)t_3}{r_o^{n+2} \rho^{n+N+3}} \begin{pmatrix} C_n^o \\ D_n^o \end{pmatrix} \right.$$

$$\mp \frac{2H_n^{+1}}{r_o^2}\begin{pmatrix} E_n^o \\ F_n^o \end{pmatrix}\Bigg\}\begin{matrix}\cos(n-N-1)\Theta \\ \sin(n-N-1)\Theta\end{matrix} + \frac{1}{2}\sum_{n=1}^{\infty}\Bigg\{\frac{(2n+N+3)t_1}{r_o^{n+2}\rho^{n+N+3}}\begin{pmatrix} A_n^o \\ B_n^o \end{pmatrix}$$

$$+\left[\frac{2(1+N)t_4 - 2nt_2}{r_o^n\rho^{n+N+1}} + \frac{(2n+N+3)t_3}{r_o^{n+2}\rho^{n+N+3}}\right]\begin{pmatrix} C_n^o \\ D_n^o \end{pmatrix} \mp \frac{2H_n^{-1}}{r_o^2}\begin{pmatrix} E_n^o \\ F_n^o \end{pmatrix}\Bigg\}\times$$

$$\begin{matrix}\cos(n+N+1)\Theta \\ \sin(n+N+1)\Theta\end{matrix}, \qquad (6.44a)$$

$$M_\Theta(1) = \tilde{M}_\Theta^1 + \frac{2(D-D_{12})}{r_o^{2\,N+3}}A_o^o\cos(1+N)\Theta - \frac{p^*(1+N)N_o^3}{r_o^2\rho^{N+1}}F_o^o\sin(1+N)\Theta$$

$$+\frac{1}{2}\sum_{n=1}^{\infty}\Bigg\{-\frac{(1-N)t_1}{r_o^{n+2}\rho^{n+N+3}}\begin{pmatrix} A_n^o \\ B_n^o \end{pmatrix} + \left[\frac{2(1+N)t_4}{r_o^n\rho^{n+N+1}} - \frac{(1-N)t_3}{r_o^{n+2}\rho^{n+N+3}}\right]\begin{pmatrix} C_n^o \\ D_n^o \end{pmatrix}$$

$$\mp \frac{2H_n^{+1}}{r_o^2}\begin{pmatrix} E_n^o \\ F_n^o \end{pmatrix}\Bigg\}\begin{matrix}\cos(n-N-1)\Theta \\ \sin(n-N-1)\Theta\end{matrix} + \frac{1}{2}\sum_{n=1}^{\infty}\Bigg\{-\frac{(2n+N+3)t_1}{r_o^{n+2}\rho^{n+N+3}}\begin{pmatrix} A_n^o \\ B_n^o \end{pmatrix}$$

$$-\left[\frac{2(1+N)t_4 + 2nt_2^+}{r_o^n\rho^{n+N+1}} + \frac{(2n+3+N)t_3}{r_o^{n+2}\rho^{n+N+3}}\right]\begin{pmatrix} C_n^o \\ D_n^o \end{pmatrix} - \frac{2H_n^{-1}}{r_o^2}\begin{pmatrix} E_n^o \\ F_n^o \end{pmatrix}\Bigg\}\begin{matrix}\cos(n+N+1)\Theta \\ \sin(n+N+1)\Theta\end{matrix}$$

(6.44b)

$$M_{\rho\theta(1)} = \tilde{M}^{1}_{\rho\theta} + \frac{p^{*}N_{o,\rho}}{r_{o\rho}^{2\,N}} F_o^o \cos(1+N)\theta - \frac{2(D-D_{12})(1+N)}{r_{o\rho}^{2\,N+3}} A_o^o \sin(1+N)\theta$$

$$+ \frac{1}{2}\sum_{n=1}^{\infty}\left\{ \mp \frac{2(n+N+2)t_1}{r_o^{n+2}\,\rho^{n+n+3}} \begin{pmatrix} A_n^o \\ B_n^o \end{pmatrix} \mp \left[\frac{4n(n-1)(1+N)D_{66}}{r_{o\rho}^{n}\,\rho^{n+n+1}} + \frac{2(2+n+N)t_3}{r^{n+2}\rho^{n+N+3}} \right] \right.$$

$$\left. \begin{pmatrix} C_n^o \\ D_n^o \end{pmatrix} + \frac{H_n^{+2}}{r_o^2} \begin{pmatrix} E_n^o \\ F_n^o \end{pmatrix} \right\} \begin{matrix} \sin(n-N-1)\theta \\ \cos(n-N-1)\theta \end{matrix} + \frac{1}{2}\sum_{n=1}^{\infty} \mp \left\{ \frac{4D_{66}n(n+1)N}{r^{n+2}\rho^{n+N+3}} \begin{pmatrix} A_n^o \\ B_n^o \end{pmatrix} \right.$$

$$\left. \mp \left[\frac{4D_{66}n(n-1)(1+n+N)}{r_{o\rho}^{n\;n+N+1}} + \frac{2(2+n+N)t_3}{r^{n+2}\rho^{n+N+3}} \right] \begin{pmatrix} C_n^o \\ D_n^o \end{pmatrix} + \frac{H_n^{-2}}{r_o^2} \begin{pmatrix} E_n^o \\ F_n^o \end{pmatrix} \right\} \times$$

$$\begin{matrix} \sin(1+n+N)\theta \\ \cos(1+n+N)\theta \end{matrix}, \qquad (6.44c)$$

$$Q_{\rho(1)} = \tilde{Q}'_{\rho} \frac{\tilde{\lambda}kK_o(\tilde{\lambda}\rho)}{r_{o\rho}^{N+1}} F_o^o \sin(1+N)\theta + \frac{1}{2}\sum_{n=1}^{\infty}\left\{ \frac{4Dn(1-n)N}{r_o^{n+1}\,\rho^{n+N+2}} \begin{pmatrix} C_n^o \\ D_n^o \end{pmatrix} \mp \frac{H_n^{+3}}{r_o} \right.$$

$$\left. \begin{pmatrix} E_n^o \\ F_n^o \end{pmatrix} \right\} \begin{matrix} \cos(n-N-1)\theta \\ \sin(n-N-1)\theta \end{matrix} + \frac{1}{2}\sum_{n=1}^{\infty}\left\{ \frac{4Dn(1-n)(2+2n+N)}{r_o^{n+1}\,\rho^{n+N+2}} \begin{pmatrix} C_n^o \\ D_n^o \end{pmatrix} \mp \frac{H_n^{-3}}{F_n^o} \times \right.$$

$$\left. \begin{pmatrix} E_n^o \\ F_n^o \end{pmatrix} \right\} \begin{matrix} \cos\,(n+N+1)\theta \\ \sin\,(n+N+1)\theta \end{matrix} \qquad (6.44d)$$

$$Q_{\theta(1)} = \tilde{Q}'_{\theta} - \frac{\tilde{\lambda}kK_o''(\tilde{\lambda}\rho)}{r_o\rho^N} F_o^o \cos(1+N)\theta + \frac{1}{2}\sum_{n=1}^{\infty}\left[\mp\frac{4Dn(1-n)N}{r_o^{n+1}\rho^{n+N+2}}\begin{pmatrix}C_n^o\\D_n^o\end{pmatrix}\right.$$

$$\left. - \frac{H_n^{+4}}{r_o}\begin{pmatrix}E_n^o\\F_n^o\end{pmatrix}\right]\begin{matrix}\sin(n-N-1)\theta\\ \cos(n-N-1)\theta\end{matrix} + \frac{1}{2}\sum_{n=1}^{\infty}\left[\mp\frac{4Dn(1-n)(2+2n+N)}{r_o^{n+1}\rho^{n+N+2}}\begin{pmatrix}C_n^o\\D_n^o\end{pmatrix}\right.$$

$$\left. - \frac{H_n^{-4}}{r_o}\begin{pmatrix}E_n^o\\F_n^o\end{pmatrix}\right]\begin{matrix}\sin(n+N+1)\theta\\ \cos(n+N+1)\theta\end{matrix} \qquad (6.44e)$$

where

$$t_1 = 2D_{66}n(n+1)$$

$$H_n^{\pm 1} = \frac{p^*nN_{n,\rho}^1}{\rho^N} \mp \frac{p^*n^2N_n^1}{\rho^{N+1}} - \frac{(1+N)p^*N_n^3}{2\rho^{N+1}},$$

$$H_n^{\pm 2} = \frac{p^*}{\rho^N}N_{n,\rho} \mp \frac{np^*N_n^3}{\rho^{N+1}} \mp \frac{4p^*n(1+N)}{\rho^{N+1}}N_n^1,$$

$$H_n^{\pm 3} = \frac{nk}{\rho^N}\left(\frac{\tilde{\lambda}K_n'}{\rho} - \frac{K_n}{\rho^2}\right) \mp \frac{n^2k}{\rho^{N+2}}K_n \mp \frac{(1+N)k\tilde{\lambda}}{N+1}K_n',$$

$$H_n^{\pm 4} = \frac{k\tilde{\lambda}^2}{\rho^N}K_n'' \quad \frac{n\tilde{\lambda}k}{\rho^{n+1}}K_n' \mp \frac{n(1+N)k}{\rho^{N+2}}K_n. \qquad (6.45)$$

The notation $N_{n,\rho}$ signifies $\frac{dN_n}{d\rho}$. From the preceding chapter, it is seen that the solution given in Eqs. (6.38) and (6.39) corresponds to the local effect since, when ρ goes into infinity, the solution of Eqs. (6.38) and (6.39) will vanish. Therefore, the stress resultants and couples given in Eqs. (6.43) and (6.44) are the

local stress distributions and vanish at infinity. As mentioned before, the entire stress field includes the local and plate bending states of stress. The bending states of stress are denoted by M_ρ^∞, M_θ^∞, $M_{\rho\theta}^\infty$, Q_ρ^∞, and Q_θ^∞; therefore, the complete stress field is expressed as follows:

$$\begin{bmatrix} M_\rho^T \\ M_\theta^T \\ M_{\rho\theta}^T \\ Q_\rho^T \\ Q_\theta^T \end{bmatrix} = \begin{bmatrix} M_\rho^\infty \\ M_\theta^\infty \\ M_{\rho\theta}^\infty \\ Q_\rho^\infty \\ Q_\theta^\infty \end{bmatrix} + \sum_{n=0}^{\infty} \varepsilon^n \begin{bmatrix} M_{\rho(n)} \\ M_{\theta(n)} \\ M_{\rho\theta(n)} \\ Q_{\rho(n)} \\ Q_{\theta(n)} \end{bmatrix} \qquad (6.46)$$

where the superscript T in the left-hand side of Eq. (6.46) represents the quantities for the total field.

Now consider the case of an infinite plate subject to the bending moment M_1 along the edge where x = constant and bending moment M_2 along the edge where y = constant. The hole is located in the center of the plate and is free from loading on its edge. Before applying the boundary conditions at infinity, the applicable bending moments M_1 and M_2 in the rectangular Cartesian coordinate are transformed to curvilinear coordinates (ρ, θ) using the transformation laws.

$$\bar{M}_{\rho}^{\infty} = \frac{1}{2}(M_1 + M_2) + \frac{1}{2}(M_1 - M_2)\cos 2\alpha,$$

$$\bar{M}_{\theta}^{\infty} = \frac{1}{2}(M_1 + M_2) - \frac{1}{2}(M_1 - M_2)\cos 2\alpha,$$

$$\bar{M}_{\rho\theta}^{\infty} = \frac{1}{2}(M_2 - M_1)\sin 2\alpha,$$

$$\bar{Q}_{\rho}^{\infty} = 0 \ . \qquad (6.47)$$

By using Eq. (6.6), Eq. (6.47) takes the following form:

$$\bar{M}_{\rho}^{\infty} = \frac{1}{2}(M_1 + M_2) + \frac{1}{2}(M_1 - M_2)\cos 2\theta + \frac{N(M_1 - M_2)}{2\rho^{N+1}}[\cos(1 + N)\theta - \cos(N-1)\theta]$$
$$+ \frac{\varepsilon^2 N(M_1 - M_2)}{2\rho^{2N+2}}[\cos 2(N + 2)\theta - \cos 2\theta] + O(\varepsilon^3),$$

$$\bar{M}_{\rho\theta}^{\infty} = \frac{1}{2}(M_1 - M_2)\sin 2\theta - \frac{\varepsilon N(M_1 - M_2)}{2\rho^{N+1}}[\sin (N + 3)\theta + \sin (N - 1)\theta]$$
$$- \frac{\varepsilon^2 N^2(M_1 - M_2)}{2\rho^{2N+2}}[\sin 2(N + 2)\theta - \sin 2\theta] - O(\varepsilon^3),$$

$$\bar{Q}_{\rho}^{\infty} = 0. \qquad (6.48)$$

6.6. Boundary Conditions

From the boundary conditions of Eq. (3.43), the boundary conditions at infinity and on the hole edge are given below.

$$\text{At infinity, } \rho \to \infty: \quad M_\rho^T = \overline{M}_\rho^\infty,\ M_{\rho\theta}^T = \overline{M}_{\rho\theta}^\infty,\ Q_\rho^T = \overline{Q}_\rho^\infty. \tag{6.49}$$

$$\text{At the hole edge:} \quad M_\rho^T = 0,\ M_{\rho\theta}^T = 0,\ Q_\rho^T = 0\ . \tag{6.50}$$

Note that the second parenthesis in Eq. (6.46) vanishes when ρ goes into infinity. Eq. (6.49) may then be rewritten as follows:

$$M_\rho^\infty = \overline{M}_\rho^\infty,\ M_{\rho\theta}^\infty = \overline{M}_{\rho\theta}^\infty,\ Q_\rho^\infty = \overline{Q}_\rho^\infty, \tag{6.51}$$

If the second boundary condition Eq. (6.50) is applied along with Eqs. (6.51), (6.48), and (6.46), the following equations are obtained for the zero and first orders of ε:

$O(\varepsilon^\circ)$:

$$M_{\rho_{(0)}} + \frac{1}{2}(M_1 + M_2) + \frac{1}{2}(M_1 - M_2)\cos 2\theta = 0,$$

$$M_{\rho\theta_{(0)}} - \frac{1}{2}(M_1 - M_2)\sin 2\theta = 0,$$

$$Q_{\rho_{(0)}} = 0. \tag{6.52}$$

$O(\varepsilon)$:

$$M_{\rho_{(1)}} + \frac{N}{2}(M_1 - M_2)\{\cos(N+3)\theta - \cos(N-1)\theta\} = 0,$$

$$M_{\theta_{(1)}} - \frac{N}{2}(M_1 - M_2)\{\sin(N+3)\theta + \sin(N-1)\theta\} = 0,$$

$$Q_{\rho_{(1)}} = 0. \tag{6.53}$$

From Eqs. (6.52) and (6.43) the following non-zero coefficients are obtained:

$$A_o^o = -\frac{(M_1 + M_2)r_o^2}{2(D_{11} - D_{12})}, \quad E_2^o = -\frac{2(M_1 - M_2)D_{11}}{k[(D_{11} + D_{12})K_2 + 2D_{11}K_o]},$$

$$C_2^o = -\frac{(M_1 - M_2)K_2 r_o^2}{2[(D_{11} + D_{12})K_2 + 2D_{11}K_o]},$$

$$A_2^o = -\frac{r_o^4 k}{8D_{11}D_{66}}[(D_{11} + D_{66})K_2 - D_{11}K_o]E_2^o . \tag{6.54}$$

Similarly, the following expressions are obtained from Eqs. (6.44) and (6.53):

$$\tilde{M}_\rho^1 - \frac{4D_{66}}{r_o^2}A_o^o \cos(1 + N)\theta + \frac{1}{2}U_{N-1}^o \cos(N - 1)\theta + \frac{1}{2}U_{N+3}^o \cos(N + 3)\theta$$

$$+ \frac{N}{2}(M_1 - M_2)[\cos(N + 3)\theta - \cos(N - 1)\theta] = 0,$$

$$\tilde{M}_{\rho\theta}^1 - \frac{4D_{66}(1 + N)}{r_o^2}A_o^o \sin(1 + N)\theta - \frac{1}{2}V_{N-1}^o \sin(N - 1)\theta$$

$$- \frac{N}{2}(M_1 - M_2)[\sin(N + 3) + \sin(N - 1)\theta] = 0,$$

$$\tilde{Q}^1_\rho + \frac{1}{2} W^o_{N-1} \cos(N - 1)\theta + \frac{1}{2} W^o_{N+3} \cos(N + 3)\theta = 0, \quad (6.55)$$

where the quantities U^o_i, V^o_i, and $W^o_i (i = N-1, N+3)$ are defined as

$$U^o_{N-1} = \frac{(1 - N)t_1}{r_o^4} A^o_2 + \left[\frac{-2(1 + N)t_4}{r_o^2} + \frac{(1 - N)t_3}{r_o^4}\right] C^o_2 + \frac{2H_2^{+1}}{r_o^2} E^o_2,$$

$$U^o_{N+3} = \frac{(N + 7)t_1}{r_o^4} A^o_2 + \left[\frac{2(1 + N)t_4 - 4t_2}{r_o^2} + \frac{(N + 7)t_3}{r_o^4}\right] C^o_2 + \frac{2H_2^{-1}}{r_o^2} E^o_2,$$

$$V^o_{N-1} = -\frac{2(N + 4)t_1}{r_o^4} A^o_2 - \left[\frac{8(1 + N)D_{66}}{r_o^2} + \frac{2Nt_3}{r_o^4}\right] C^o_2 + \frac{H_2^{+2}}{r_o^2} E^o_2,$$

$$V^o_{N+3} = \frac{24D_{66}N}{r_o^4} A^o_2 + \left[\frac{8D_{66}(3 + N)}{r_o^2} + \frac{2(4 + N)t_3}{r_o^4}\right] C^o_2 + \frac{H_2^{-2}}{r_o^2} E^o_2,$$

$$W^o_{N-1} = -\frac{8DN}{r_o^3} C^o_2 + \frac{H_2^{+3}}{r_o} E^o_2,$$

$$W^o_{N+3} = \frac{8D(6 + N)}{r_o^3} C^o_2 + \frac{H_2^{-3}}{r_o} E^o_2. \quad (6.56)$$

The quantities $\tilde{M}^1_\rho$, $\tilde{M}^1_{\rho\theta}$, $\tilde{M}^1_\theta$, $\tilde{Q}^1_\rho$, and $\tilde{Q}^1_\theta$ are obtained from Eq. (6.41) when i = 1. Substituting these quantities into Eq. (6.55) yields the following:

$$\frac{2D_{66}}{r_o^2} A_o^1 + \sum_m \left\{ - \frac{2D_{66}m(m+1)}{r_o^{2+m}} A_m^1 + \left[\frac{2(m-1)[(D+D_{12}) - mD_{66}]}{r_o^m} \right.\right.$$

$$\left.\left. - \frac{8p^*Dm(1-m^2)}{kr_o^{m+2}} \right] C_m^1 + \frac{2p^*mN_m^1}{r_o^2} E_m^1 \right\} \cos m\theta - \bar{U}_m^o \cos m\theta = 0,$$

$$\sum_m \left\{ - \frac{2D_{66}m(m+1)}{r_o^{m+2}} A_m^1 - \left[\frac{2D_{66}m(m-1)}{r_o^m} + \frac{8p^*Dm(1-m^2)}{kr_o^{m+2}} \right] C_m^1 + \frac{p^*N_m^3}{r_o^2} E_m^1 \right\} \times$$

$$\sin m\theta - \bar{V}_m^o \sin m\theta = 0,$$

$$\sum_m \left[\frac{km}{r_o} K_m(\tilde{\lambda}\rho) E_m^1 - \frac{4Dm(m-1)}{r_o^{m+1}} C_m^1 \right] \cos m\theta + W_m^o \cos m\theta = 0 \tag{6.57}$$

where $m = N-1$, $N+1$, and $N+3$ and $\bar{U}_i^o$, $\bar{V}_i^o$, $i = N-1$, $N+1$, $N+3$, and W_{N+1}^o are defined as

$$\bar{U}_{N-1}^o = \frac{N}{2}(M_1 - M_2) - \frac{1}{2}U_{N-1}^o, \quad \bar{U}_{N+1}^o = \frac{4D_{66}}{r_o^2} A_2^o,$$

$$U_{N+3}^o = -\frac{N}{2}(M_1 - M_2) - \frac{1}{2}U_{N+3}^o,$$

$$\bar{V}_{N-1}^o = \frac{N}{2}(M_1 - M_2) + \frac{1}{2}V_{N-1}^o, \quad V_{N+1}^o = \frac{4D_{66}(1+N)}{r_o^2} A_o^o$$

$$V_{N+3}^o = \frac{N}{2}(M_1 - M_2) - \frac{1}{2}V_{N+3}^o,$$

$$W^{o}_{N+1} = 0 \ . \qquad (6.58)$$

By solving the algebraic equations, the constants in Eq. (6.57) are obtained as follows:

$$E^{1}_{m} = \frac{2D(\bar{U}^{o}_{m} - \bar{V}^{o}_{m} - \frac{D + D_{12}}{2Dm} W^{o}_{m} r_{o})}{k[(D + D_{12})K_{m} + 2DK_{m-2}]} \ , \ A^{m}_{o} = 0,$$

$$C^{1}_{m} = \frac{W^{o}_{m} r_{o}^{m+1}}{4Dm(m + 1)} + \frac{k r_{o}^{m} K_{m}}{4D(m - 1)} E^{1}_{m},$$

$$A^{1}_{m} = \frac{1}{4D_{66}m(m + 1)} \Big\{ \{2(m - 1)[(D + D_{12}) - 2mD_{66}]r_{o}^{2} - \frac{16p^{*}D}{k} m(1 - m^{2})\} C^{1}_{m}$$

$$+ p^{*} r_{o}^{m} (2mN^{1}_{m} + N^{3}_{m}) E^{1}_{m} - r_{o}^{m+2} \bar{U}^{o}_{m} - V_{o}^{m+2} \bar{V}^{o}_{m} \Big\} \qquad (6.59)$$

with $m \neq 0$.

Now consider the case for $N = 1$, which corresponds to the elliptical hole case. The value of m for this case will be zero; hence Eq. (6.58) cannot be applied directly. However, the solution for this case can be calculated by directly inserting the value of $m = 0, 2, 4$ into Eq. (6.57). By calculating this set of algebraic equations, it is found that the results have the same formula as Eq. (6.59) but the m will now stand for $N + 1$ and $N + 3$ only and the value of A^{1}_{o} will no longer be zero.

Substituting the non-zero coefficient into Eqs. (6.46), (6.44), and (6.43), the solution for the complete problem is obtained. In most cases, only the stress around the hole edge is of interest. This problem can be solved by directly setting $\rho = 1$ in Eq. (6.46). However, the simplest way to calculate M_θ^T around the hole edge is to evaluate the sum of M_θ^T and M_ρ^T and then set $\rho = 1$ on the hole edge since the value of M_ρ^T is zero when $\rho = 1$. In this way, the expression for M_θ^T around the hole edge can be obtained as follows:

$$M_\theta^T\Big|_{\rho=1} = (M_1 + M_2) + \frac{4(D_{11} + D_{12})}{r_o^2} C_2^o \cos 2\theta$$

$$+ \varepsilon\left[- \frac{8(D_{11} + D_{12})}{r_o^2} C_2^o \cos(N + 3)\theta + \sum_m \frac{4(m - 1)(D_{11} + D_{12})}{r_o^m} C_m^1 \cos m\theta \right]$$

$$+ O(\varepsilon^2) \, . \qquad (6.60)$$

The resultant shear stress, Q_θ^T, can be evaluated directly from Eq. (6.46) in the form

$$Q_\theta^T\Big|_{\rho=1} = -\left[\frac{\tilde{\lambda}k}{r_o} K_2'(\tilde{\lambda}) E_2^o + \frac{8D}{r_o^3} C_2^o\right] \sin 2\theta + \varepsilon\Big\{ -$$

$$\sum_m \left[\frac{\tilde{\lambda}k}{r_o} K_m'(\tilde{\lambda}) E_m^1 + \frac{4Dm(m - 1)}{r_o^{m+1}} C_m^1\right] \sin m\theta - \frac{1}{2}\Big(+ \frac{8D}{r_o^3} C_2^o + \frac{H_2^{+4}}{r_o} E_2^o \Big) \sin(1 - N)\theta$$

$$+ \frac{1}{2}\left[\frac{8D}{r_o^3}(6 + N)C_2^o - \frac{H_2^{-4}}{r_o}E_2^o\right]\sin(3 + N)\theta\Big\} + O(\varepsilon^2) \quad (6.61)$$

where the m is equal to N - 1, N + 1, and N + 3 when $N \neq 1$. For N = 1, the m will be N + 1 and N + 3 only.

In Eq. (6.60), when only the zero-order term is retained and the coefficient C_2^o in Eq. (6.54) is used, the zero-order solution of M_θ^T with $\rho = 1$ is obtained as

$$M_\theta^T\Big|_{\rho=1} = M_1 + M_2 - \frac{2(D_{11} + D_{12})(M_1 - M_2)K_2(\tilde{\lambda})}{[(D_{11} + D_{12})K_2(\tilde{\lambda}) + 2D_{11}K_o(\tilde{\lambda})]}\cos 2\theta + O(\varepsilon). \quad (6.62)$$

Eq. (6.62) is exactly the same expression as Eq. (5.8) for the circular hole case. This is the expected result. Similarly, for the resultant shear Q_θ^T, the following expression applies for zero order:

$$Q_\theta^T\Big|_{\rho=1} = \frac{2(M_1 - M_2)D_{11}\lambda K_1(\tilde{\lambda})}{[(D_{11} + D_{12})K_2(\tilde{\lambda}) + 2D_{11}K_o(\tilde{\lambda})]}\sin 2\theta + O(\varepsilon). \quad (6.63)$$

Eq. (6.63) is the same expression as Eq. (5.11) for the circular hole case.

In conclusion, the zero-order solutions of Eqs. (6.60) and (6.61) are the solutions for the circular hole case; however, their higher order solutions are the modified terms that indicate solutions

for deviations from a circular hole. These modified terms depend on the values of ε and N, which vary for the different types of hole examined. In order to avoid the tedious expressions, M_θ^T and Q_θ^T at $\rho = 1$ for different hole shapes (elliptical, diamond-shaped, and triangular) are not presented in this dissertation. Instead, the numerical solutions for different cases are given by the curves indicated in Figures

6.7. Numerical Results

Several numerical examples are presented in this investigation. Most are given for St/Al/St laminated composite plates. Figure 33 gives plots of Eq. (6.60) around the hole for $\varepsilon = 1/9$ and $N = 3$; Figure 34 gives M_θ^T/M_0 for $\varepsilon = 1/4$ and $N = 2$; and Figure 35 is for $\varepsilon = 1/6$ and $N = 3$. All these cases have the same hole size $R = 1.25$ inch. As expected, the diamond-shaped hole case has the highest stress concentration factor. As the size of hole decreases, the stress distribution pattern for M_θ^T around the hole changes; however, the stress concentration factor increases. This is indicated in Figures 35 and 36 for the same ε and N but with a different value for R. The deviations between the one-term and two-term solutions are given in Figures 36 through 38 for different hole types. From Figures 38 it is seen that the perturbation solution is very close to the exact solution given by Eq. (5.50). Figure 39 shows the one-term and two-term solutions for the elliptical hole as well as the exact solution given in Eq. (5.52).

From both figures it is seen that the perturbation solution of the first order only will give a higher value than the exact one. However, these solutions do agree quite well. This may also be justified because the elliptical hole is very close to the circular hole. If we examine the diamond-shaped hole in Figure 36, the deviation between the one-term and two-term solutions is considerable. Therefore, it is suspected that the two-term solution is not sufficiently accurate.

In order to investigate the effect of ε in the perturbation solution, comparisons of Eqs. (5.50) and (6.60) at $\Theta = 90°$ with $N = 1$ are studied for different values of ε. Table VI gives the results. It may be seen that, since the value of ε is less than 0.1, the accuracy of the perturbation solution is less than $\pm 3\%$. This value is acceptable for both mathematicians and engineers. However, when the ε value is greater than 0.1, the percentage of accuracy drops drastically.

A comparison of the perturbation solution with the finite element solution is discussed in Chapter 7.

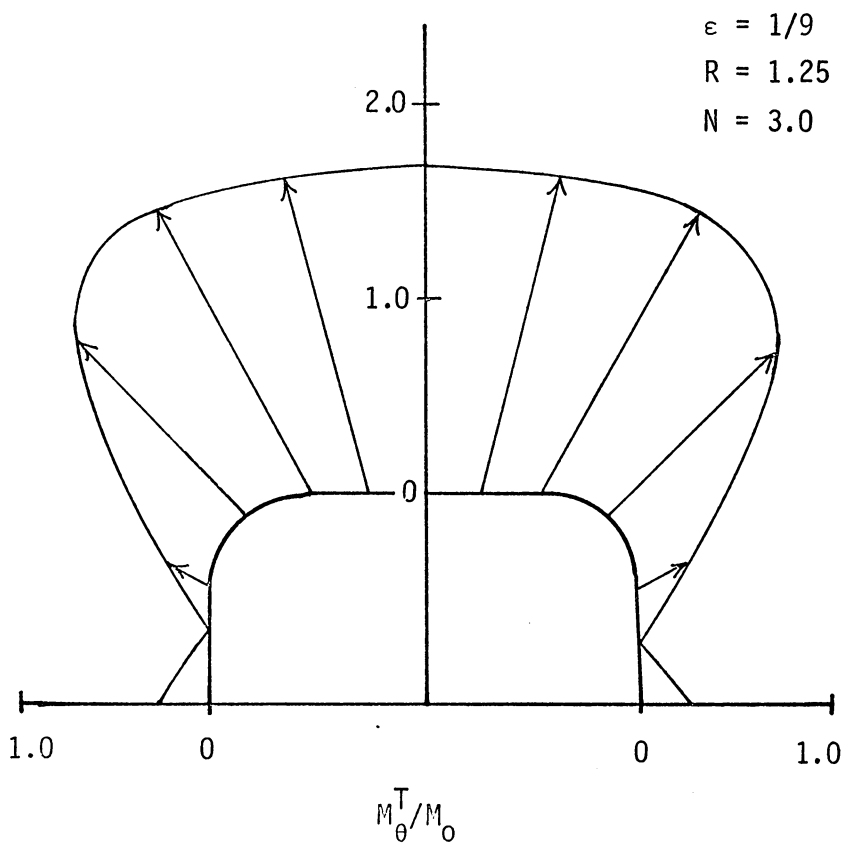

Figure 33. Distribution of M_θ/M_o Around Square Hole in $(St/Al)_s$ Sandwich Plate, R = 1.25

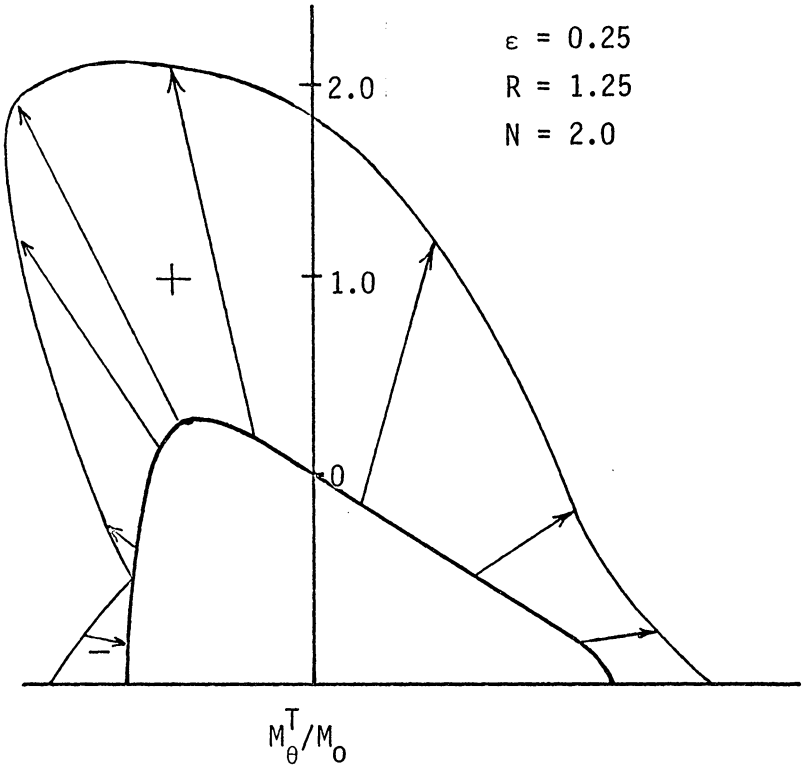

Figure 34. Distribution of M_θ/M_o Around Triangular Hole in $(St/Al)_s$ Sandwich Plate, R = 1.25

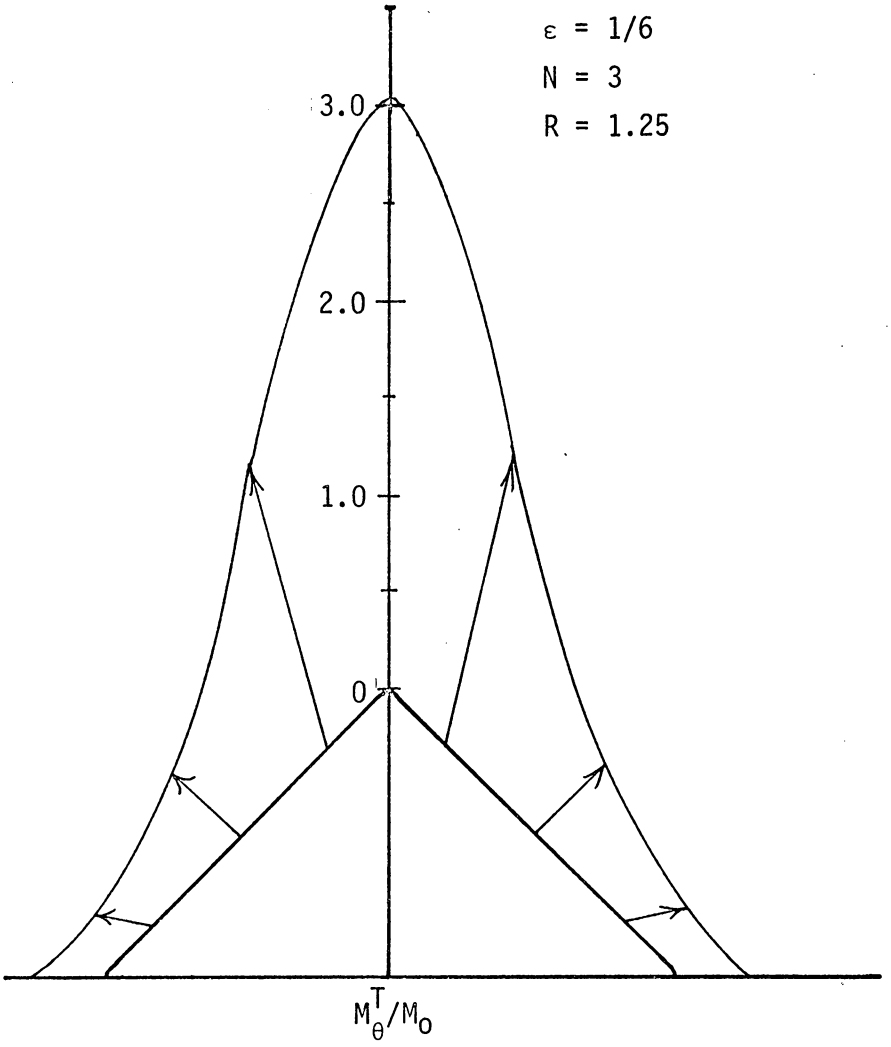

Figure 35. Distribution of M_θ/M_o Around Diamond-Shaped Hole in $(St/Al)_s$ Sandwich Plate, R = 1.25

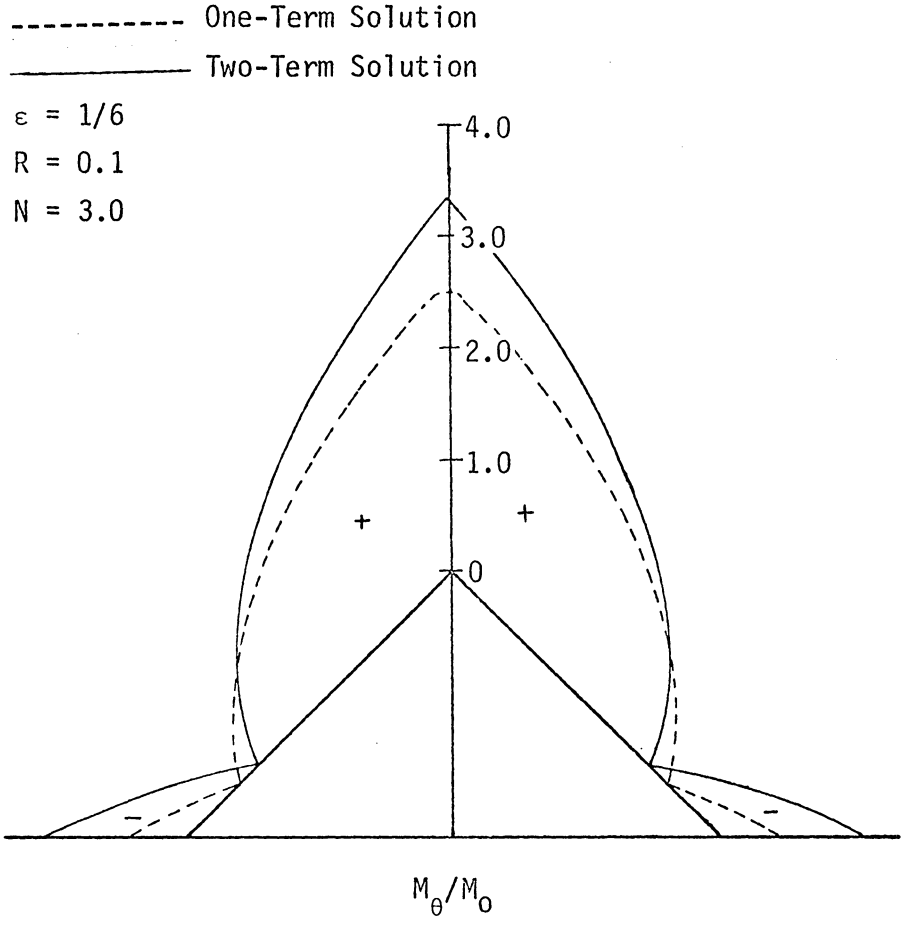

Figure 36. Distribution of M_θ/M_o Around Diamond-Shaped Hole in $(St/Al)_s$ Sandwich Plate, R = 0.1, for Perturbation Solution

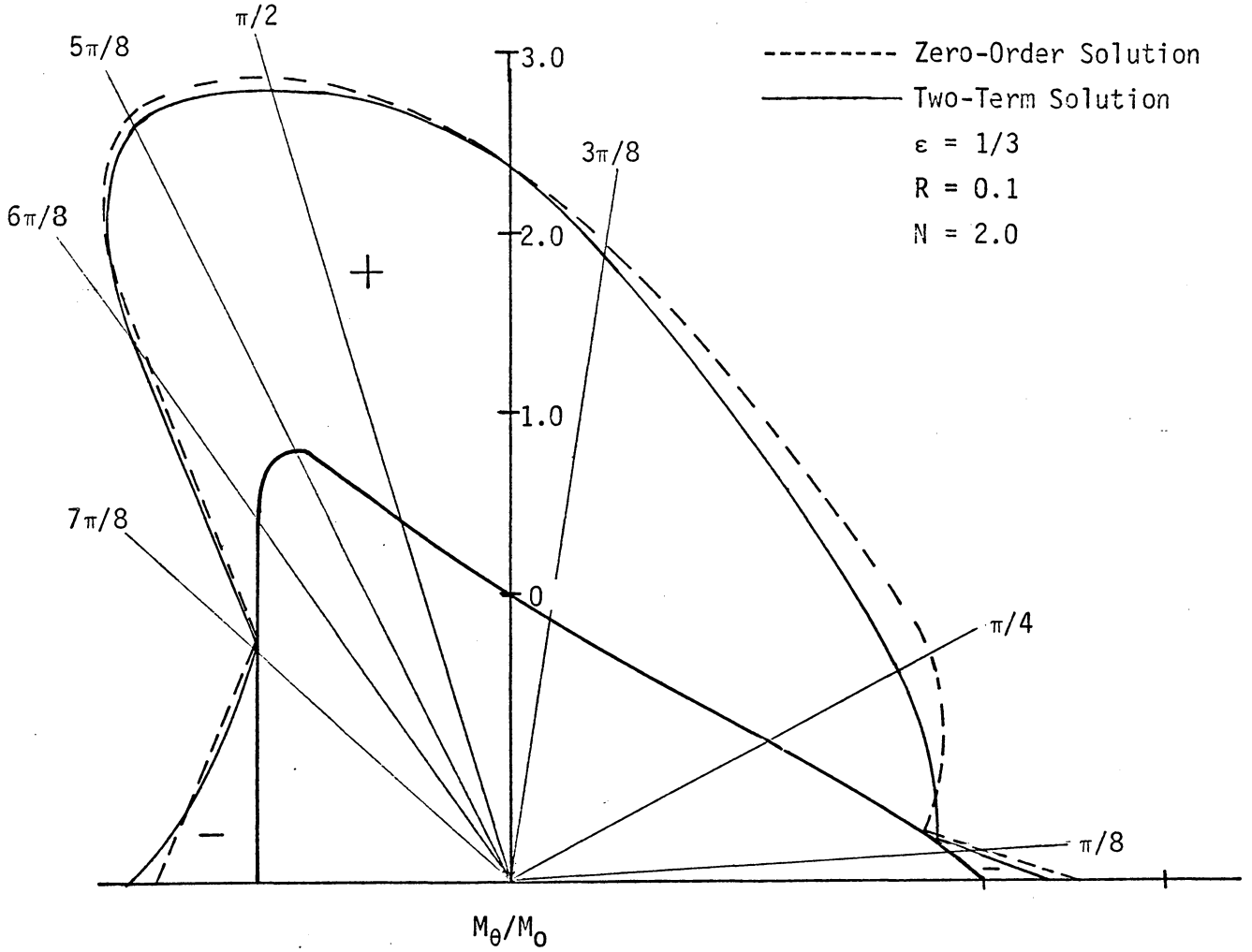

Figure 37. Distribution of M_θ/M_o Around Triangular Hole in $(St/Al)_s$ Sandwich Plate, R = 0.1

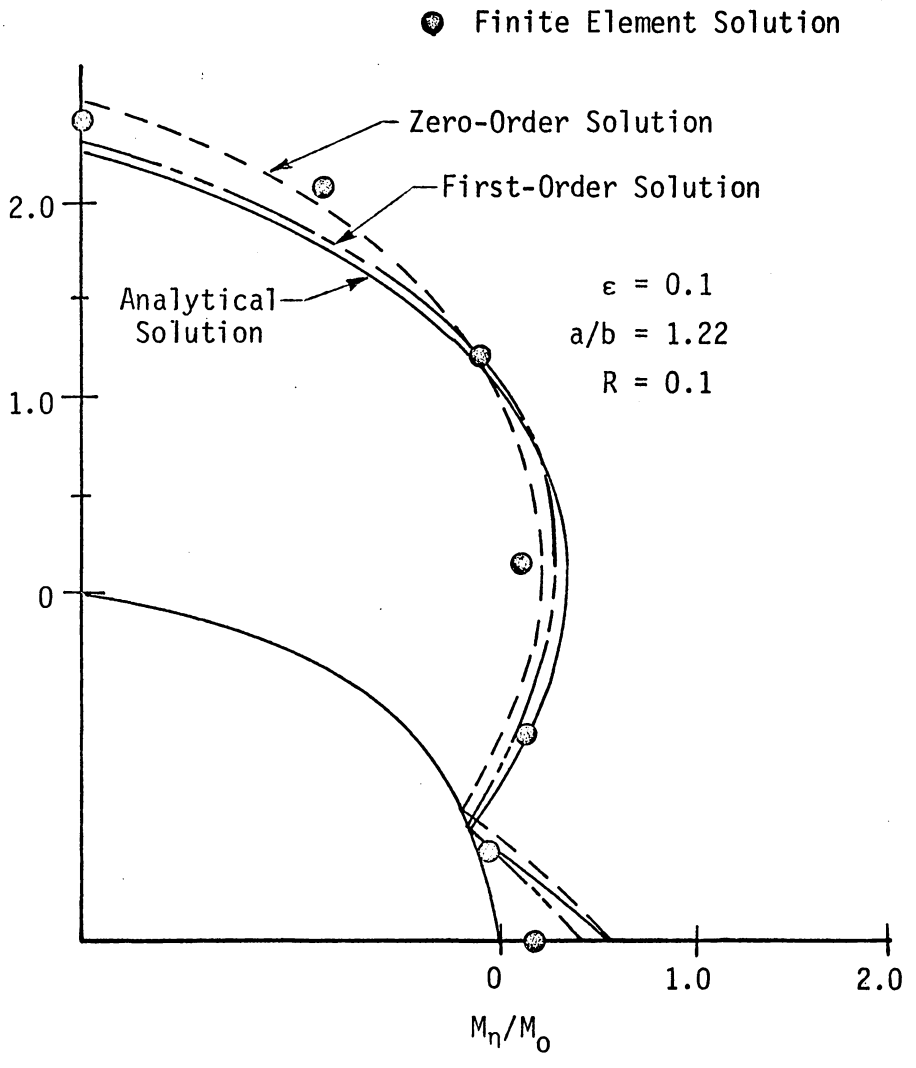

Figure 38. Distribution of M_η/M_o Around Elliptical Hole in $(St/Al)_S$ Sandwich Plate for Perturbation, Finite Element, and Analytical Solutions

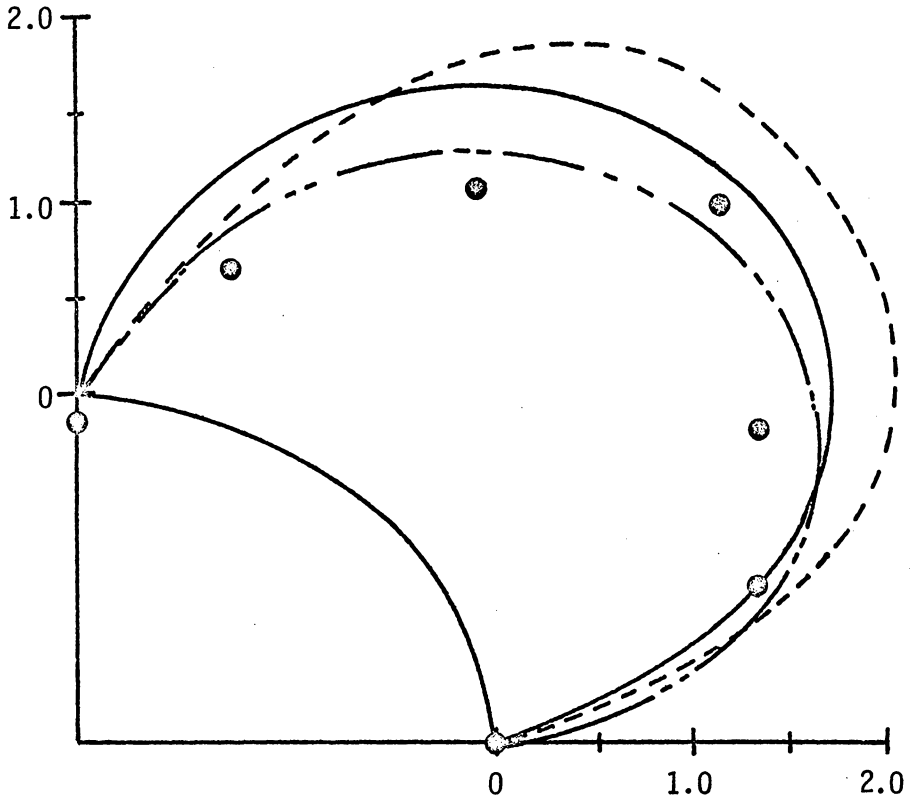

Figure 39. Distribution of Q_η/M_o Around Elliptical Hole in (St/Al/St) Sandwich Plate for Perturbation, Finite Element, and Analytical Solutions

TABLE IV. EFFECT OF ϵ IN THE PERTURBATION SOLUTION

ϵ	M_Θ^T/M_o Eq. (5.50)	M_Θ^T/M_o Eq. (6.60)	a/b	%
0.2	2.03	2.431	1.50	19.8
0.1	2.27	2.332	1.22	3.1
0.05	2.39	2.432	1.11	1.7
0.01	2.50	2.513	1.02	0.5

where a = semi-major axis, b = semi-minor axis

VII. FINITE ELEMENT SOLUTION

As mentioned in Chapter II,the three-dimensional finite element analysis for the state of stress around a circular hole in a laminated composite plate under uniform tension, has been studied by Barker, Dana, and Pryor [19]; that work has also been extended by Dana [28]. They used a curved, isoparametric cubic, three dimensional element (see reference [28] Figure 2, or [18] Figure 12) with 24 nodal points and 72 degrees of freedom (DOF) to model the individual layers of the laminate. This element initially was coded by Lin [18] and tested by him for a Al-St laminate undergoing cylindrical bending by a sinusoidal load in comparison with results of Pagano [38]. Their results show that the finite element analysis for a three-ply laminate agreed well with the exact elasticity solution. A most efficient FORTRAN coded computer program was developed by Dana using the conjugate gradient iterative method. The great advantage of this technique is that it does not require the global stiffness matrix but only the unique element stiffness matrices. The nodal displacements are then determined by minimizing the total potential energy of the system at the element level. In doing this, the storage requirements are greatly reduced, and the roundoff errors will not accumulate during the iterative process.

The three nodal displacements (u, v, w) at each node obtained from the minimization technique are used in conjunction with the shape function to give the six stress components at each node. In

this section, the same element is used to study the laminated composite plate under pure bending with a hole. For convenient discussion, this section is divided into two parts. One is for the isotropic homogeneous laminated composite plate with a hole. Its solutions are employed to compare with the analytical solutions obtained in Chapters V and VI. The second part describes orthotropic homogeneous laminated composites with a circular hole. Four different types of stacking sequences are investigated. They are $(90/0)_s$, $(0/90)_s$, $(-45/45)_s$ and $(45/-45)_s$ fiber orientations. Since there are at present no analytical solutions associated with these types, only the finite element solutions are given in this section. Fortunately, the classic solution for single-layer orthotropic and orthotropic anisotropic plates has been given by Lekhnitskii [21]. A comparative investigation between the finite element solution and the classical solutions for single-layer plates may then be studied.

The geometry of the finite element mesh for the laminated composite plate is shown in Figure 40. The specimen has a length 2a, width 2b, thickness h, and a hole diameter D. The plate comprises three layers or laminas, each with a thickness t, and it is subjected to a pure rotation by applying rotational displacements at $x = \pm a$.

Two types of laminates are idealized with a finite element mesh. The first mesh type (Figure 40-I) is the model for the first group of laminated composites and orthotropic laminated

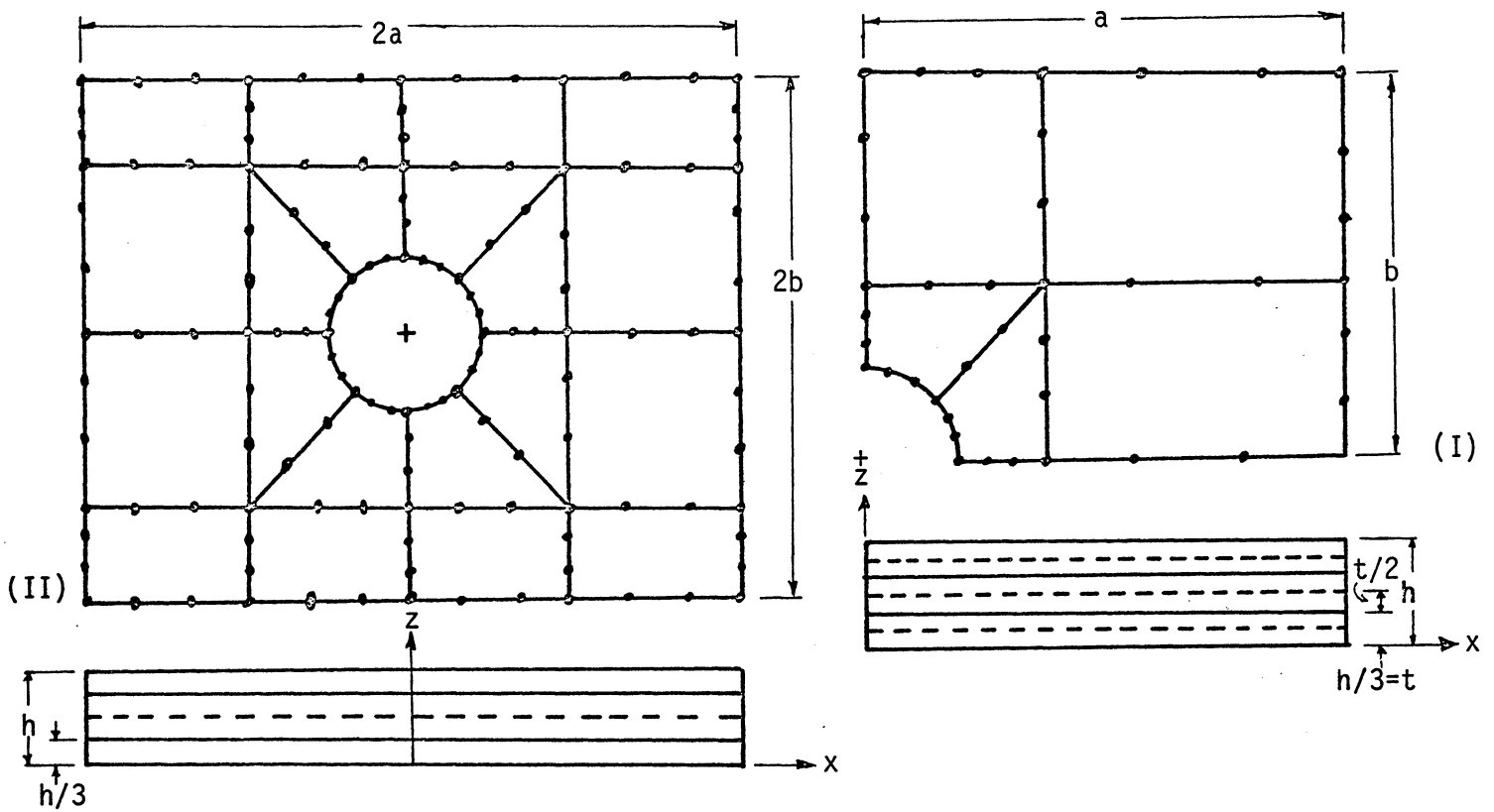

Figure 40. Finite Element Meshes, Types I and II

composites with the laminates pierced by a hole. There are two planes of symmetry, so that only a quarter of the laminate is modeled. Two elements are used through the thickness of each lamina. The laminate dimensions are a = 1 inch, b = 1 inch, and h = 0.3 inch. Therefore, each element thickness is 0.05 inch; the diameter of the hole is 0.2 inch. Thirty elements are used, six of which are unique. The mesh has 287 nodal points and 861 degrees of freedom.

The second mesh type (see Figure 40-II) is the model for angle-ply laminates. From Pagano's analysis [38], it can be seen that for the pure bending case, there are no planes of symmetry; therefore, the entire laminate must be modeled. As a result, four times more elements are required for modeling an angle-ply laminate than for the cross-ply laminate. For the sake of computing time, only one element is used to model the thickness of each lamina. This type of mesh has 80 elements, of which 18 are unique. There are 680 nodal points with 2040 DOF.

In the analytical solution, the stresses were expressed in terms of stress resultants and couples. To compare the finite element solution with the analytical values, the stresses given by the finite element solution must be converted to stress resultants and couples by Eqs. (3.18) and (3.19) The integration is performed numerically by using the trapezoidal rule through the thickness of each element. Stresses from the finite element

program may be displayed in either rectangular or polar coordinates. However, since the stresses around the hole are of interest the stress must be expressed as a function of the hole edge coordinate. Therefore, a modified subroutine was added to transform the stresses to the hole edge coordinates.

The stress M_0, as seen in Chapters V and VI is known as an applied moment at the far ends of plate. In this analysis, the value of M_0 is evaluated by averaging the far-end moments in the laminate.

Experience shows that it is very difficult to specify the boundary condition to produce pure bending by applying in-plane loading on the ends of laminated plate because it is difficult to obtain a convergent solution. In the present analysis the pure bending is provided by specifying pure initial rotation at the ends of laminates with respect to the center of the plate thickness. The maximum initial displacements on the far end boundaries at $x = \pm 1.0$ for $z = 0$ and 0.3 were taken to be equal to ± 0.0006 inch.

The material properties of aluminum and steel were taken as $E = 30 \times 10^6$ psi, $\nu = 0.33$, $G = 11.25 \times 10^6$ psi for steel (St), $E = 10 \times 10^6$ psi, $\nu = 0.32$, $G = 3.788 \times 10^6$ psi for aluminum (Al). For the orthotropic material the properties were taken as follows:

$$E_{11} = 20 \times 10^6 \text{ psi}, \quad E_{22} = 2.1 \times 10^6 \text{ psi}$$

$$\nu_{12} = \nu_{13} = \nu_{23} = 0.21, \quad G_{12} = G_{23} = G_{13} = 8.5 \times 10^5 \text{ psi}.$$

The comparative study of the finite element and analytical solutions is given in Figures 38-39 and 41-46. Figures 38 and 39 are for the elliptical hole case; the solutions calculated using three different techniques agree well. Figures 41 and 42 are for square holes and diamond-shaped holes, respectively. They show the two-term perturbation and finite element solutions. It can be seen that the finite element solution will have a higher value than the two-term perturbation solution. This is not surprising since the accuracy of the two-term perturbation solution for this case suffered considerably. The higher the order of the terms included in the solution, the more accurate the perturbation solutions become, and the black dots in Figures 41 and 42 will be closer to the finite element solution.

Figure 45 shows the finite element and exact solutions. The finite element solution is quite accurate. The normal stress distribution through the plate thickness is given in Figures 43 and 31 for circular and elliptical holes, respectively. Upon examination of Figure 44, it is seen that the finite element method gives poor accuracy for the shear stresses. This is due to two reasons: (1) a coarse mesh is used through the plate thickness in the model and (2) the 72DOF three-dimensional element has a linear shape function in the thickness. Therefore, due to the latter, a finer mesh may be required in the plate thickness in order to achieve more accurate results. However, unfortunately, that would

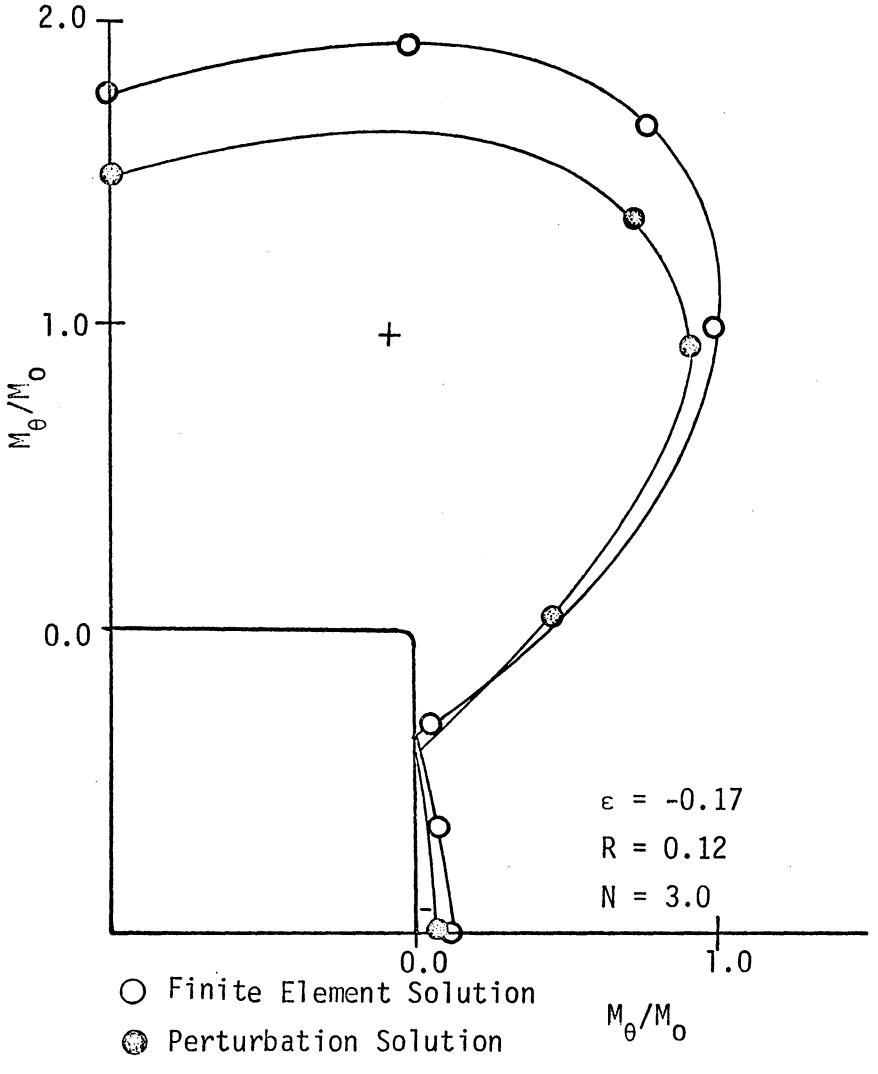

Figure 41. Variation of M_θ/M_o Around Square Hole in $(St/Al)_s$ Sandwich Plate for Finite Element and Perturbation Solutions

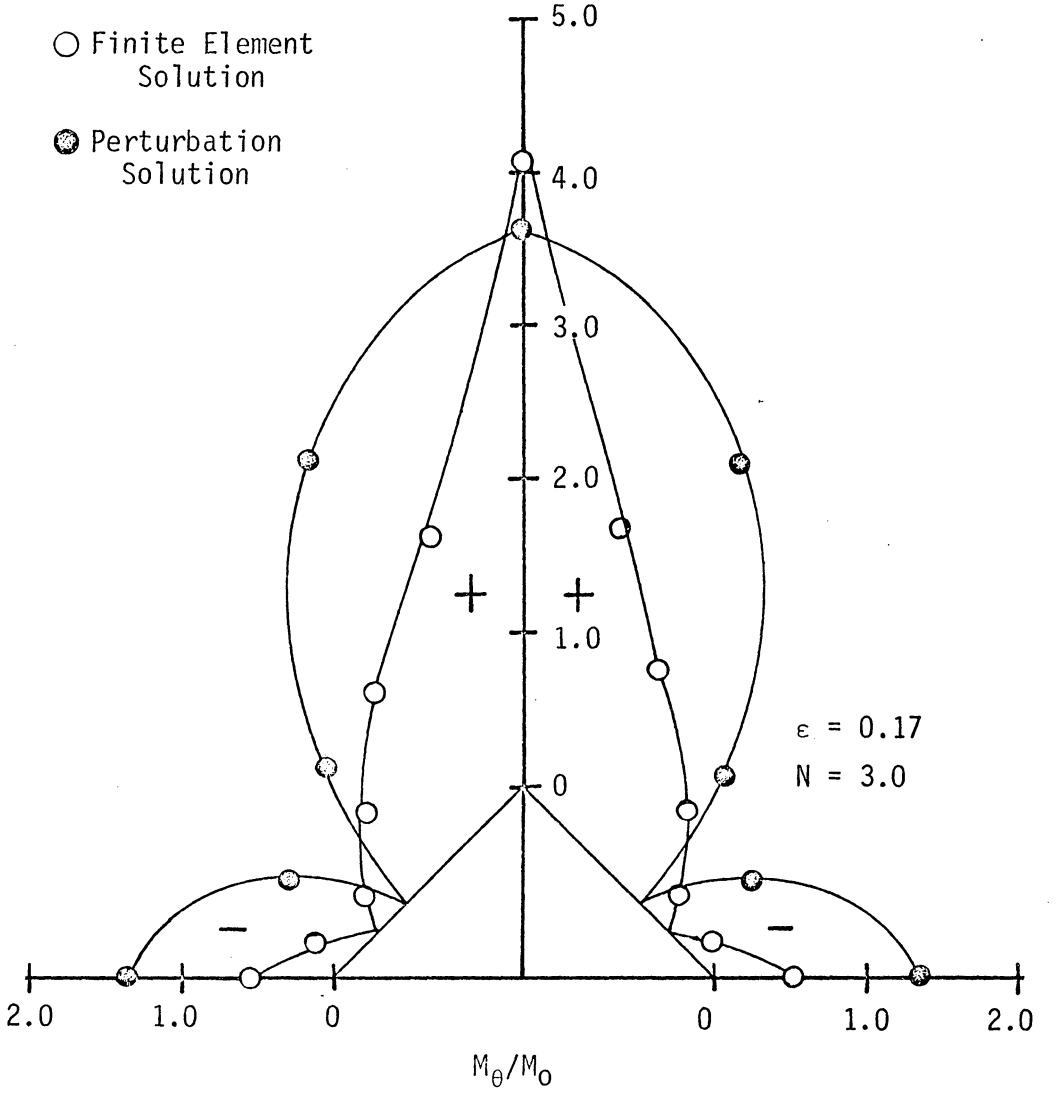

Figure 42. Distribution of M_θ/M_o Around Diamond-Shaped Hole in $(St/Al)_s$ Sandwich Plate, R = 0.09, for Perturbation and Finite Element Solutions

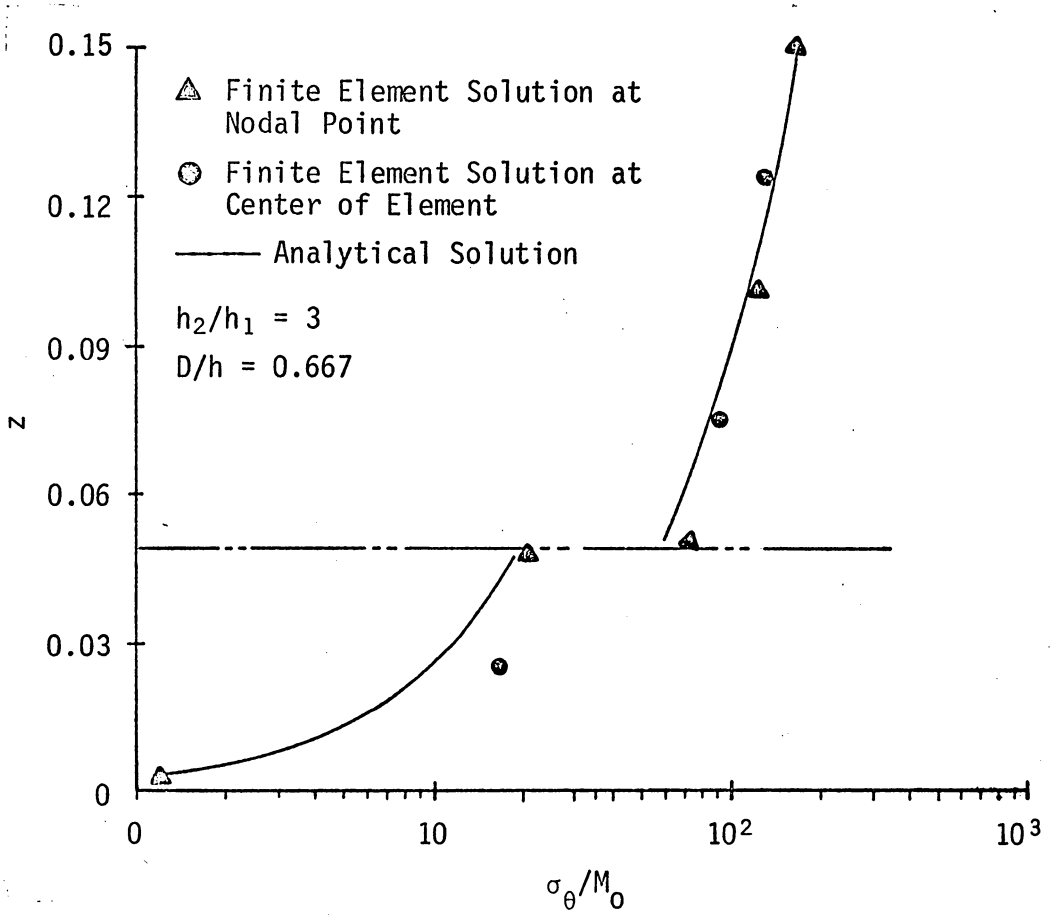

Figure 43. Distribution of σ_θ/M_o Through Plate Thickness at Circular Hole in $(St/Al)_s$ Sandwich Plate for Finite Element and Analytical Solutions

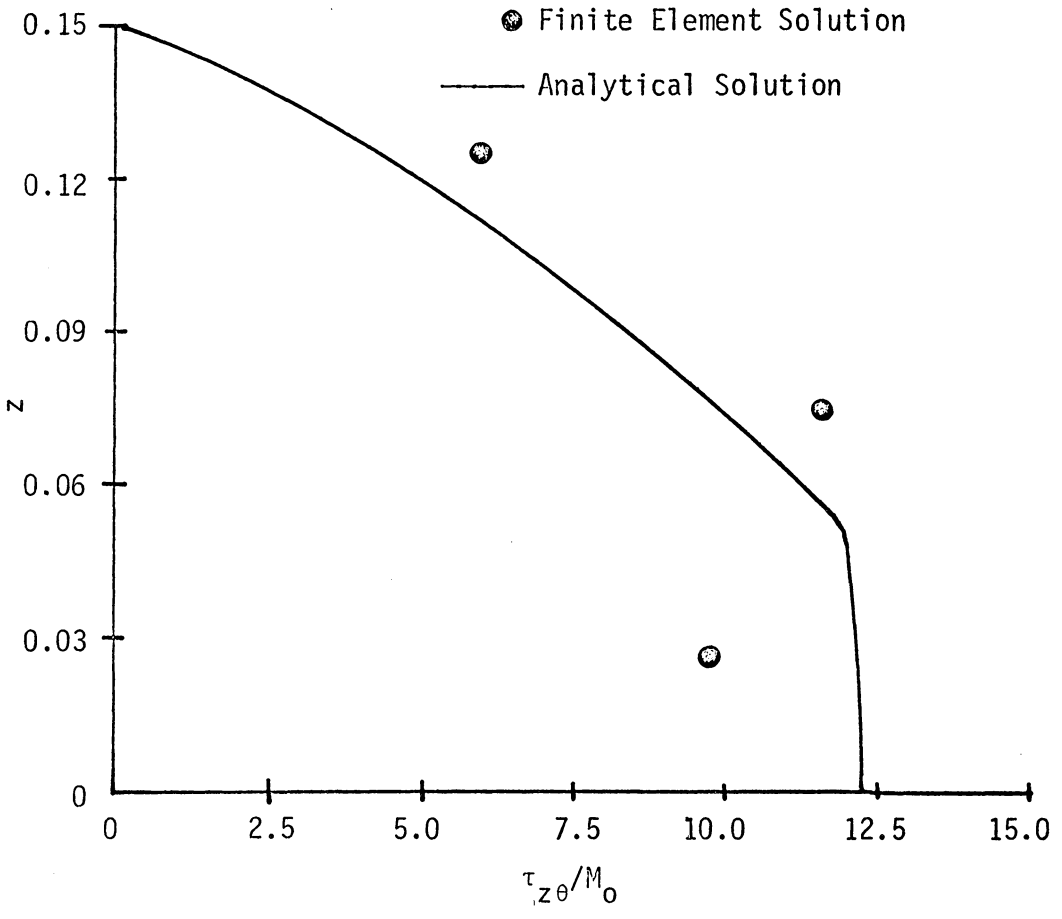

Figure 44. Distribution of $\tau_{z\theta}/M_o$ Through Plate Thickness at Circular Hole in $(St/Al)_s$ Sandwich Plate for Finite Element and Analytical Solutions

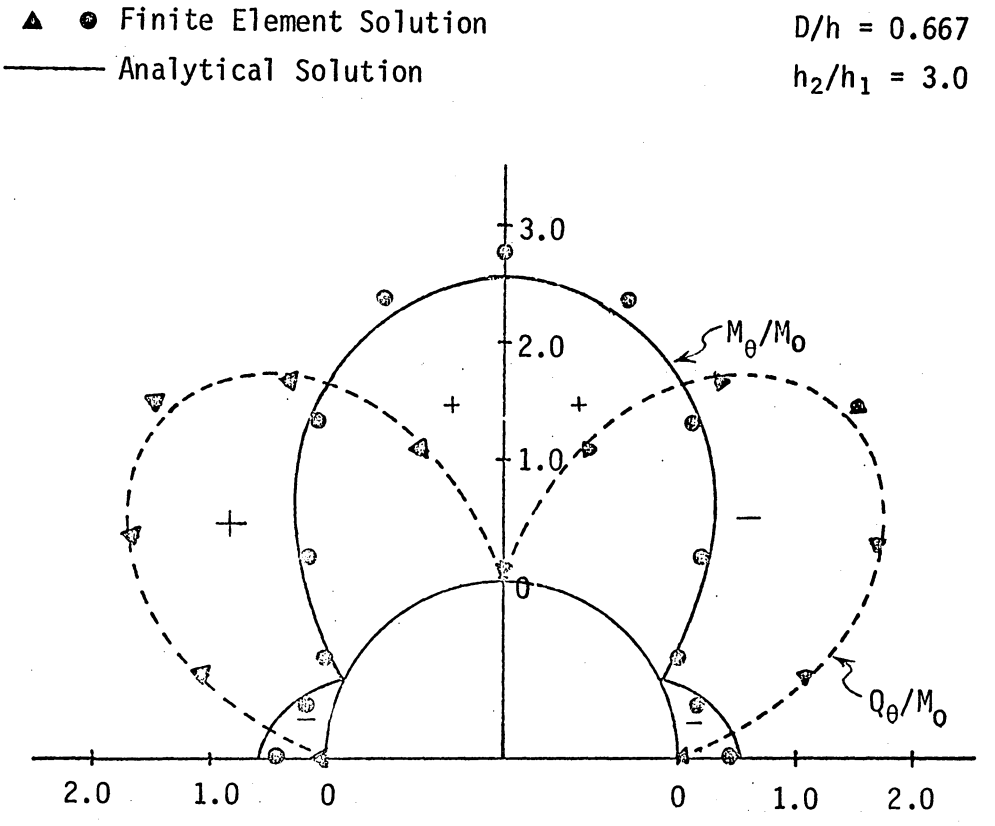

Figure 45. Distribution of M_θ/M_o and Q_θ/M_o Around Circular Hole in $(St/Al)_s$ Sandwich Plate for Finite Element and Analytical Solutions

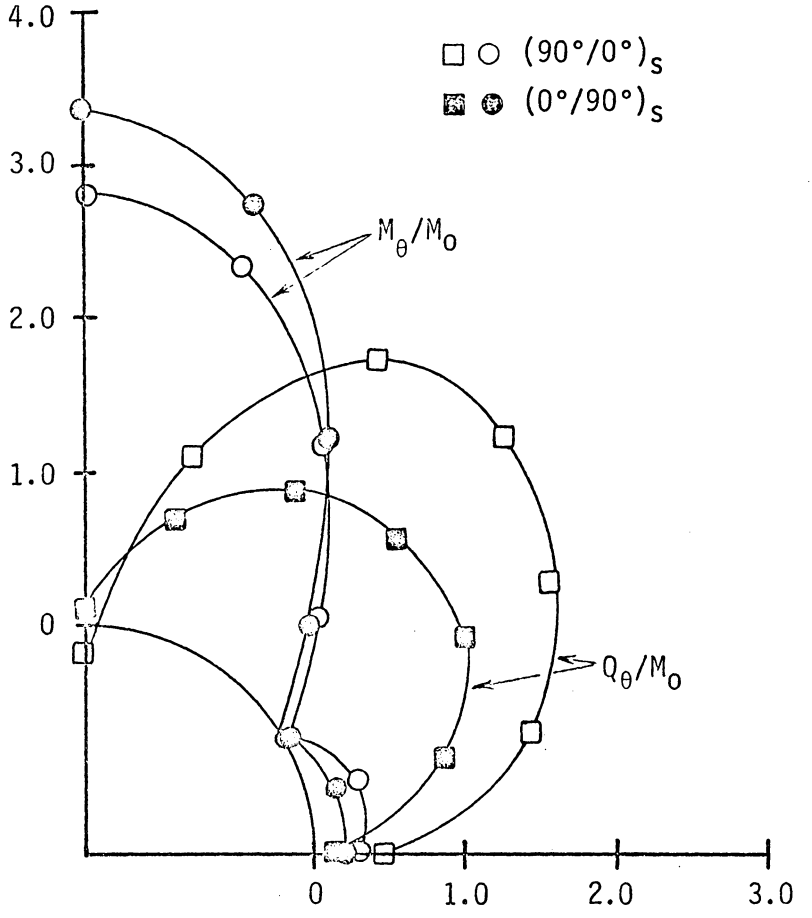

Figure 46. Distribution of M_θ/M_o and Q_θ/M_o Around Circular Hole in $(0°/90°)_s$ and $(90°/0°)_s$ Sandwich Plates for Finite Element Solution

increase the computing time and the required computer storage. It would create a difficulty in the program.

A comparison of the finite element solution with Reissner's solution for a single-layer isotropic plate under pure bending is shown in Figures 47 through 49. From Figure 49 the same conclusion can be drawn - the shear stress distribution in the plate thickness definitely deviates from the Reissner's Theory.

A comparison of the finite element solution with Lekhnitskii's classical solution for orthotropic plates is shown in Figure 50. In Figure 46, the orthotropic laminated sandwich plate is studied. Sandwich plates having two different stacking sequences, $(0°/90°)_s$ and $(90°/0°)_s$, are illustrated. The distinct deviation between these two plates can be observed.

In order to study the angle-ply laminated composite plate, the results for $(45°/-45°)_s$ and $(-45°/45°)_s$ sandwich plates are presented.

The stress distributions for M_θ/M_o and Q_θ/M_o around the hole for these two plates are shown in Figures 51 and 52. The point at which the maximum M_o occurs will shift ahead or behind the 90° point depending on the stacking sequence of the composite. It is clear that the influence of stacking sequence on the stress distribution is pronounced.

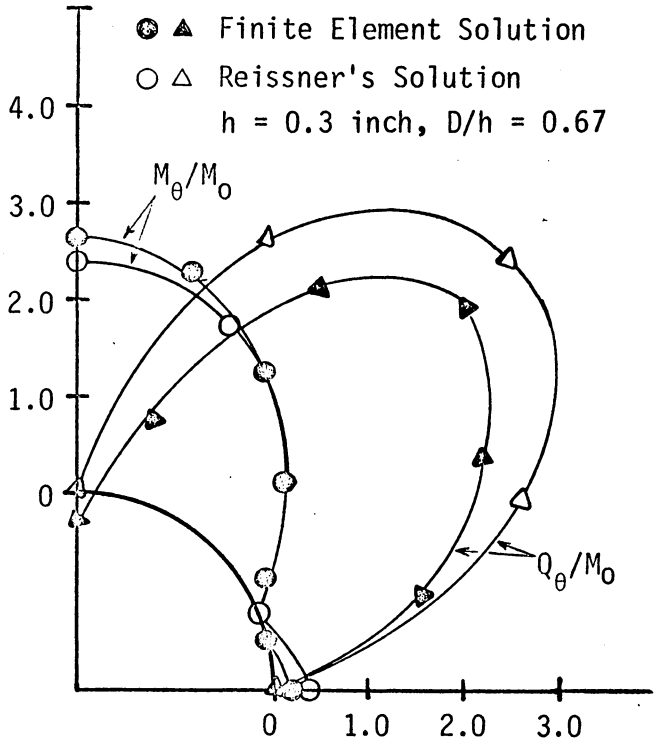

Figure 47. Distribution of M_θ/M_o and Q_θ/M_o Around Circular Hole in Single-Layer, Isotropic Plate for Finite Element and Reissner's Theory Solutions

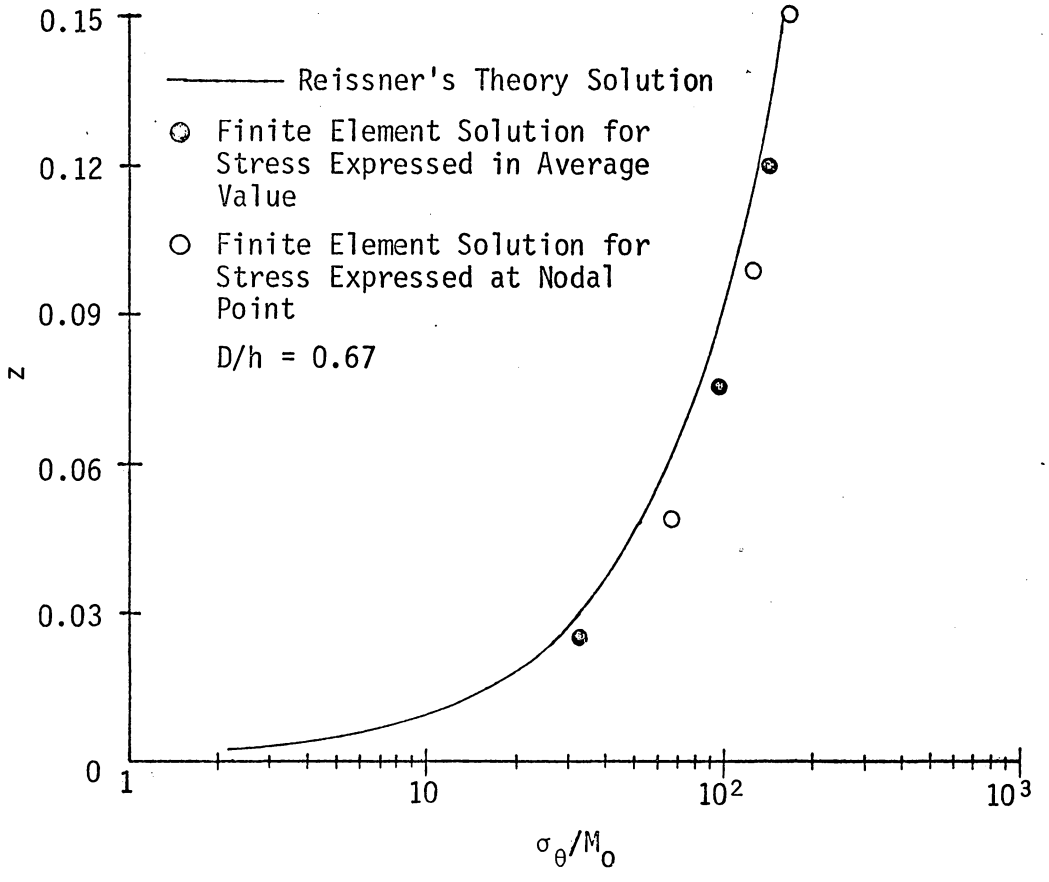

Figure 48. Distribution of σ_θ/M_o at Circular Hole Through Plate Thickness in Single-Layer, Isotropic Plate for Finite Element and Reissner's Theory Solutions

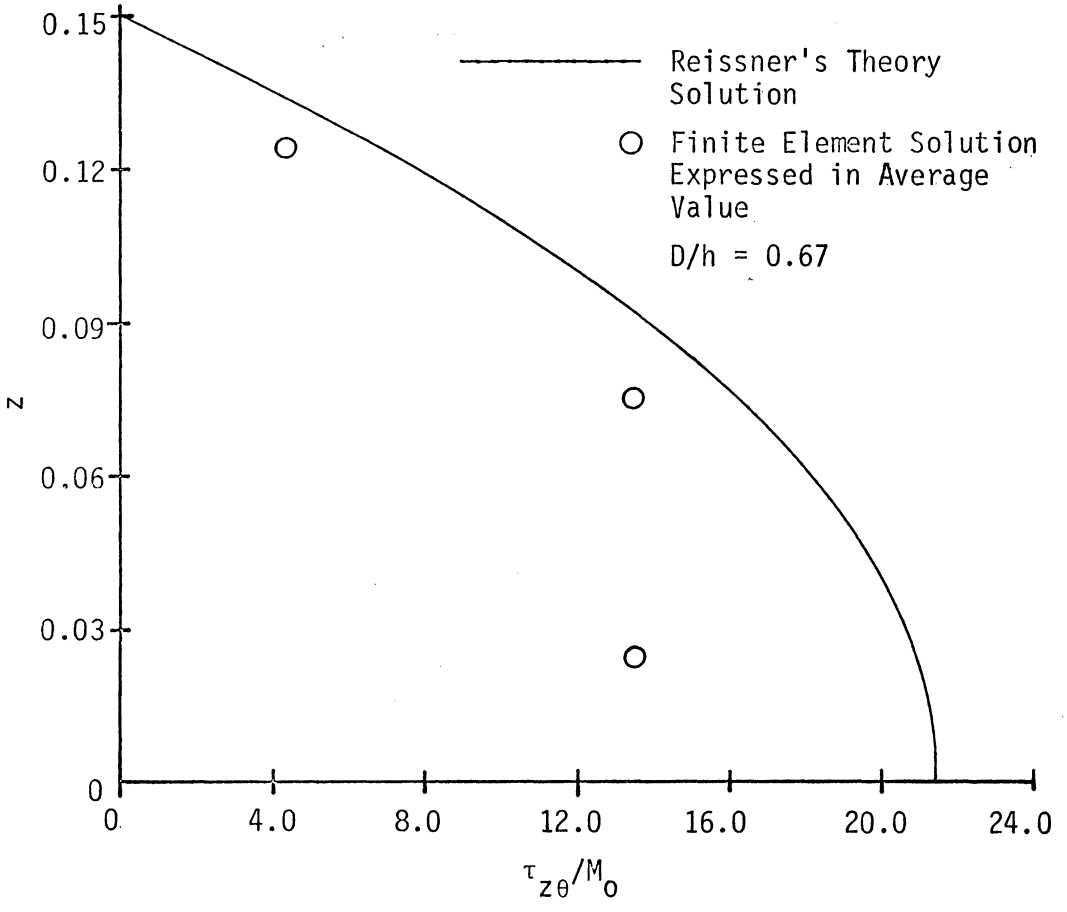

Figure 49. Distribution of $\tau_{z\theta}/M_o$ at Circular Hole Through Plate Thickness in Single-Layer, Isotropic Plate for Finite Element and Reissner's Theory Solutions

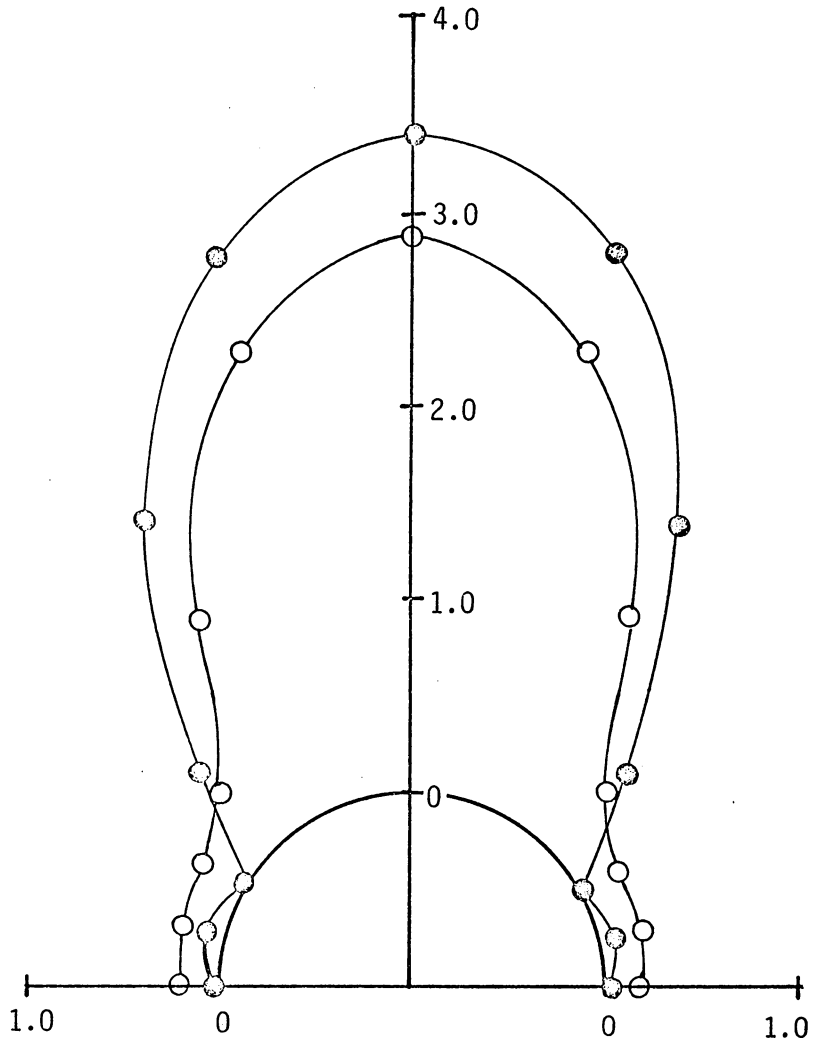

Figure 50. Distribution of M_θ/M_0 Around Circular Hole in Single-Layer, Orthotropic Plate for Finite Element and Lekhnitskii's Theory Solutions

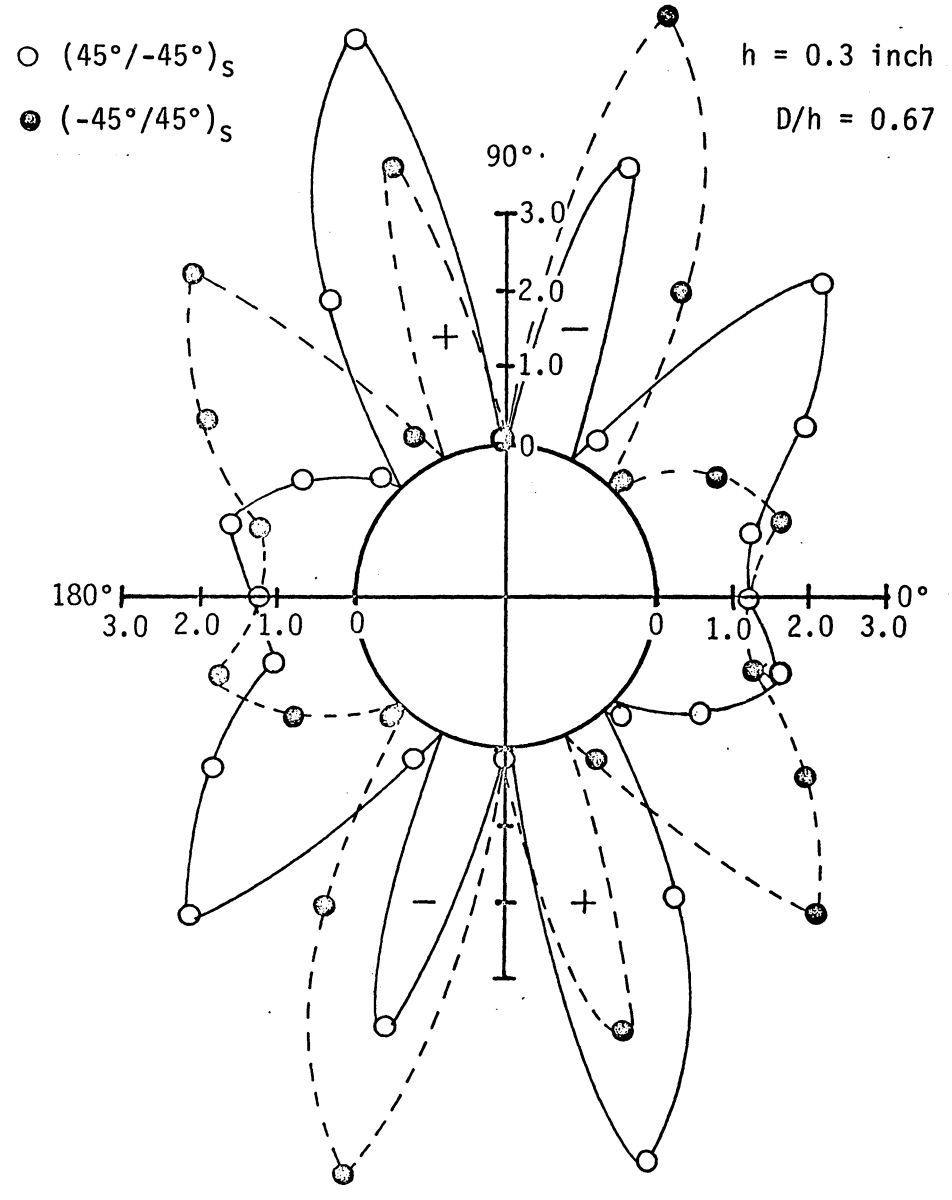

Figure 51. Distribution of Q_θ/M_0 Around Circular Hole in $(45°/-45°)_s$ and $(-45°/45°)_s$ Sandwich Plates for Finite Element Solution

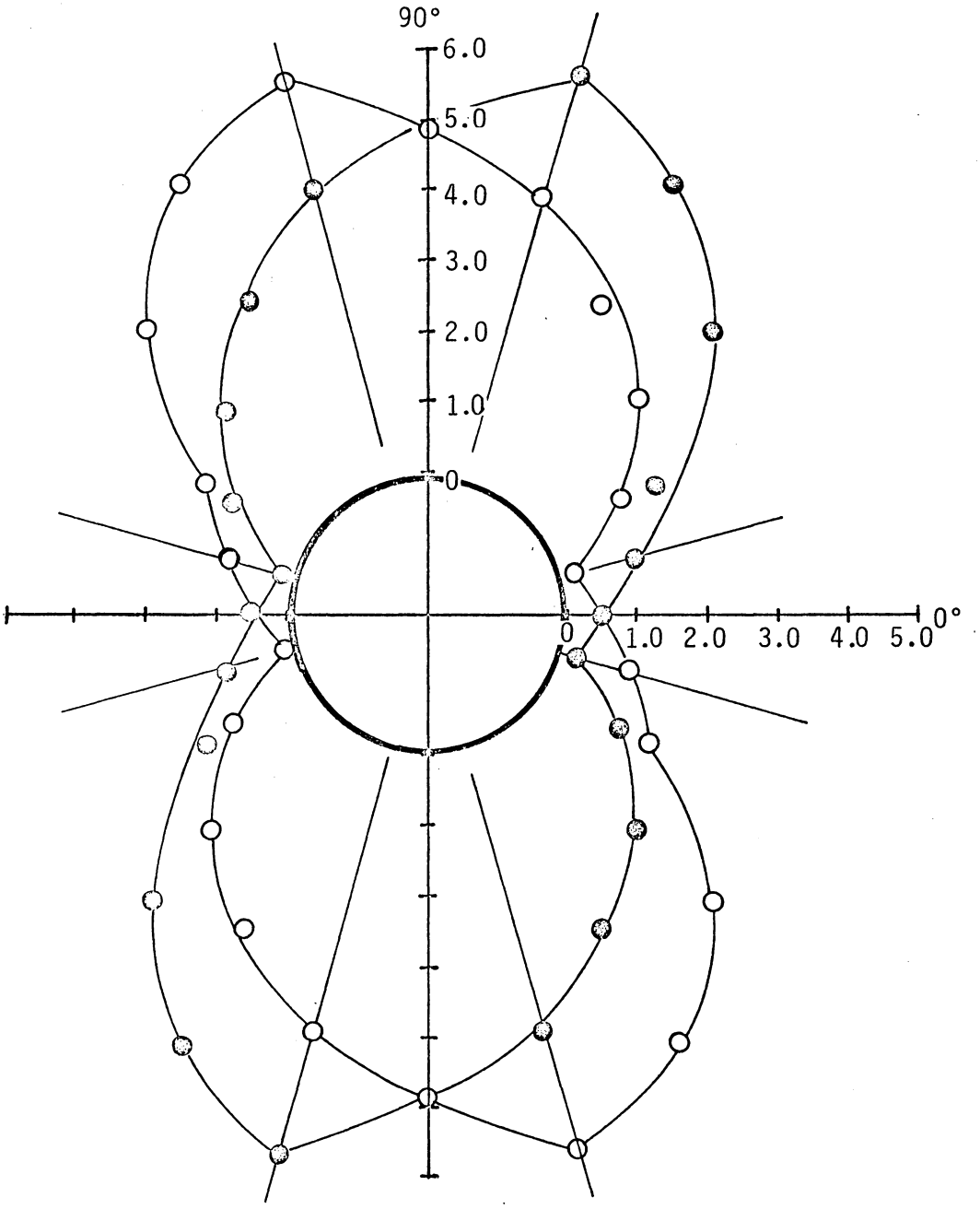

Figure 52. Distribution of M_θ/M_o Around Circular Hole in $(45°/-45°)_s$ and $(-45°/45°)_s$ Sandwich Plates for Finite Element Solution

8. CONCLUSIONS

The shear deformation lamination theory has been used to investigate the stress distribution around a hole in laminated composites under pure bending. The analysis shows that the stress couples in the tangential direction and the shear resultants have the same order of magnitude at the hole edge. The analysis also presents the deviation between the classic lamination theory and the theory presented. The results indicate that the stress resultants and couples are influenced by the quantity D/h. The stress resultants and couples decrease and approach the classical lamination solution as the quantity D/h increases to a very large value.

With a higher-order lamination theory, the existence of a so-called boundary layer near the free boundary of the hole is demonstrated. The thickness of the boundary layer depends strongly on the value of D/h. For specified laminated composite plates, the peak value of Q_θ/M_o at the hole edge increases as D/h increases, while the peak value of Q_R/M_o decreases. When the curvature of the hole edge approaches zero ($D/h \to \infty$), the peak value of Q_θ/M_o reaches a maximum value, and the boundary layer thickness for this case is approximately the plate thickness. The D/h value as well as the stacking sequence affect the boundary layer. For example, the peak value of Q_θ/M_o for $(Al/St/Al/St)_s$ laminates is 2.412, whereas, for $(St/Al/St/Al)_s$ laminates, it is 1.93.

The boundary form perturbation technique is used to investigate elliptical, square, and diamond-shaped holes. Owing to the algebraic complications, only the zero- and first-order solutions are presented. Comparative studies of the exact and perturbation solutions for elliptical holes indicate that the two-term perturbation solution gives fairly good accuracy. A comparative investigation of the finite element method and the perturbation solution for square and diamond-shaped holes shows that the results agree with each other.

The 72 DOF finite element solution gives good accuracy in predicting the stress distribution for M_θ/M_o, Q_θ/M_o around the hole and the ratio σ_θ/M_o through the plate thickness. However, it gives poor results for the distribution of $\tau_{\theta z}/M_o$ through the plate thickness. Therefore, in order to achieve better results for $\tau_{\theta z}/M_o$, additional elements must be used in the thickness direction. Unfortunately, this extension will create difficulties in handling the computer program on the IBM 360 computer because of the requirements for wider band width and larger storage capacity.

REFERENCES

1. C. B. Smith, "Some New Types of Orthotropic Plates Laminated of Orthotropic Materials," J. Applied Mechanics, Vol. 20 (1953), p. 286.

2. K. S. Pister and S. B. Dong, "Elastic Bending of Layered Plates," ASCE Proceedings, Vol. 85, No. EMH (1959), p. 4.

3. E. Reissner and Y. Stavsky, "Bending and Stretching of Certain Types of Heterogeneous Aeolotropic Elastic Plates," J. Applied Mechanics, Vol. 28, Series E, No. 2, September 1961, p. 402.

4. Y. Stravsky, "Bending and Stretching of Laminated Aeolotropic Plates,: Journal of ASCE Proceedings, Engineering Mechanics Division, December 1961, p. 31.

5. S. B. Dong, K. S. Pister, and R. L. Taylor, "On the Theory of Laminated Anisotropic Shells and Plates," J. of Aerospace Science, August 1962, p. 969.

6. L. R. Calcote, The Analysis of the Laminated Composite Structures, Van Nostrand Reinhold Co. (1969).

7. J. E. Ashton, J. C. Halpin, and P. H. Petit, Primer on Composite Materials Analysis, Technomic Pbk. (1969).

8. J. E. Ashton and J. M. Whitney, Theory of Laminated Plates, Technomic Pbk. (1970).

9. G. H. Dietz, Composite Engineering Laminates, MIT Press, Cambridge, Mass. (1969).

10. E. Reissner, "The Effect of Transverse Shear Deformation on the Bending of Elastic Plates," J. Applied Mechanics, Vol. 12, No. 2, June 1945, p. 69.

11. R. D. Mindlin, "Influence of Rotary Inertia and Shear on Flexural Motions of Isotropic Elastic Plates," J. Applied Mechanics, Vol. 18, No. 1, ASME, March 1951, p. 31.

12. Y. Stravsky, "On the Theory of Heterogeneous Anisotropic Plates, PhD Thesis, MIT, Cambridge, Mass. (1959).

13. S. A. Ambartsumyan, Theory of Anisotropic Plates, Translated from Russian by Technomic Pbk (1969).

14. J. M. Whitney, "The Effect of Transverse Shear Deformation on the Bending of Laminated Composite Plates," J. Composite Materials, Vol. 3, No. 3, July 1969, p. 534.

15. P. C. Yang, C. H. Norris, and Y. Stravsky, "Elastic Wave Propagation in Heterogeneous Plates," Intl. J. Solids and Structures, Vol. 2 (1966), p. 665.

16. C. T. Sun, J. D. Achenbach, and G. Herrmann, "Continuum Theory for a Laminated Medium," J. Applied Mechanics, Vol. 35, No. 3, ASME Series E, September 1968, p. 467.

17. C. W. Pryor, "Finite Element Analysis of Laminated Anisotropic Plates," PhD Dissertation, VPI&SU (1970).

18. F. T. Lin, "The Finite Element Analysis of Laminated Composites," PhD Dissertation, VPI&SU (1972).

19. R. M. Barker, J. R. Dana, and C. W. Pryor, "Stress Concentration Near Holes in Laminates," ASCE Specialty Conference on Composite Materials, Pittsburgh, Pa., November 13, 1972.

20. S. G. Savin, Stress Concentration Around the Holes, Pergamon Press (1961).

21. S. G. Lekhnitsky, "Anisotropic Plates," Foreign Technology Division, Wright-Patterson AFB, Ohio, March 1968.

22. A. E. Green and W. Zerna, Theoretical Elasticity, Oxford Press (1968).

23. I. M. Daniel and R. E. Rowlands, "Determination of Strain Concentration in Composites by Moire' Techniques," J. Composite Materials, Vol. 5, April 1971, p. 250.

24. T. Chiba and R. A. Heller, "Alleviation of Stress Concentration with Analogue Reinforcement," VPI&SU Report VPI-E-72-4, Apeil 1962.

25. M. E. Waddoups, J. R. Eisenmann, and B. E. Kaminski, "Macroscopic Fracture Mechanics of Advanced Composite Materials," J. of Composite Materials, Vol. 5, October 19-1, pp. 446-454.

26. O. M. Guz, "Stress Concentration Near a Circular Aperture in a Spherical and Isotropic Shell," PMM, Vol. 7, No. 4 (1961).

27. O. M. Guz, "Approximate Method of Calculation of Stress Concentration Near Circular Aperture in Shell," PMM, Vol. 8, No. 6 (1962).

28. J. R. Dana, "Three-Dimensional Finite Element Analysis of Thick Laminated Composites - Including Interlaminar and Boundary Effects Near Circular Holes," PhD Dissertation, VPI&SU (1973).

29. A. I. Lur'e, Three-Dimensional Problems of the Theory of Elasticity, Interscience Publishers, New York, 1964.

30. D. Frederick and T. S. Chang, Continuum Mechanics, 2nd Printing, Allyn & Bacon, Inc. (1969).

31. N. I. Muskhelishvili, Some Basic Problems of the Mathematical Theory of Elasticity, P. Nordhoff, Ltd., Groningen, Holland (1953).

32. Woinowsky-Krieger and Timoshenko, Theory of Plate and Shell, 2nd Ed., McGraw-Hill (1959).

33. R. B. Pipes and N. J. Pagano, "Interlaminar Stresses in Composite Laminates Under Uniform Axial Extension," J. Composite Materials, Vol. 4, October 1970, p. 538.

34. P. M. Naghdi, "The Effect of Elliptical Holes on the Bending of Thick Plates," J. Applied Mechanics, Vol. 22, March 1955, p. 89.

35. N. W. McLachlan, Theory and Application of Mathieu Functions, Oxford Press (1947).

36. M. Abramovitz and I. Stegum, Handbook of Mathematical Functions, Dover Publications, Inc., New York.

37. G. N. Savin, "Concentration of Stresses Around Curvilinear Holes in Plates and Shells," Proceedings, 11th Intl. Congress of Applied Mechanics, 1964, Springer Verlag Publications (1965).

38. N. J. Pagano, "Exact Solutions for Rectangular Bidirectional Composites and Sandwich Plates," J. Composite Materials, Vol. 4, January 1970, p. 20.

APPENDIX

APPENDIX

1. Derivation of Eq. (G.9a) from (G.8):

$$r = [\rho^2 + \varepsilon(\bar{\zeta}f + \zeta\bar{f}) + \varepsilon^2 f\bar{f}]^{1/2}$$

$$= \rho[1 + \varepsilon(\bar{\zeta}f + \zeta\bar{f})/\rho^2 + \varepsilon^2 f\bar{f}/\rho^2]^{1/2}$$

$$= \rho\{1 + \frac{1}{2}[\varepsilon(\bar{\zeta}f + \zeta\bar{f})/\rho^2 + \varepsilon^2 f\bar{f}/\rho^2]$$

$$- \frac{1}{8}[\varepsilon(\bar{\zeta}f + \zeta\bar{f})/\rho^2 + \varepsilon^2 f\bar{f}/\rho^2 + \ldots\}$$

$$= \rho[1 + \frac{\bar{\zeta}f + \zeta\bar{f}}{2\rho^2}\varepsilon - \frac{(\bar{\zeta}f - \zeta\bar{f})^2}{8\rho^4}\varepsilon^2 + \ldots] .$$

2. Derivation of Eq. (G.9b):

$$\text{Let } \theta = \Theta + \varepsilon\theta_1 + \varepsilon^2\theta_2 + \ldots; \text{ then}$$

$$\tan\Theta + \frac{\partial}{\partial\Theta}(\tan\theta)(\varepsilon\theta_1 + \varepsilon^2\theta_2 + \ldots)$$

$$+ \frac{1}{2!}\frac{\partial^2}{\partial\Theta^2}(\tan\Theta)(\varepsilon\theta_1 + \varepsilon^2\theta_2 + \ldots)^2 + \ldots$$

Since

$$\frac{\partial}{\partial\Theta}(\tan\Theta) = \frac{1}{\cos^2\Theta}, \quad \frac{\partial^2}{\partial\Theta^2}(\tan\Theta) = \frac{2\sin\Theta}{\cos^3\Theta}$$

Hence,

$$\tan\theta = \tan\Theta + \frac{1}{\cos^2\Theta}(\varepsilon\theta_1 + \varepsilon^2\theta_2 + \ldots)$$

$$+ \frac{2}{2!}\frac{\sin\Theta}{\cos^3\Theta}(\varepsilon^2\theta_1^2 + 2\varepsilon^3\theta_1\theta_2 + \ldots) + \ldots$$

$$= \tan\Theta + \frac{\theta_1}{\cos^2\Theta} + \left(\frac{\theta_2}{\cos^2\Theta} + \frac{\sin\Theta}{\cos^3\Theta}\theta_1^2\right)\varepsilon^2 + \ldots \quad \text{(A.1)}$$

From Eq. (6.4),

$$\tan\theta = \frac{\sin\Theta + \dfrac{f(\zeta) - \bar{f}(\bar{\zeta})}{2\rho_i}}{\cos\Theta + \dfrac{f(\zeta) + \bar{f}(\bar{\zeta})}{2\rho}}$$

$$= \tan\Theta\left(1 + \varepsilon\frac{f - \bar{f}}{2\rho_i\sin\Theta} - \varepsilon\frac{f + \bar{f}}{2\rho\cos\Theta} - \varepsilon^2\frac{f^2 - \bar{f}^2}{4\rho^2\sin\Theta\cos\Theta}\right.$$

$$\left. + \varepsilon^2\frac{f^2 + 2f\bar{f} + \bar{f}^2}{4\rho^2\cos^2\Theta} + \ldots\right)$$

$$= \tan\Theta + \tan\Theta \frac{\varepsilon}{\sin\Theta\cos\Theta}\left(\frac{f - \bar{f}}{2\rho_i}\cos\Theta - \frac{f + \bar{f}}{2\rho}\sin\Theta\right)$$

$$+ \tan\Theta \frac{\varepsilon^2}{\sin\Theta\cos\Theta}\left(-\frac{f^2 - \bar{f}^2}{4\rho_i^2} + \tan\Theta\frac{f^2 + \bar{f}^2 + f\bar{f}}{4\rho^2}\right) + \ldots \tag{A.2}$$

Comparing Eqs. (a.1) and (A.2), the following is obtained:

$$\theta_1 = \frac{f - \bar{f}}{2\rho_i}\cos\Theta - \frac{f + \bar{f}}{2\rho}\sin\Theta \tag{A.3}$$

and

$$\theta_2 + \tan\Theta\theta_1 = -\frac{f^2 - \bar{f}^2}{4\rho_i^2} + \tan\Theta\frac{f^2 + \bar{f}^2 + 2f\bar{f}}{4\rho^2} \tag{A.4}$$

Using (A.3) and (A.4), we have

$$\theta_2 = \frac{f^2 + \bar{f}^2}{4\rho^2}\sin 2\Theta - \frac{f^2 - \bar{f}^2}{4\rho_i^2}\cos 2\Theta. \tag{A.5}$$

The vita has been removed from the scanned document

STRESS DISTRIBUTION AROUND HOLES IN LAMINATED COMPOSITE PLATES

by

Chi-Hung Huang

(ABSTRACT)

A solution is presented for the stress distribution around holes in laminated composite plates under pure bending. The shear deformation, lamination theory is derived and employed for the analysis of circular, elliptical, square, and diamond-shaped holes piercing the laminated composite plate. Each layer of the laminate is assumed to be homogeneous and to have isotropic properties. Functional analysis employing complex variable methods is used to solve the governing equations. Using conformal mapping and boundary form perturbation techniques, the circular hole solution has been extended to the solution of the curvilinear hole case.

These analytical solutions are compared with the solution obtained from a 72 DOF finite element method. The stress resultants and stress couples around the hole, the interlaminar stresses, as well as the tangential stress through the plate thickness are studied. In addition, the boundary layer phenomenon in the vicinity of the hole is presented.